DOE/EV/04682--4

ORO-4682-4

SORPTION OF GRAPHITES AT HIGH TEMPERATURES

DOE/EV/04682--4

DE82 011151

FINAL REPORT

for Period

February 1, 1977 - June 30, 1978

N. I. Kazi

T. D. Pyecha

L. R. Zumwalt (Principal Investigator)

North Carolina State University

Raleigh, North Carolina

June 30, 1980

DISCLAIMER

SORPTION OF GRAPHITES AT HIGH TEMPERATURES

FINAL REPORT

for Period

February 1, 1977 - June 30, 1978

N. I. Kazi

T. D. Pyecha

L. R. Zumwalt (Principal Investigator)

North Carolina State University

Raleigh, North Carolina

June 30, 1980

PREPARED FOR THE UNITED STATES DEPARTMENT OF ENERGY

UNDER CONTRACT NO. E - (40-1)-4682

Contract Period April 30, 1977 - June 30, 1978

ABSTRACT

The topics of this report include: 1) corrected data and new data on cesium sorption by bulk graphite (H-451) with a discussion of anomalies and a comparison of the data; 2) a review of the exponential (Freundlich) isotherm theory and a derivation of the modified-exponential isotherm; 3) a report on a study by the pseudo-isopiestic method of cesium by H-451 graphite powder (size range 44 to 74 μm) of the type used in the Knudsen cell mass spectrometer method; 4) a comparison of the results on particulate graphite (powder) obtained by the Knudsen cell method and also a comparison of cesium sorption results obtained with the bulk graphite; 5) development of a theory for the kinetics of sorption of a system (cesium and graphite) which shows an exponential (Freundlich) type of sorption; 6) comparison of theoretical with observed kinetics for sorption of cesium by graphite (H-451) powder and a comparison of bulk graphite vs. particulate graphite sorption kinetics. 7) report of a study of the effects of barium on cesium sorption by H-451 graphite at 1000°C; and 8) a thermodynamic treatment of mixed sorption and its application to mixed barium-cesium and strontium-cesium sorption by graphite.

The most important conclusions of this report are:

1. The kinetics of absorption and desorption of cesium by bulk nuclear-grade graphite and even by the graphite in particulate form (size range 44 to 74 μm) is such that, in general, several days are required to reach a near equilibrium state. Accordingly, the pseudo-isopiestic method, although time consuming, appears to be the best method to assure the obtainment of equilibrium data in the cesium vapor pressure range of about 10 Pa down to 10^{-4} Pa.
2. The kinetics data of the pseudo-isopiestic experiment with graphite powder was found to be very well represented mathematically by

a kinetics equation which is based on the site (trap) activation energy, ϵ, being approximately equal to the site interaction (sorption) energy, χ. In accordance with theory for modified-exponential sorption, the sites are taken to be non-uniformly distributed having a number which decreases exponentially with interaction energy, χ, which has a finite upper limit χ_L.

3. The kinetics data of the pseudo-isopiestic experiments with solid graphite do not fit the kinetics equation quite as well as does the data obtained with a powdered graphite sample. The fit, however, is reasonably good and at short times, the data appears to reflect rapid evaporation of cesium from external graphite surfaces while at very long times the kinetics are believed to be controlled by a slow diffusion of atoms to residual sites within the bulk of the graphite.

4. In binary sorption studies, where data were obtained of the effects of barium or strontium in graphite (H-451) on the equilibrium vapor pressure of cesium, a thermodynamic treatment was found the most useful. The vapor pressure is given by an equation which contains the activity coefficient, γ_1, defined as the ratio of true cesium vapor pressure to the ideal vapor pressure. The logarithm of the activity coefficient is functionally expressed by a polynomial in terms of x_2, the mole fraction of the second component (strontium or barium).

TABLE OF CONTENTS

page

LIST OF TABLES v

LIST OF FIGURES vii

1. INTRODUCTION 1

1.1 Review of the Pseudo-isopiestic Method 1

1.2 Kinetic Behavior - Time to Reach Equilibrium 5

2. CESIUM-GRAPHITE (H-451) ISOTHERMS 7

2.1 Analysis of the Corrected Data of Experiments 5, 7, and 9 7

2.2 Hysteresis and Other Anomalies - Experiments 5,7 and 9. 15

2.3 Experiments 15, 30 and 36 23

2.4 Comparison of Data of Experiments 15, 30 and 36 at 1273 K 28

2.5 The Exponential or Freundlich Isotherm - Derivation of the Modified-Exponential Isotherm 31

3. COMPARISON OF THE CESIUM SORPTION AND DESORPTION BEHAVIOR OF BULK VERSUS PARTICULATE GRAPHITE 36

3.1 Discussion of the Knudsen Cell and Pseudo-Isopiestic Method 36

3.2 A Pseudo-Isopiestic Study of Cesium Sorption by Particulate Graphite (H-451) - Experimental Runs by Kevin M. Vaughan 38

3.3 Comparison of Results Obtained with Graphite Powder . . 42

3.4 Comparison of Bulk Graphite vs Particulate Graphite Equilibrium Cesium Sorption 45

4. KINETICS OF CESIUM-GRAPHITE SORPTION AND DESORPTION 48

4.1 Kinetic Theory of an Exponential (Freundlich) Sorption System 48

4.2 Comparison of Theoretical with Observed Kinetics in the Case of Graphite Powder 59

4.3 Kinetics of Cesium -Graphite Sorption and Desorption for Bulk H-451 Graphite 60

4.3.1 Comparison of Theoretical with Observed Kinetics for Experiment 36 60

TABLE OF CONTENTS (continued)

page

4.3.2 Comparison of Theoretical with Observed Kinetics for Experiment 16 78

5. BINARY SORPTION 80

5.1 Cesium Sorption Isotherms of Barium-Impregnated H-451 Graphite 80

5.2 Cesium Sorption Isotherms on Strontium-Impregnated H-451 Graphite 95

5.3 Application of the Thermodynamic and FREVAP Models to Binary Sorption 109

6. SUMMARY AND CONCLUSIONS 117

6.1 Summary 117

6.2 Conclusions 118

7. ACKNOWLEDGEMENTS -- CONTACTS WITH OTHER LABORATORIES . . 121

8. LIST OF REFERENCES 122

APPENDIX I 123

APPENDIX II 128

APPENDIX III 130

APPENDIX IV 132

APPENDIX V 138

LIST OF TABLES

page

Table 2.1 Experiment 5: Cesium Sorption on H-451 Graphite at 1273 K 9

Table 2.2 Experiment 7: Cesium Sorption on H-451 Graphite at 126 and 1177 K 10

Table 2.3 Experiment 9: Cesium Sorption on H-451 Graphite at 1076, 1173, 1271 and 1367 K 11

Table 2.4 Cesium Desorption Isotherm Coefficients for H-451 Graphite -- Experiments 5, 7 and 9 20

Table 2.5 Experiment 15: Cesium Sorption on H-451 Graphite (Finned Sample) at 1366 K 26

Table 2.6 Experiment 30: Cesium Sorption on H-451 Graphite (Impregnation Blank) at 1273 K and 1373 K 27

Table 2.7 Experiment 36: Cesium Sorption on H-451 Graphite (Impregnation Blank) at 1272 K 29

Table 3.1 Experiment 41: Cesium Sorption on H-451 Graphite Powder (44 to 74 μm size) at 1272 K 41

Table 4.1 Kinetics Best Fit Parameters for Cesium Sorption by H-451 Graphite Powder 67

Table 4.2 Data Points and Best Choice and Next Best Choice for the Kinetics Parameters A_s and f 77

Talbe 5.1 Experiment 33: Cesium Sorption on Barium Impregnated H-451 Graphite-H-451 Sample Weight: Before Impregnation = 3.7342 gm 85

Table 5.2 Experiment 32: Cesium Sorption on Barium Impregnated H-451 Graphite - H-451 Sample Weight: Before Impregnation = 3.7375 gm 86

Table 5.3 Experiment 31: Cesium Sorption on Barium Impregnated H-451 Graphite - H-451 Sample Weight: Before Impregnation = 3.7227 gm 87

Table 5.4 Experiment 35: Cesium Sorption on Barium Impregnated H-451 Graphite - H-451 Sample Weight: Before Impregnation = 3.7326 gm 88

Table 5.5 Experiment 36: Cesium Sorption on Barium-Free H-451 Graphite 89

LIST OF TABLES (continued)

page

Table 5.6 Cesium Desorption Isotherm Parameters for Barium-Impregnated H-451 Graphite at 1273 K 93

Table 5.7 Cesium Desorption Isotherm Coefficients for Strontium Impregnated H-451 Graphite 97

Table 5.8 Experiment 13: Cesium Sorption at 1271 K on H-451 Graphite (Finned Sample) Impregnated to 0.924 mmol Sr/kg Graphite 104

Table 5.9 Experiment 12: Cesium Sorption at 1269 K on H-451 Graphite (Finned Sample) Impregnated to 3.520 mmol Sr/kg Graphite 105

Table 5.10 Experiment 18: Cesium Sorption at 1273 K on H-451 Graphite Impregnated to 5.189 mmol Sr/kg Graphite. 106

Table 5.11 Experiment 15: Cesium Sorption at 1273 K on H-451 Graphite Impregnated to 7.810 mmol Sr/kg Graphite. 107

Table 5.12 Experimental and Predicted Data Points 114

LIST OF FIGURES

		page
Figure 1.1	Experimental Arrangement for Pseudo-isopiestic Method	2
Figure 1.2	Distillation and Sorption Apparatus	4
Figure 1.3	Experiment 36: Kinetics Data - Cesium Sorption on H-451 Graphite at 1273 K	6
Figure 2.1	Freundlich Fit of Cesium Sorption on H-451 Graphite (Linear Plot)	12
Figure 2.2	Freundlich Fit of Cesium Sorption on H-451 Graphite (Log-Log Plot)	13
Figure 2.3	Freundlich Relation for Cesium Sorption on H-451 Grahite with 95% Confidence Bands	14
Figure 2.4	Cesium Sorption by H-451 Graphite at 1076 ± 10 K -- Experiment 9	16
Figure 2.5	Cesium Sorption by H-451 Graphite at 1175 ± 10 K -- Experiments 7, 9	17
Figure 2.6	Cesium Sorption by H-451 Graphite at 1271 ± 10 K -- Experiments 5, 7 and 9	18
Figure 2.7	Cesium Sorption by H-451 Graphite at 1367 ± 10 K -- Experiment 9	19
Figure 2.8	Cesium Sorption on H-451 Graphite at 1369 ± 10 K -- Experiments 15 and 30	25
Figure 2.9	Cesium Sorption on H-451 Graphite at 1273 K by the Pseudo-isopiestic Method --Expts. 15, 30, 36 . . .	30
Figure 3.1	Cesium-Graphite (H-451) Powder, Sorption Isotherms with Experiment 41 Data Points-	42
Figure 3.2	Cesium-Graphite (H-451) Solid, Sorption Isotherms Comparison of Knudsen Cell and Pseudo-isopiestic Results	46
Figure 4.1	Potential Energy Diagram of a Hole and a Trap . . .	51
Figure 4.2	A Possible Physical Concept of Potential Energy Diagram (Figure 4.1) with Cesium Atom on Surface, in Hole and in Trap	51
Figure 4.3	Annealing Function Diagram Plot. As the Isothermal Annealing Progresses, the Curve is Displaced along ε but does not Alter in Shape.	58
Figure 4.4	Annealing Function Approximated by a Step Function.	58

LIST OF FIGURES (continued)

page

Figure 4.5 Kinetics data and Curves for Going from Point 2 to Point 3 -- Experiment 41 (A_s = 5 x $10^{-4}s^{-1}$, f = 1.00) 61

Figure 4.6 Kinetics data and Curves for Going from Point 3 to Point 4 -- Experiment 41 (A_s = 7 x $10^{-4}s^{-1}$, f = 0.95) 62

Figure 4.7 Kinetics data and Curves for Going from Point 4 to Point 5 -- Experiment 41 (A_s = 10 x $10^{-4}s^{-1}$, f = 1.00) 63

Figure 4.8 Kinetics data and Curves for Going from Point 4 to Point 5 -- Experiment 41 (A_s = 10 x $10^{-4}s^{-1}$, f = 0.70) 64

Figure 4.9 Kinetics data and Curves for Going from Point 7 to Point 8 -- Experiment 41 (A_s = 7 x $10^{-4}s^{-1}$, f = 0.90) 65

Figure 4.10 Kinetics data and Curves for Going from Point 8 to Point 9 -- Experiment 41 (A_s = 7 x $10^{-4}s^{-1}$, f = 0.95) 66

Figure 4.11 Experiment 36: Kinetic Behavior of Cesium on H-451 Graphite at 1273 K. R08 - R09 Kinetics Plot . . . 69

Figure 4.12 Experiment 36: Kinetic Behavior of Cesium on H-451 Graphite at 1273 K. R09 - R10 Kinetics Plot . . . 71

Figure 4.13 Experiment 36: Kinetic Behavior of Cesium on H-451 Graphite at 1273 K. R10 - R11 Kinetics Plot . . . 72

Figure 4.14 Experiment 36: Kinetic Behavior of Cesium on H-451 Graphite at 1273 K. R11 - R12 Kinetics Plot . . . 73

Figure 4.15 Experiment 36: Kinetic Behavior of Cesium on H-451 Graphite at 1273 K. R12 - R13 Kinetics Plot . . . 74

Figure 4.16 Experiment 36: Kinetic Behavior of Cesium on H-451 Graphite at 1273 K. R13 - R14 Kinetics Plot . . . 75

Figure 4.17 Experiment 36: Kinetic Behavior of Cesium on H-451 Graphite at 1273 K. R14 - R15 Kinetics Plot . . . 76

Figure 4.18 Experiment 16: Kinetic Behavior of Cesium on H-451 Graphite at 1273 K 79

Figure 5.1 Experiment 33: Cesium Sorption by Barium-Impregnated H-451 Graphite at 1273 K. Average Barium Concentration for Desorption is 4.86 mmol Ba/kg. 81

LIST OF FIGURES (continued)

page

Figure 5.2 Experiment 32: Cesium Sorption by Barium-Impregnated H-451 Graphite at 1273 K. Average Barium Concentration for Desorption is 5.08 mmol Ba/kg 82

Figure 5.3 Experiment 31: Cesium Sorption by Barium-Impregnated H-451 Graphite at 1273 K. Average Barium Concentration for Desorption is 6.76 mmol Ba/kg 83

Figure 5.4 Experiment 35: Cesium Sorption by Barium-Impregnated H-451 Graphite at 1273 K. Average Barium Concentration for Desorption is 9.18 mmol Ba/kg 84

Figure 5.5 Experiment 35: Kinetic Behavior of Cesium in Barium-Impregnated H-451 Graphite at 273 K. 91

Figure 5.6 Least-Squares Fit for Cesium Desorption Isotherms over Barium-Impregnated H-451 Graphite at 1273 ± 10 K 92

Figure 5.7 Cesium Desoprtion Isotherms for Barium-Impregnated H-451 Graphite at 1273 K 94

Figure 5.8 Freundlich fit of Cesium Sorption on Strontium-Impregnated H-451 Graphite 98

Figure 5.9 Cesium Vapor Pressure as a Function of Strontium Concentration at Various Cesium Concentrations 99

Figure 5.10 Cesium Sorption at 1271 K on H-451 Graphite with an Average of 0.59 mmol Sr/kg graphite (Expt. 13) 100

Figure 5.11 Cesium Sorption at 1269 K on H-451 Graphite with an Average of 2.00 mmol Sr/kg graphite (Expt. 12) 101

Figure 5.12 Cesium Sorption at 1273 K on H-451 Graphite with an Average of 2.46 mmol Sr/kg graphite (Expt. 18) 102

Figure 5.13 Cesium Sorption at 1273 K on H-451 Graphite with an Average of 3.38 mmol Sr/kg graphite (Expt. 17) 103

Figure 5.14 Cesium Desorption Isotherms for Barium-Impregnated H-451 Graphite at 1273 K. FREVAP Model with Unit Correction Factor and Thermodynamic Model with Unit Activity Coefficient 111

Figure 5.15 Cesium Desorption Isotherms for Barium-Impregnated H-451 Graphite at 1273 K. Thermodynamic Model with Activity Coefficient 112

LIST OF FIGURES (continued)

page

Figure 5.16 Logarithm of Activity Coefficient (γ) for Cesium Sorbed by Strontium-Impregnated H-451 Nuclear Graphite 115

Figure 5.17 Cesium Vapor Pressure as a Function of Strontium Concentration at Various Cesium COncentrations . . 116

Figure IV-1 Plot of the Logarithm of Activity Coefficient as a Function of Barium Mole Fraction 136

1. INTRODUCTION

This is the final report of a series (1,2,3) on the sorption of graphite at high temperatures (800 to 1100°C). The experimental studies in this period concentrated on near isotropic H-451 nuclear grade graphite of the Great Lakes Carbon Co. as the material of interest. The topics of the report include: 1) corrected data and new data on cesium sorption by bulk graphite (H-451) with a discussion of anomalies and a comparison of the data; 2) a review of the exponential (Freundlich) isotherm theory and a derivation of the modified-exponential isotherm; 3) a report on a study by the pseudo-isopiestic method of cesium by H-451 graphite powder (size range 44 to 74 μm) of the type used in the Knudsen cell mass spectrometer method; 4) a comparison of the results on particulate graphite (powder) obtained by the Knudsen cell method and also a comparison of cesium sorption results obtained with the bulk graphite; 5) development of a theory for the kinetics of sorption of a system (cesium and graphite) which shows an exponential (Freundlich) type of sorption; 6) comparison of theoretical with observed kinetics for sorption of cesium by graphite (H-451) powder and a comparison of bulk graphite vs particulate graphite sorption kinetics; 7) report of a study of the effects of barium on cesium sorption by H-451 graphite at 1000°C; 8) a thermodynamic treatment of mixed sorption and its application to mixed barium-cesium and strontium-cesium sorption by graphite.

1.1 Review of the Pseudo-isopiestic Method

The technique used in this study for the measurements of the cesium vapor pressure over the sample was the pseudo-isopiestic method. A schematic drawing of the apparatus is shown in Figure 1.1. In this method, cesium vapor from a pure cesium source held at one temperature saturates

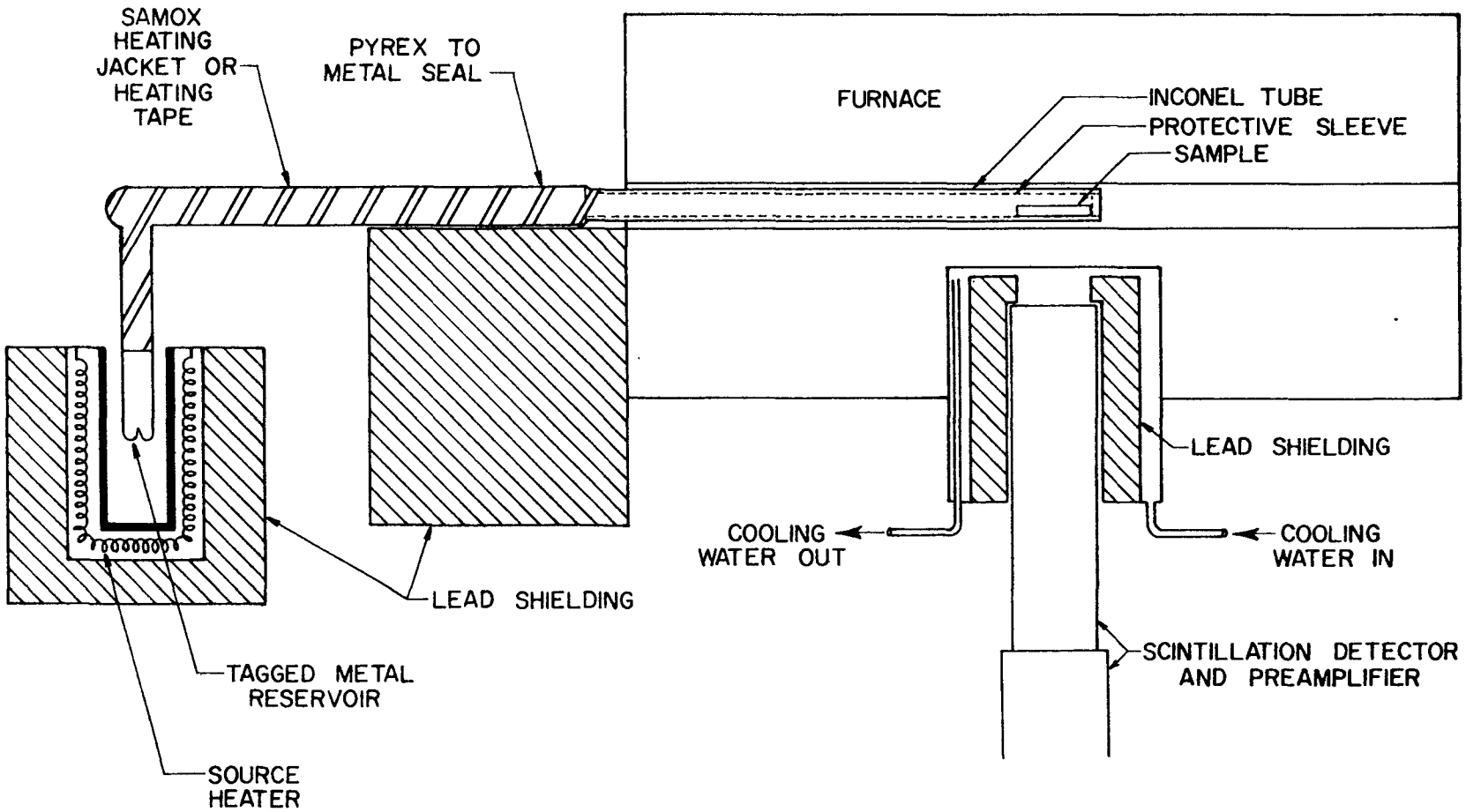

Figure 1.1 Experimental Arrangement for Pseudoisopiestic Method

the graphite sample held at another temperature, and in due time, the sample closely approaches equilibrium with the vapor. In this research, the graphite sample unimpregnated or impregnated with barium tagged by Ba-133 or with strontium tagged by Sr-85 was maintained at a constant temperature of 1000°C throughout the experiment and was allowed to interact with cesium vapor tagged by Cs-137. Therefore, the content of the isotopes present in the graphite sample could be determined in situ by a scintillation detector system placed beneath the furnace containing the graphite sample. The pseudo-isopiestic method generally gives vapor pressure-sorbate concentration data which have a high degree of accuracy and which unlike the high-temperature Knudsen cell mass spectrometer method are almost certain to be close to equilibrium.

Since there is a temperature difference between the cesium source and the graphite sample, a pressure difference in general exists between the two. The pseudo-isopiestic method does not attempt to equate pressures at the sample and the source. Liang (7) suggested a correction is used to find the sample vapor pressure of cesium which is described in Appendix III. Liang's expression for this given in Equation (AIII-1), has been tried by some workers who reported 2-3% accuracy for atmospheric gases with a temperature difference of no more than 300°C.

The cesium vapor pressure over the sample varied from 10^{-4} Pa to 10 Pa as the temperature of the cesium source varied over the range from 25°C to 200°C. The maximum cesium vapor pressure that could be attained was limited by the temperature of the glass-metal seal of the sorption apparatus indicated in Figure 1.2 (this figure also shows the distillation attachment for source preparation). It was important that the cesium source be maintained as the coldest region of the apparatus so as

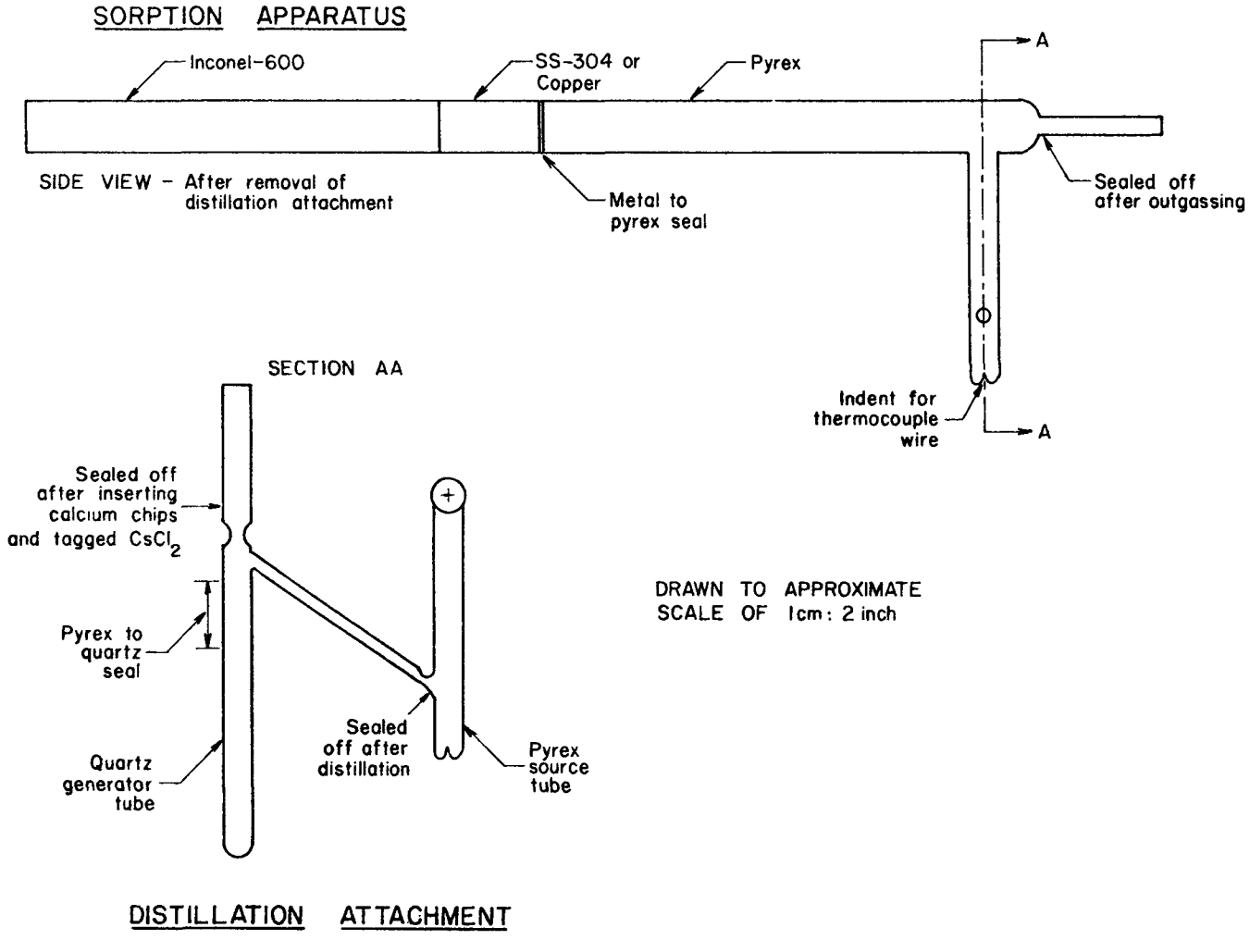

Figure 1.2 Distillation and Sorption Apparatus

to ensure a monotonic increase in the temperature distribution along the mid-section of the sorption apparatus towards the graphite sample. The sample temperature was held constant at 1000°C, a high temperature value that seems to be convenient for purposes of comparison with other work involving different grades of nuclear graphite and different experimental techniques.

1.2 Kinetic Behavior - Time to Reach Equilibrium

The kinetic behavior of cesium sorption on H-451 graphite is displayed graphically in Figure 1.3. This information was collected during the course of Experiment 36 and indicates the time required for attainment of an equilibrium condition prior to obtaining the cesium concentration for the listed sorption isotherm points. The time taken to achieve equilibrium varied from 6 to 20 days, the longer times being required for lower cesium vapor pressures or after large changes in vapor pressure.

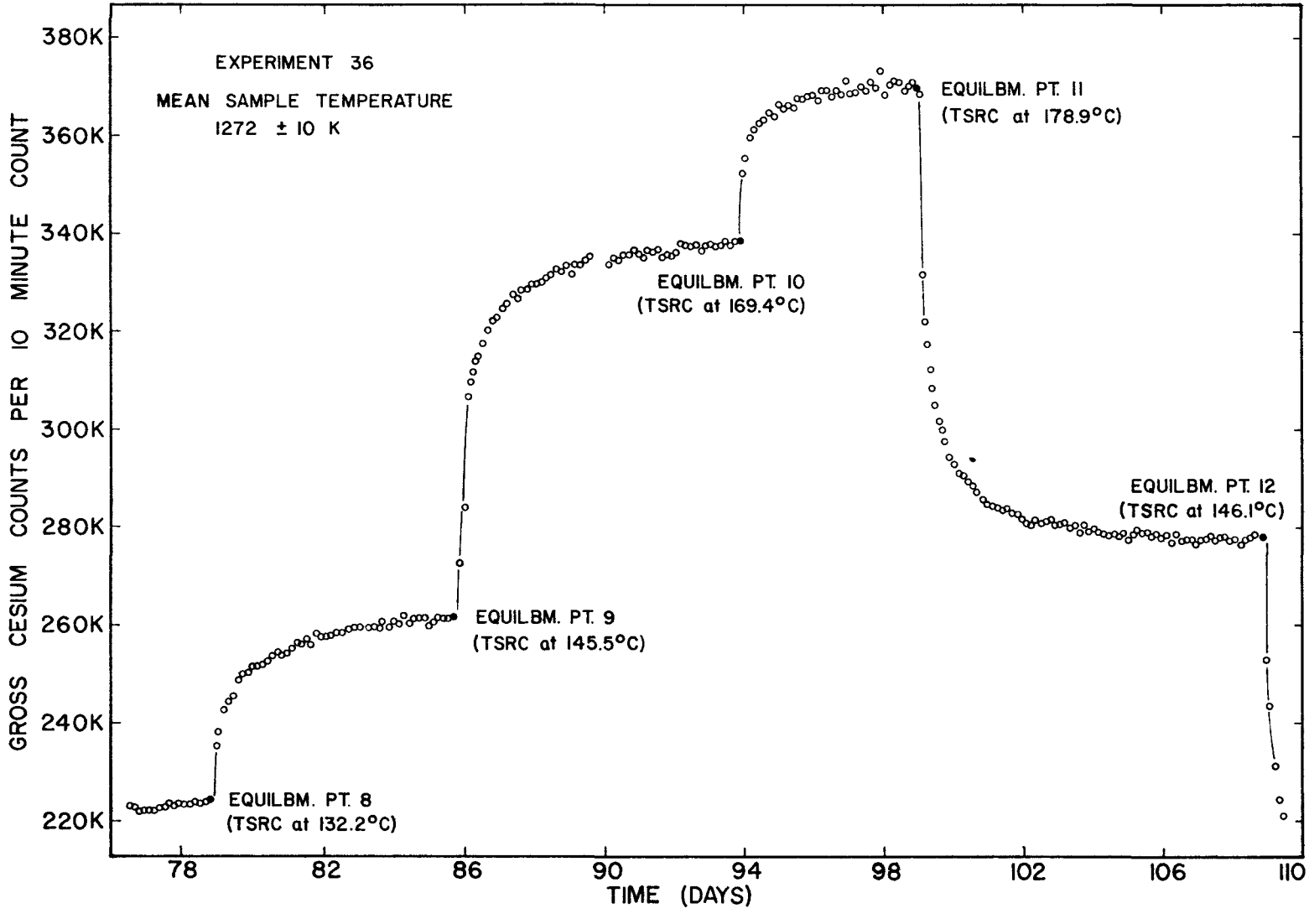

Figure 1.3. Experiment 36: Kinetics Data - Cesium Sorption on H-451 Graphite at 1273 K

2. CESIUM-GRAPHITE (H-451) ISOTHERMS

Since the last report two additional cesium-graphite (H-451) isotherm experiments (Expts 30 and 36) have been done on solid graphite samples. Also the data of previous experiments (Expts 5, 7, 9 and 15) have been corrected and made as accurate as possible. This is reported below.

2.1 Analysis of the Corrected Data of Experiments 5, 7 and 9

The corrected results of Experiments 5, 7 and 9 given in Table 2.1, 2.2 and 2.3, respectively, have been analyzed using a non-linear least-squares fit method. The equilibrium, desorption isotherms are expressed by Equation 2.1 which corresponds to the exponential or Freundlich isotherm in a logarithmic form,

$$\ln P = A + B\left(\frac{10^3}{T}\right) + \left[D + E\left(\frac{10^3}{T}\right)\right] \ln C \qquad (2.1)$$

where P is in pascals, C is in mmol Cs/kg graphite, and T is in degrees kelvin.

The estimated values of the sorption coefficients A, B, D and E were obtained by a non-linear least squares fit of the equilibrium data points selected from three separate experiments (Expertiments 5, 7 and 9) over the sample temperature range of 1076 K to 1367 K ± 10 K and the cesium vapor pressure range of 1×10^{-4} to 10 Pa. These estimated values and the statistical results of the least squares fit are tabulated in Table 2.4. The high correlation among the coefficients as shown on the correlation matrix indicates the excellent degree to which all of the desorption data, and at the higher vapor pressures ($\geq 10^{-1}$ Pa) the sorption data, fit the Freundlich isotherm model (Equation 2.1) well. All of the observed equilibrium points from these three experiments, along with the fitted expression, are displayed on Figures 2.1 (linear plot) and 2.2

(log-log plot). The closed (solid) symbols indicate the points obtained during desorption from a greater concentration. The dotted line on Figure 2.1 on the 1271 K isotherm indicates the hysteresis observed between sorption and desorption. The calculated desorption isotherms and their respective 95% confidence bands are shown on Figure 2.3.

The equilibrium isotherms obtained at each experimental mean temperature are displayed in Figures 2.4 through 2.7. The solid line on each indicates the fitted Freundlich relation (Equation 2.1) using the coefficient estimates of Table 2.4. The number, beside each experimental point, is the cardinal number of the sequence of points which were obtained in a given experiment. The equilibrium data points given in Tables 2.1, 2.2 and 2.3 are also tabulated in the sequence obtained. Included in the tabulations are the rates of change in the cesium concentrations observed during the 24-hour period (approximately) immediately prior to and including the times at which the equilibrium point counting rates were obtained and also the times ($t_{0.9}$) observed for the cesium concentration on the sample to change by 90% after each change in vapor pressure or sample temperature. That is,

$$C(t_{0.9}) = 0.9\ (C_o - C_{eq})/C_o \qquad (2.2)$$

where C_o and C_{eq} are the sample tube background corrected cesium concentrations (mmol Cs/kg graphite) obtained immediately prior to the change in temperature (or vapor pressure) and upon reaching the new equilibrium concentration, respectively. The "Final sample concentration" noted in the tables were determined on a separate NaI detection system of low background.

The most complete experimental isotherm is that which was obtained at

TABLE 2.1: EXPERIMENT 5: Cesium Sorption on H-451 Graphite at 1273 K.

Sample Temperature (± 10 K)	Source Temperature (± 2 K)	Cesium vapor pressure at sample (Pa)	Cesium concentration[a] (mmol Cs/kg graphite)	Rate at equilibrium (10^{-7} mmol kg-s)	Time to 90% change in concentration (hours)	Time at vapor pressure (hours)	Time at sample temperature (hours)
1273[e]	298	3.65 (-4)[b]	0.068	≤ 1.2	9.8	71.5	72
1272[e]	308	9.49 (-4)	0.418	≤ 1.2	14.9[c]	98.2	194
1273[e]	365	7.34 (-2)	2.758	11.3	178.5[c]	236.7	434
1273[e]	383	2.00 (-1)	4.914	6.5	148.5	236.4	675
1273	398	4.09 (-1)	6.164	9.2	130.0	163.4	841
1273	423	1.24	7.718	9.2	137.2[c]	192.5	1057
1273	448	3.72	9.276	≤ 1.2	67.1[c]	189.5	1249
1273	473	1.03 (1)	10.680	≤ 1.2	13.1[c]	92.7	1345
1273	398	4.09 (-1)	6.197	5.2	30.8	117.9	1465
1273	311	1.25 (-3)	2.446	7.0	143.5	240.8	1708
295[e]	295	1.30 (-4)	6.367	33.2[d]	204.8	228.7	229
Sample tube background			1.011				
Final sample concentration			6.287				

H-451 sample weight = 3.713 g before experiment

(a) In situ equilibrium concentrations corrected for sample tube background.

(b) Read as 3.65×10^{-4}.

(c) May not be characteristic of equilibrium approach due to abnormal temperature or detection system fluctuations early in the approach. However, conditions were stable at the equilibrium point.

(d) Cesium source not oxidized.

(e) Not included in the least squares fit to Equation 2.1.

TABLE 2.2: EXPERIMENT 7: Cesium Sorption on H-451 Graphite at 126 and 1177 K.

Sample Temperature (± 10 K)	Source Temperature (± 2 K)	Cesium vapor pressure at sample (Pa)	Cesium concentration (mmol Cs/kg graphite) [a]	Rate at equilibrium (10^{-7} mmol/kg-s)	Time to 90% change in concentration (Hours)	Time at vapor pressure (hours)	Time at sample temperature
1268[e]	273	2.42 (-5)[b]	0.084	< 1.2	(c)	97.3	97
1273[e]	335	9.30 (-3)	1.134	4.1	142.0	209.3	313
1273[e]	313	1.50 (-3)	0.823	1.4	91.1	142.8	460
1273[e]	295	2.70 (-4)	0.682	1.5	90.9	121.5	585
1273[e]	273	2.43 (-5)	0.523	< 1.2	280.8	336.8	934
1268[e]	335	9.42 (-3)	1.320	3.3	116.3	164.9	1104
1268[e]	273	2.42 (-5)	0.733	1.7	101.4	180.4	1305
1268[e]	298±5	3.64 (-4)	0.706	< 1.2	(c)	124.4	1490
1268	464	7.24	10.968	< 1.2	42.0[c]	195.9	1710
1268	424	1.31	7.798	3.4	24.6	94.0	1808
1266	403	5.21 (-1)	6.571	6.6	41.2	76.5	1905
1265	374	1.25 (-1)	4.758	5.0	102.5	188.3	2113
1264	357	4.44 (-2)	3.718	1.7	201.8	286.8	2408
1265	464	7.38	11.143	< 2.0	48.3[c]	160.4	2595
1179	438	2.42	11.864	< 2.0	(c)	92.8	92
1181	423.5	1.28	10.733	< 2.0	28.1	117.3	214
1178	403.5	5.29 (-1)	9.558	3.4	45.3	78.2	306
1173	373.5	1.18 (-1)	7.663	5.4	103.3	137.5	449
1173	357	4.30 (-2)	6.383	3.3	165.8	218.0	696
1275	423	1.28	7.586	< 1.2	5.3	102.3	102
295[e]	273	1.04 (-5)	23.425	< 1.2[d]	1.5	52.3	52
Sample tube background			0.455				
Final sample concentration			23.644				

H-451 Sample weight: before experiment = 3.7204 g
after experiment = 3.7668 g

(a) In situ equilibrium concentrations corrected for sample tube background contribution.
(b) Read as 2.42×10^{-5}.
(c) Not obtainable or may not be characteristic of equilibrium approach due to abnormal temperature or detection system fluctuations early in the run. However, conditions were stable at the equilibrium point.
(d) Cesium source not oxidized; cold spot developed at the metal-to-Pyrex seal region during cooldown.
(e) Not included in the least squares fit to Equation 2.1.

TABLE 2.3: EXPERIMENT 9: Cesium Sorption on H-451 Graphite at 1076, 1173, 1271 and 1367 K.

Sample Temperature (± 10 K)	Source Temperature (± 2 K)	Cesium vapor pressure at sample (Pa)	Cesium concentration (mmol Cs/kg graphite) [a]	Rate at equilibrium (10^{-7} mmol/kg-s)	Time to 90% change in concentration (hours)	Time at vapor pressure (hours)	Time at sample temperature (hours)
297 [e]	295	1.31 (-4) [b]	0.028	3.9	(c)	117.2	117
1073	437	2.32	14.034	29.5	180.0	294.0	294
1077	423	1.25	13.036	< 1.2	38.6	78.3	390
1076	403	5.12 (-1)	11.362	< 1.2	86.3	190.3	598
1078	373.5	1.15 (-1)	9.174	4.5	182.0	287.0	893
1078	353.5	3.28 (-2)	8.171	4.1	128.9	162.1	1080
1077	438	2.42	15.810	21.2	136.7	214.8	1301
1173	438	2.42	11.487	4.0	10.6	79.8	80
1173	403	5.17 (-1)	8.794	5.0	60.6	139.1	223
1175	353	3.30 (-2)	5.850	5.5	132.9	219.6	470
1173	438	2.42	11.576	5.7	69.3	170.0	682
1173	463	6.95	14.886	12.8	42.8	99.5	803
1367	463	6.95	8.063	3.9	1.8	64.4	64
1367	423	1.26	5.707	< 1.2	8.9	61.6	141
1366	403.5	5.37 (-1)	4.620	8.1	19.3	56.2	212
1366	373.5	1.24 (-1)	3.033	3.0	47.9	116.7	331
1368	353	3.47 (-2)	1.975	3.0	92.3	167.6	500
1368	310.5	1.24 (-3)	0.858	4.2	155.4	214.8	719
1076 [e]	308	8.74 (-4)	1.314	< 1.2	300.8	423.3	423
1271	447.5	3.65	9.544	6.5	33.0	173.0	173
1271	403.5	5.27 (-1)	6.648	33.2	47.8	139.7	315
1271	373.5	1.22 (-1)	4.789	5.9	87.8	167.5	484
1271	423	1.24	7.787	7.3	42.9	119.4	606
294 [e]	294	1.30 (-4)	8.687	(d)	(d)	20.2	(d)
Sample tube background			0.521				
Final sample concentration			9.723				

H-451 sample weight = 3.7044 g before experiment

(a) In situ equilibrium concentrations corrected for sample tube background concentration.
(b) Read as 1.31×10^{-4}.
(c) Not observed.
(d) Cesium source oxidized.
(e) Not included in the least squares fit to Equation 2.1.

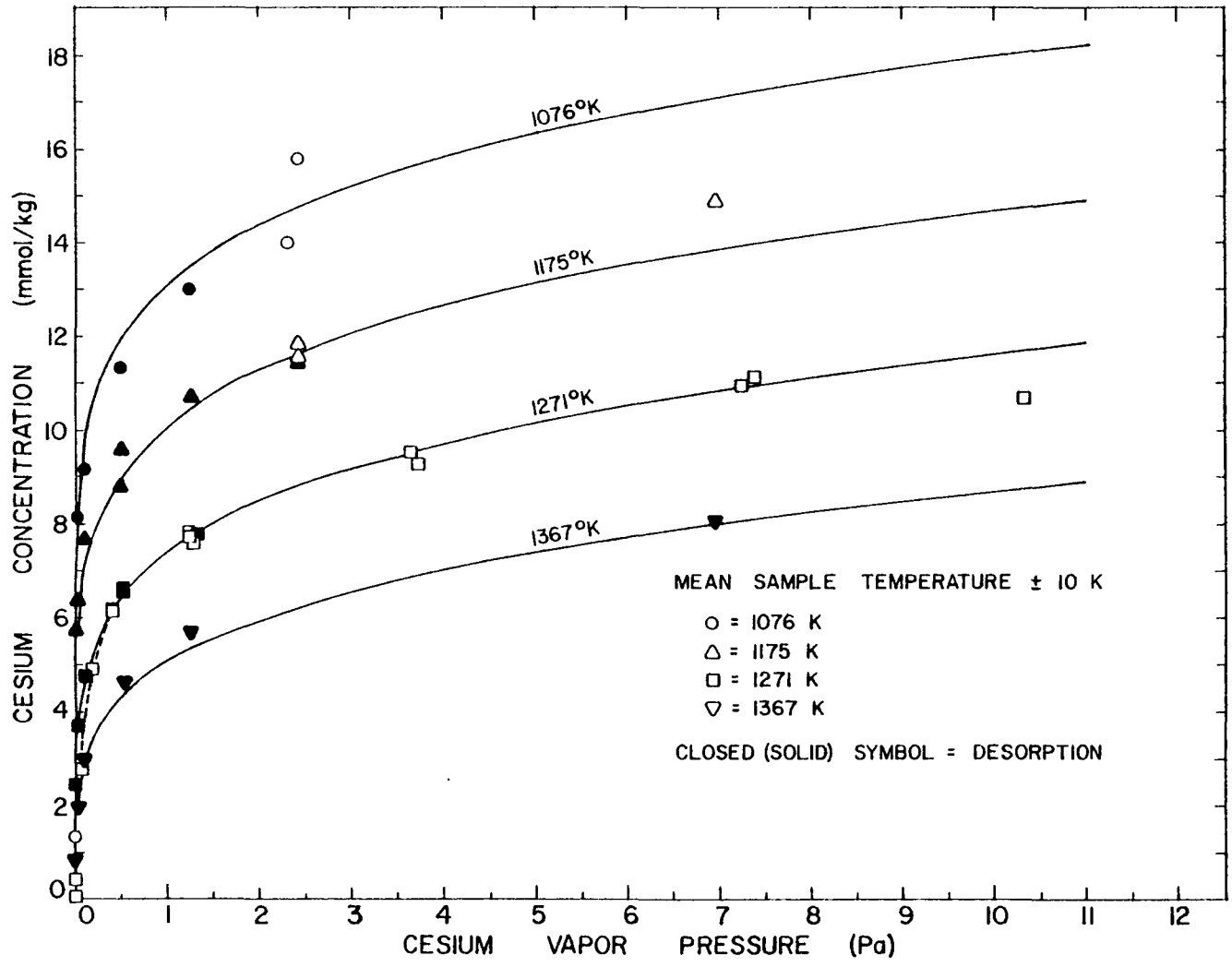

Figure 2.1. Freundlich Fit of Cesium Sorption on H-451 Graphite (Linear Plot)

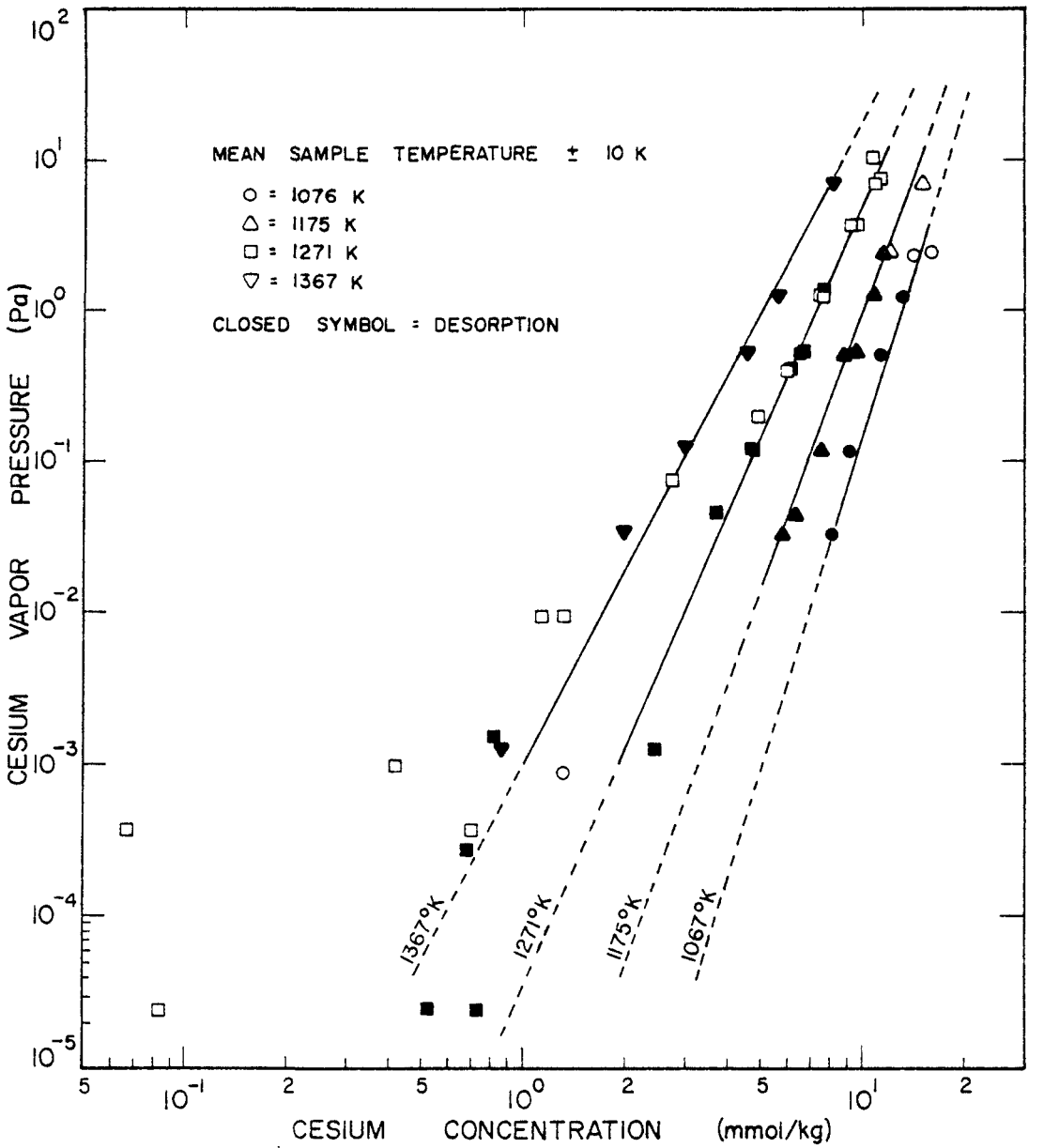

Figure 2.2. Freundlich Fit of Cesium Sorption on H-451 Graphite (Log-Log Plot)

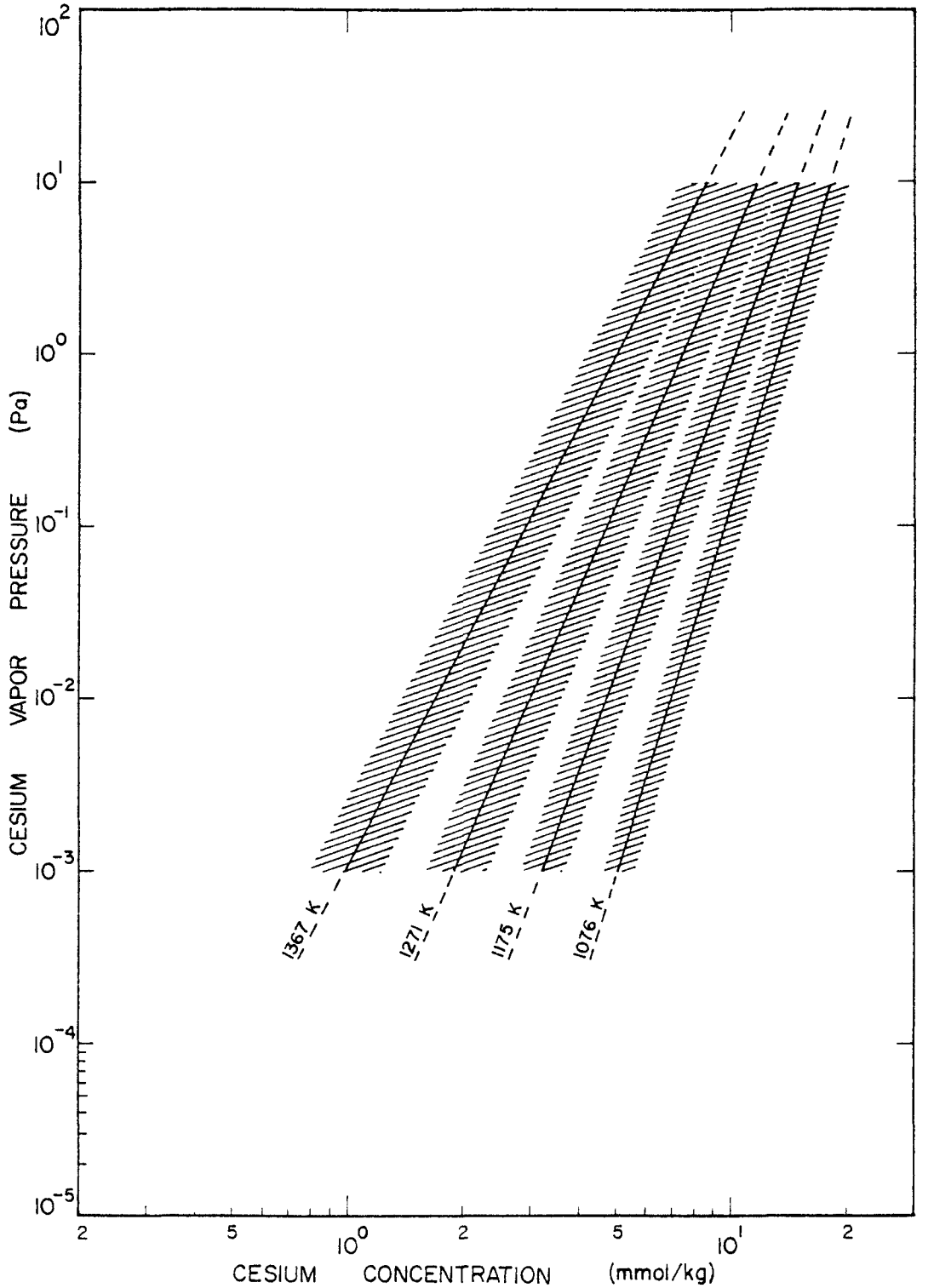

Figure 2.3. Freundlich Relation for Cesium Sorption on H-451 Graphite with 95% Confidence Bands

1271 ± 10 K (Figure 2.6). This is composed of data from three separate experiments and indicates the high degree of reproducibility at the higher vapor pressures among the samples studied. The desorption branch at this sample temperature, and also at the other sample temperatures, is described well by the Freundlich relation as demonstrated by the linearity in the figures. Above approximately 0.3 Pa the sequence of sorbing or desorbing the cesium and the cesium sorption history of the sample is largely immaterial, and the cesium sorption is reversible. As indicated in the tabulated data, the graphite sample of Experiment 5 (Table 2.1) was subjected to a monotonically increasing, then decreasing, cesium vapor pressure. The sample of Experiment 7 (Table 2.2) was initially subjected to cesium vapor at various pressures below 10^{-2} Pa with no significant effect on the subsequent equilibrium behavior at the higher vapor pressures (above 1×10^{-1} Pa) and upon desorption from the higher vapor pressures. Similarly, the equilibrium sorption behavior of Experiment 9 (Table 2.3) is in complete agreement after previous sorption and desorption at sample temperatures of 1076, 1175 and 1367 K. Additionally, no clear tendency towards either cesium saturation or multi-layer cesium sorption is apparent within the range of the maximum vapor pressures attainable (≤ 10.3 Pa) during these experiments.

2.2 Hysteresis and Other Anomalies - Experiments 5, 7 and 9

At the low cesium vapor pressures (≤ 0.2 Pa), a definite hysteresis (irreversibility) is evident between desorption and sorption (Figure 2.6). While the desorption branch is essentially linear on the log-log plot throughout the vapor pressure range studied, the sorption branch is highly non-linear and is dependent upon the amount of cesium previously sorbed on the graphite sample. This is illustrated by the sorption sequence

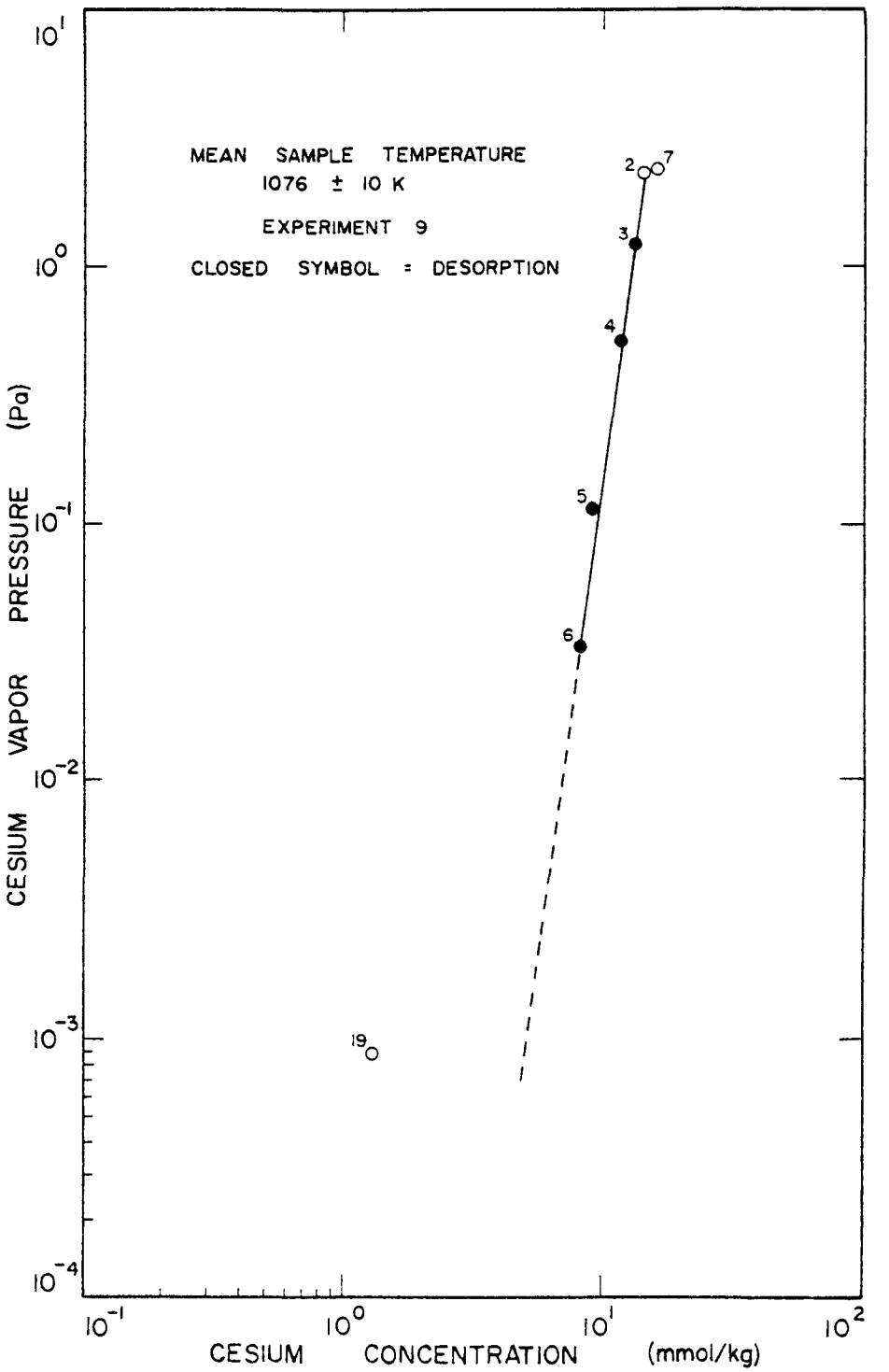

Figure 2.4. Cesium Sorption by H-451 Graphite at 1076 ± 10 K -Experiment 9

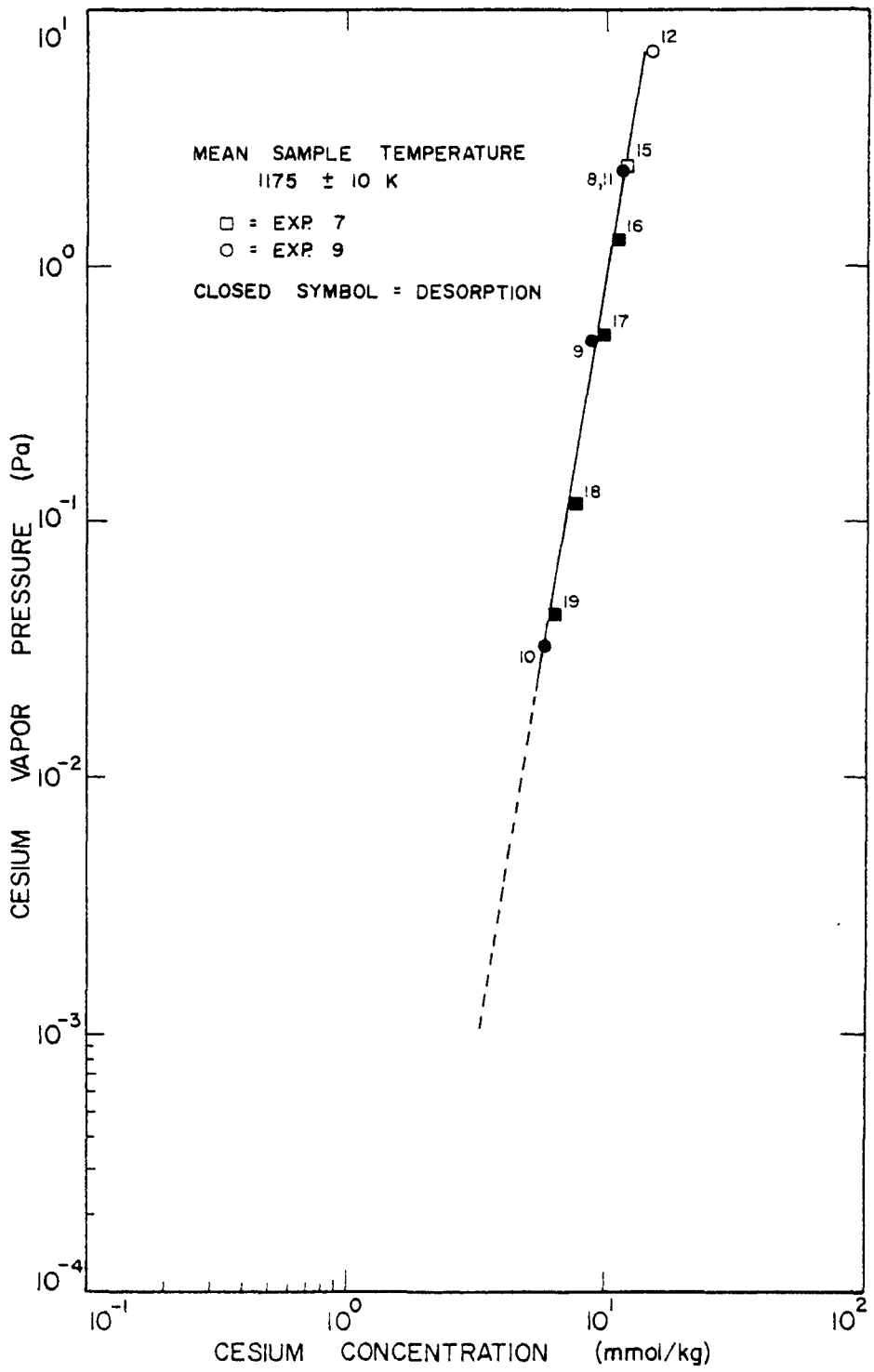

Figure 2.5. Cesium Sorption by H-451 Graphite at 1175 ± 10 K. --- Experiment 7, 9

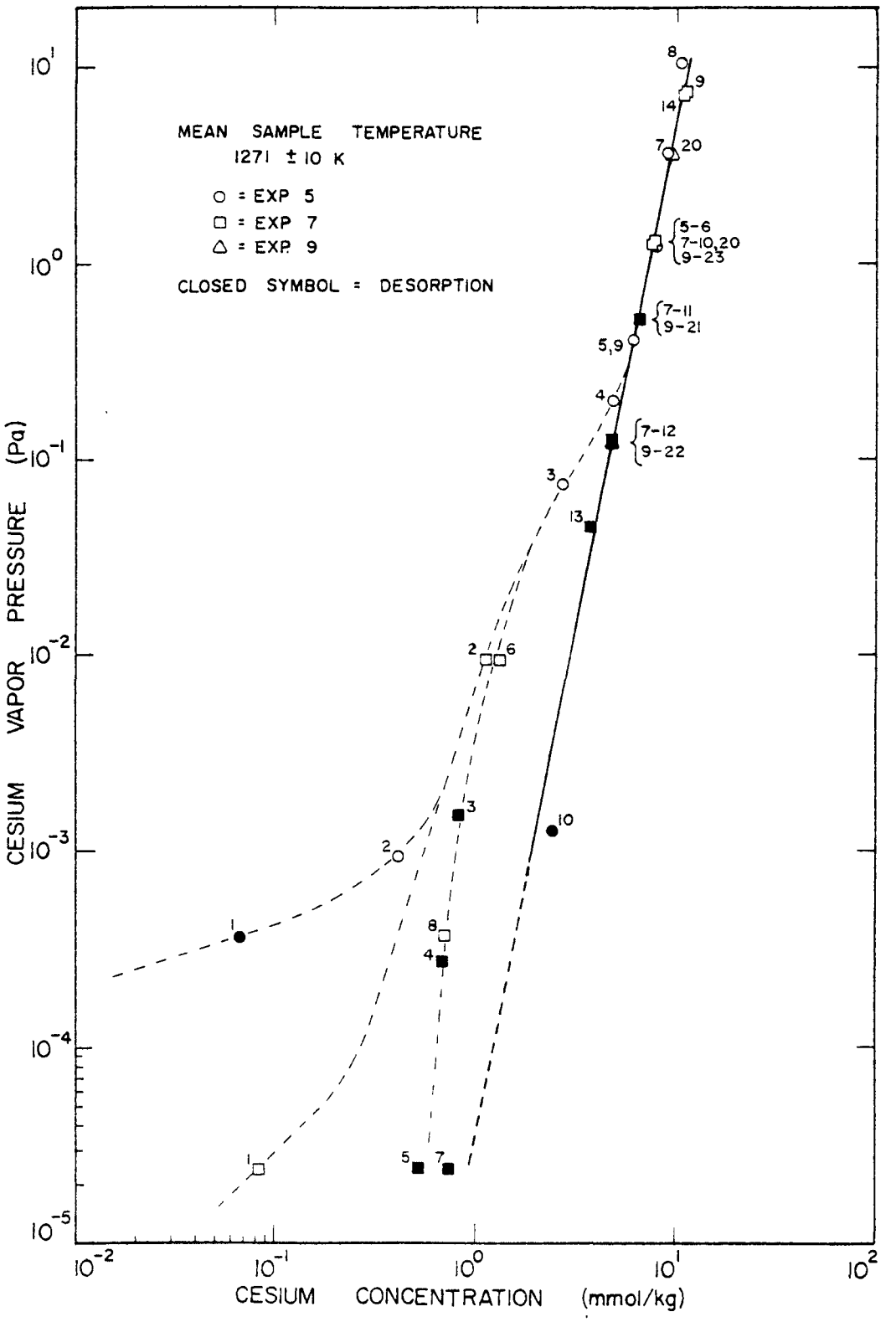

Figure 2.6. Cesium Sorption by H-451 Graphite at 1271 ± 10 K. ---Experiments 5, 7, 9

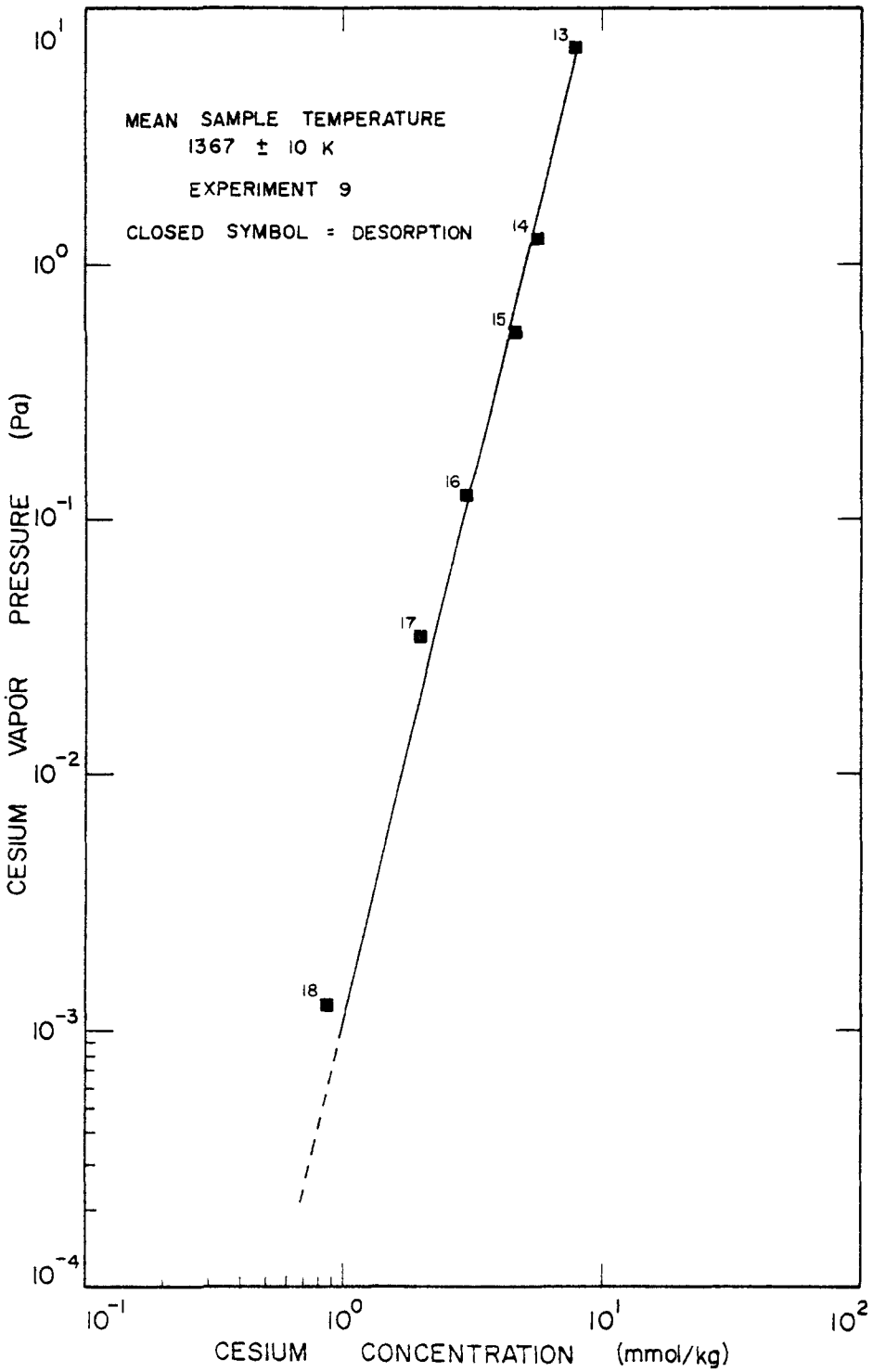

Figure 2.7. Cesium Sorption by H-451 Graphite at 1367 ± 10 K. ---Experiment 9

TABLE 2.4: Cesium Desorption Isotherm Coefficients for H-451 Graphite — Experiments 5, 7 and 9

Non-weighted, non-linear least squares fit of

$$C = \exp\{[\ln P - A - B \frac{10^3}{T}]/[D + E \frac{10^3}{T}]\}$$

where: P = cesium vapor pressure (pascals)

C = cesium equilibrium concentration (mmol Cs/kg graphite)

T = graphite sample temperature (K)

Coefficient	Estimated value ± σ[(a)]
A	36.774 ± 4.467
B	-59.722 ± 5.658
D	- 6.921 ± 1.848
E	15.282 ± 2.373
Mean square error (MSE) of fit:[(b)]	0.1836
Number of data points fitted:	39

Asymptotic correlation matrix:

	A	B	D	E
A	1.000	-0.997	-0.984	-0.990
B	-0.997	1.000	0.973	-0.986
D	-0.984	0.973	1.000	-0.996
E	0.990	-0.986	-0.996	1.000

(a) σ = standard (root-mean-square) deviation

(b) MSE = $(\frac{1}{n-k-1})\sum_{i=1}^{m}(y_i-\hat{y}_i)^2$, where n is the number of data points fitted (=39), k is the number of independent variables in the above relation (=23), y is the observed concentration, and $\hat{y}$ is the calculated concentration.

of Experiments 5, 7 and 9 at 1271 K (Figure 2.6) and by the single equilibrium point, Point 19, of the 1076 K isotherm (Figure 2.4). This latter point was obtained upon sorption at 1076 K in Experiment 9 after sequential desorption at 1367 K and confirms the presence of hysteresis at this lower sample temperature. Even though the first equilibrium point of Experiment 5 (Figure 2.6)--a desorption point--exhibits a rather low concentration (0.068 mmol Cs/kg graphite) for the given vapor pressure, the cesium that accumulated on this sample during the experimental preparation stages had an appreciably higher concentration (about 0.2 mmol Cs/kg graphite) which desorbed relatively rapidly, in a matter of a few hours, upon increasing the sample temperature to its experimental value of 1273 K. On the other hand, the first equilibrium point of Experiment 7 occurred after an insignificant change in concentration upon establishing the experimental conditions (sample at 1268 K and source at 273 K). Anomalous behavior of this nature at the start of each experiment (including those with the strontium-impregnated graphite samples) was not uncommon, and the amount of cesium deposited within the sample end of the sorption tube during the experimental preparation stages was variable. Although this initial pre-experimental concentration of cesium was either loosely bound to the graphite and/or to the protective sleeve or was low enough to be considered insignificant, a sample completely free of cesium could not be obtained at the start of each experiment, and the true sorption behavior at very low vapor pressures could not be resolved. Low vapor pressure conditions ($<1 \times 10^{-4}$ Pa) were not established at the other sample temperatures to further investigate low pressure hysteresis because of the difficulties involved in controlling low source temperatures and the length of time required to attain near-equilibrium concentrations.

The 1175 K isotherm of Figure 2.5 is composed of data from two experiments: Experiment 7 obtained after successive stages of sorption and desorption at 1269 K and Experiment 9 obtained after successive desorption followed by a final desorption point at 1175 K (Point 10). The reproducibility and linearity are good within the range of vapor pressures attained. However, a tendency towards an increasing cesium concentration which deviates considerably from the exponential, Freundlich relation at the higher vapor pressures ($\geq$ 7 Pa) is apparent (see Figure 2.1). At the maximum vapor pressure of Experiment 9 (Point 12 at 1173 K), the cesium sorption rate at the equilibrium point was significant (12.8×10^{-7} mmol/kg - s, Table 2.3). A similar tendency towards possible multi-layer sorption or interstitial compound formation as opposed to a sub-monolayer type surface sorption is also suggested on the 1076 K isotherm at a slightly lower pressure of 2.4 Pa (Point 7 of Figure 2.4, also see Figure 2.1). The cesium sorption rate at this point was also significantly larger than normal (21.2 mmol/kg - s). Both of these points were obtained while the sample was still sorbing at a rate of 29.5 mmol Cs/kg - s, indicating that satisfactory equilibrium had not yet been attained after more than 290 hours of exposure to cesium vapor at the indicated pressure. Similar deviations from the 1271 and 1367 K exponential isotherms were not observed. Vapor pressures above 5 Pa (corresponding to a cesium source temperature of $\geq$ 455 K) were difficult to achieve due to the formation of cold spots in the intermediate region of the sorption apparatus and the temperature limitations placed upon the Pyrex-to-metal seal area of the apparatus. Consequently, it was not possible to investigate the sorption behavior in the higher vapor pressure region above about 5 Pa, where one might find deviations (points below the exponential isotherm) due to multilayer sorption or interstitial compound formation (5).

The 1367 K desorption isotherm data of Figure 2.7, obtained in Experiment 9 after obtaining the 1076 and 1175 K isotherm data, exhibits slightly more curvature than that at the other sample temperatures relative to the calculated isotherm. A least squares fit of the equilibrium data obtained at 1076 K, 1175 K and 1217 K, neglecting the 1367 K data, produced coefficient estimates of Equation 2.1 that were in good agreement with the coefficient estimates of Table 2.4, indicating a good agreement with the Freundlich family of isotherms. The Freundlich relation using the values of Table 2.4 is represented by the straight line on Figure 2.7 which fits 1367 K data quite well.

2.3 Experiments 15, 30 and 36

Two additional experiments, Experiments 15 and 30, were conducted in an attempt to verify 1367 K behavior. However, in Experiment 15 the sample geometry, and in Experiment 30 the procedures used in preparing the sample prior to the distillation of the cesium metal source, were different from those used in Experiments 5, 7 and 9. The cylindrical graphite sample of Experiment 15 was radially finned as described previously (1) and rinsed lightly with acetone to remove loose graphite powder remaining after the machining process. The solid cylindrical sample of Experiment 30 was prepared to check for any changes in the cesium sorption behavior that may possibly have resulted from the impregnation of the sample with 0.6 cm^3 of an acetone (60%) - water (40%) solution and the related vacuum outgassing and King furnace annealing procedures used in the strontium-impregnated graphite studies discussed in Section 5.

The results of Experiment 15 and 30 studies of cesium sorption at 1369 ± 10 K are displayed on Figure 2.8 and tabulated in Tables 2.5 and 2.6. The heavy straight line on Figure 2.8 represents Equation 2.1 at

1369 K using the coefficient values of Table 2.4. The cesium desorption behavior of these experiments exhibits a lower slope, a substantial displacement towards a lower concentration (less sorption) and a greater non-linearity in comparison to the 1367 K desorption isotherm of Experiment 9 Figure 2.7). However, the low pressure hysteresis apparent in Experiment 15 below about $6x10^{-2}$ Pa is in qualitative agreement with that of the 1076 and 1271 K isotherms of Figures 2.4 and 2.6, respectively. The sample of Experiment 30 (Figure 2.8) at 1369 K, exhibits hysteresis below about $2x10^{-2}$ Pa occurring after desorption (Point 6) from the previous isotherm, followed by sorption (Points 7, 8, etc.) and final desorption (Points 16 and 17). In this case, the sorption leg is at a higher concentration than the desorption leg indicating the degree of difficulty in releasing the sorbed cesium at the lower vapor pressures even at the higher sample temperature.

An additional deviation from Freundlich sorption behavior, observed in both experiments, occurs at the higher vapor pressures above 2 Pa. The two points obtained appear to be approaching a constant concentration (saturation) of about 6 mmol Cs/kg graphite as the vapor pressure is increased. This is in contrast to the tendency of the sorbed cesium concentration to increase (i.e. fall below the Freundlich isotherm line) towards possible multi-layer sorption or interstitial compound formation as observed previously on the 1076 and 1175 K isotherms.

Experiment 36 was carried out as a reference study in the series of studies on the effect of barium impregnation on the sorption of cesium by H-451 graphite. Experiment 36 was run with no barium impregnation but with other features of the experiment the same as those of Experiments 31, 32, 33 and 35 all of which were done with barium impregnated samples. Thus

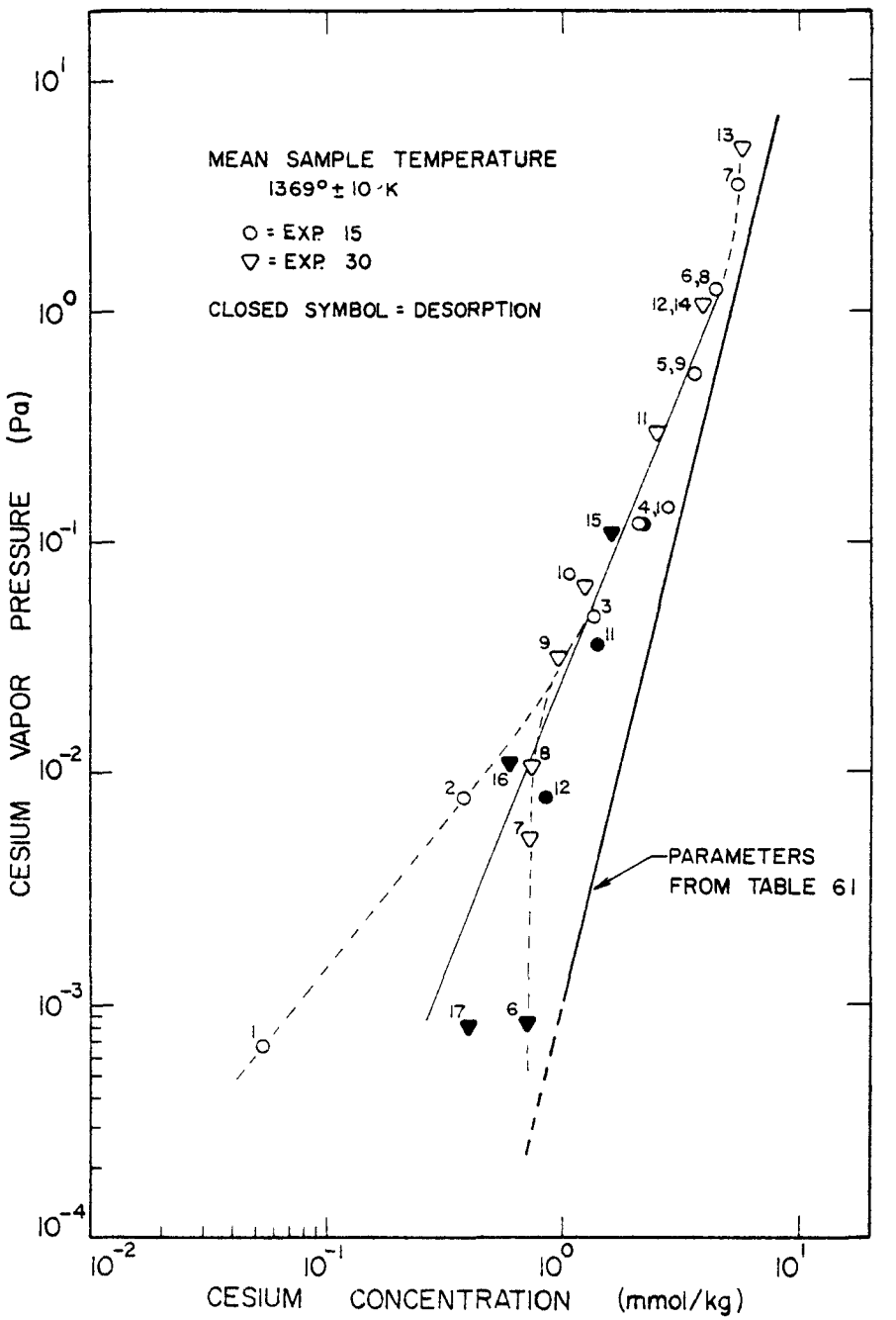

Figure 2.8. Cesium Sorption on H-451 Graphite at 1369 ± 10 K --- Experiments 15 and 30.

TABLE 2.5: EXPERIMENT 15: Cesium Sorption on H-451 Graphite (Finned Sample) at 1366 K

Run Sequence Number	Sample Temperature (± 10 K)	Cesium vapor pressure at sample (Pa)	Cesium concentration (a) (mmol Cs/kg graphite)	Rate at equilibrium (10^{-7} mmol kg-s)	Time to 90% change in concentration (hours)	Time at vapor pressure (hours)	Time at sample temperature (hours)
R01	1367	304	6.77 (-4)(b)	0.054	< 1.2	41.7	42
R02	1368	332.5	7.93 (-3)	0.384	2.8	71.4	117
R03	1365	358	4.82 (-2)	1.357	3.6	183.8	303
R04	1365	373	1.21 (-1)	2.166	3.1	154.9	476
R05	1365	403.5	5.37 (-1)	3.704	2.5	170.4	663
R06	1365	423	1.26	4.526	3.7	81.0	768
R07	1365	447.5	3.66	5.596	3.0	100.6	884
R08	1365	423.5	1.27	4.459	< 1.2	61.8	948
R09	1367	403.5	5.31 (-1)	3.624	< 1.2	108.7	1079
R10	1368	373	1.21 (-1)	2.218	8.7	131.7	1212
R11	1366	353.5	3.64 (-2)	1.411	< 1.2	230.3	1455
R12	1364	332.5	7.82 (-3)	0.840	3.2	317.4	1776
R13	1273	332.5	7.66 (-3)	1.254	< 1.2	308.2	308
	1272	424	1.31	6.035 (d)	(d)	193.1	525
EOR	296	275.5	1.37 (-4)	5.168	(e)	14.9	(e)
	Sample tube background			0.353			
	Final sample concentration			4.912			

H-451 sample weight: Before experiment = 3.118 g After experiment - 3.120 g

(a) In situ equilibrium concentrations corrected for sample tube background contribution.
(b) Read as 6.77×10^{-4}.
(c) Not obtained due to temperature fluctuation early in the approach to equilibrium.
(d) Final equilibrium not attained due to furnace failure.
(e) Cesium source oxidized as discussed in Section 4.2.3.

TABLE 2.6. EXPERIMENT 30: Cesium Sorption on H-451 Graphite (Impregnation Blank) at 1273 K and 1373 K

Run Sequence Number	Sample Temperature (± 10 K)	Source Temperature (± 2 K)	Cesium Vapor Pressure at Sample (Pa)	Cesium Concentration(a) ($\frac{\text{nmol Cs}}{\text{kg graphite}}$)	Rate at Equilibrium ($\frac{10^{-7}\ \text{nmol}}{\text{kg-s}}$)	Time to 90% Change in Concentration (hours)	Time at Vapor Pressure (hours)	Time at Sample Temperature (hours)
R01	1274	306.5	8.08(-4)(b)	0.404	< 1.2	(c)	87.6	88
R02	1275	332.5	7.55(-3)	0.766	3.5	114.2	140.9	232
R03	1272	371.5	1.07(-1)	2.885	2.8	238.6	358.6	592
R04	1272	419	1.04	5.914	≤ 1.2	253.0	475.3	1070
R05	1273	455	5.00	8.057	≤ 2.0	193.2(c)	263.2	1337
R06	1373	306	8.24(-4)	0.703	2.4	179.8(c)	450.8	451
R07	1372	327	5.13(-3)	0.721	≤ 1.2	18.3	138.4	591
R08	1372	336.5	1.06(-2)	0.736	≤ 2.0	16.7	73.1	665
R09	1374	351.5	3.12(-2)	0.946	1.2	83.5	109.1	775
R10	1373	362	6.34(-2)	1.228	1.9	65.1	125.6	902
R11	1374	390.5	3.00(-1)	2.431	2.2	110.7	189.8	1094
R12	1371	420	1.09	3.784	≤ 1.2	40.7	194.2	1290
R13	1374	455.5	5.12	5.695	≤ 1.2	9.2	95.4	1386
R14	1372	419	1.06	3.855	< 1.2	21.1	116.9	1504
R15	1374	371	1.08(-1)	1.608	< 1.2	71.7	190.7	1695
R16	1374	336.5	1.07(-2)	0.588	2.7	150.8	244.0	1943
R17	1373	306	8.02(-4)	0.390	1.9	187.7	204.8	2148
EOR	297	297	1.60(-4)	0.299	(d)	(d)	14.0	(d)
Sample Tube Background				0.272				
Sample Return in Situ				0.316				
Final Sample Concentration				0.299				

H-451 Sample Weight = 3.718 g Before Experiment

(a) In situ equilibrium concentration corrected for sample tube background contribution
(b) Read as 8.08×10^{-4}
(c) Not characteristic of the equilibrium approach
(d) End of run in situ (sample and tube)-cesium source oxidized
(e) Sample returned to in situ arrangement inside a clean sample tube

the graphite sample was a solid cylinder of standard size, 7.938 mm (5/16") dia. by 4.445 mm (1-3/4") length, and was treated with an acetone-water solution as described below in the discussion of cesium-barium mixed sorption, Experiments 31, 32, 33 and 35 (Section 5.1). The results of Experiment 36 are given in Table 2.7 and shown in Figure 2.9. (w. Expt. 15,30)

2.4 Comparison of Data of Experiments 15, 30 and 36 at 1273 K

The additional equilibrium points of Experiments 15 and 30 obtained at 1273 K similarly exhibit a lower sorbed cesium concentration relative to the previously obtained 1271 K isotherm. In regards to the reason for this, it is unlikely that the acetone solution would have such a dramatic effect since the samples were outgassed for at least 12 hours at 1391 K prior to exposing them to the cesium vapors. The only other plausible explanation is that the graphite samples were inadvertently cut from the region of the sample block corresponding to the mid-length edge of the parent log rather than the mid-length center. Consequently, it is considered likely that these results reflect the inhomogeneity of the graphite properties. The results of Experiments 15 and 30 at 1273 K appear to agree more closely with the results of Experiment 36 and are reviewed next. The equilibrium sorption and desorption points obtained at 1273 ± 10 K in Experiment 15, 30 and 36 are shown in Figure 2.9. All three experiments are seen to contribute to the sorption portion of the isotherm curve which are found to display a hysteresis behavior relative to the desorption curve. The desorption points were entirely contributed by Experiment 36. As shown on Figure 2.8 Experiments 15 and 30 were run in the desorption mode at 1367 ± 10 K.

Experiments 15, 30 and 36 appear to provide a consistent set of isotherms which at 1367 and 1273 K have, at a given Cs vapor pressure, a

TABLE 2.7

EXPERIMENT 36: Cesium Soprtion on H-451 Graphite (Impregnation Blank) at 1272 K.

Run Sequence Number	Sample Temperature (± 10 K)	Source Temperature (± 2 K)	Cesium Vapor Pressure At Sample (Pa)	Cesium Concentration(a) ($\frac{\text{mol Cs}}{\text{kg graphite}}$)	Rate at Equilibrium ($\frac{10^{-7}\ \text{mol}}{\text{kg-s}}$)	Time to 90% Change in Concentration (hours)	Time at Vapor Pressure (hours)	Time at Sample Temperature (hours)
R01	1273	298	3.65(-4)(b)	0.565	1.9	(c)	115.1	115
R02	1273	328	5.31(-3)	0.737	1.6	73	94.8	210
R03	1273	336	1.01(-2)	0.890	1.3	92	124.7	335
R04	1273	350	2.81(-2)	1.422	1.2	318	430.6	765
R05	1272	361	5.68(-2)	1.815	< 1.2	132	211.3	977
R06	1274	370.5	1.01(-1)	2.377	1.5	142	218.6	1194
R07	1273	390	2.84(-1)	3.621	3.6	248	359.9	1555
R08	1273	405.5	5.75(-1)	4.559	< 1.2	246	337.0	1892
R09	1272	418.5	1.03	5.316	< 1.2	73	166.2	2058
R10	1272	442.5	2.94	6.757	< 1.2	58	193.2	2251
R11	1272	452	4.40	7.385	< 1.2	43	123.2	2371
R12	1272	419	1.06	5.521	< 1.2	39	236.7	2611
R13	1272	370.5	1.02(-1)	3.171	< 1.2	192	504.4	3116
R14	1272	337	1.05(-2)	2.009	< 1.2	256	485.2	3601
R15	1273	298.5	3.86(-4)	1.302	< 1.2	251	484.0	4085
EOR	383	298	2.00(-4)	1.314	(d)	(d)	3.7	(d)
Sample Tube Background				0.024				
Sample Returned in situ(e)				1.279				

H-451 Sample Weight: Before Experiment = 3.747 g

(a) In situ equilibrium concentration corrected for sample tube background contribution.
(b) Read as 3.65×10^{-4}
(c) Not characteristic of the equilibrium approach.
(d) End of run in situ (sample and tube)-cesium source oxidized.
(e) Sample returned to in situ arrangement inside a clean sample tube.

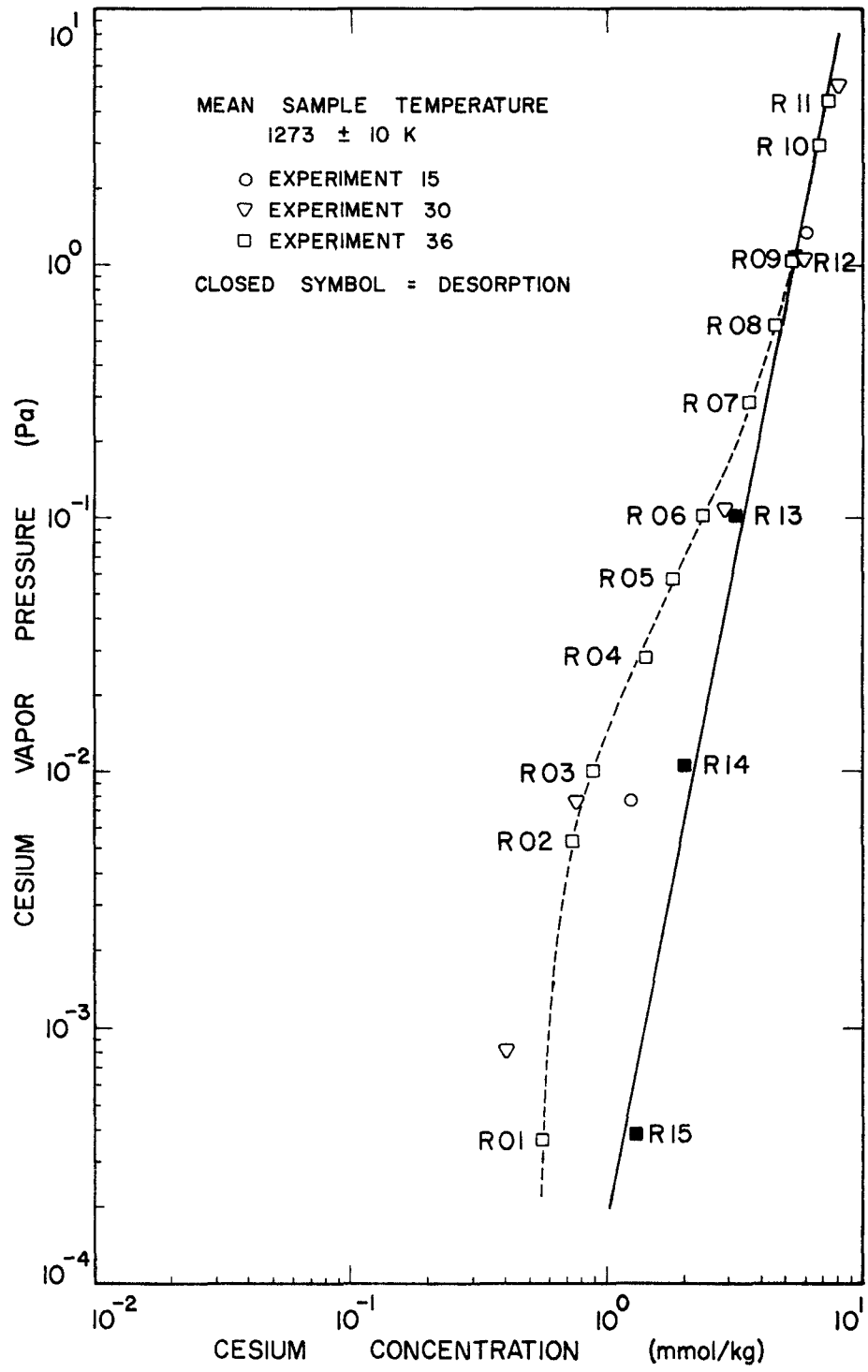

Figure 2.9. Cesium Sorption on H-451 Graphite at 1273 K by the Pseudoisopiestic Method -- Experiments 15, 30, 36. (Experiment 36 data points are given with run numbers).

lower equilibrium concentrations than do the isotherms of Experiments 5, 7 and 9. In Figure 2.9 we compare the desorption isotherm of the latter set of experiments with the desorption isotherm of Experiment 36 which has equilibrium concentrations equal to about three-fourths those of Experiment 5, 7 and 9. As mentioned above, we are inclined to attribute this difference to an inhomogeneity of the different sets of graphite samples.

2.5 The Exponential or Freundlich Isotherm—Derivation of the Modified-Exponential Isotherm

The Freundlich isotherm for single component sorption is given by,

$$P = k_F C^u \tag{2.3}$$

where k_F and u are coefficients that, in general, are a function of temperature and which is given in a particular logarithmic form by Equation 2.1. This sorption isotherm was independently treated theoretically by Zeldowich (8), Cremer and Flugge (9), and was also treated by Halsey and Taylor (10). The treatments assumed monolayer adsorption on a composite surface, where neighboring sites do not affect each other. Furthermore, it was assumed the probability, $\theta(\chi)$, for sites characterized by sorbate-sorbent interaction energy χ, to be occupied by the sorbate species is given by the Langmuir equation,

$$\theta(\chi) = \frac{f(\chi)\, P}{1 + f(\chi)P} \tag{2.4}$$

with $f(\chi)$ = a coefficient which is a function of energy χ and temperature.

The treatments also assumed the number distribution of the sites to decrease exponentially with interaction energy, χ, and the range of χ to extend to infinity. The infinite limit for χ was unrealistic but its use

facilitated analytical integration which gave an exponential isotherm as a result.

Gluekauf (11) extended the treatment to binary systems of sorbates on non-uniform surfaces where adsorption energies ranged from 0 to ∞, but he also investigated how the theoretical isotherm is affected if the energies realistically range from 0 to a finite upper limit χ_L. He found for $\chi_L >> RT$ the isotherm was of the exponential (Freundlich) type over fairly large range of surface coverages (sorbate concentrations) but at sufficiently low coverages the isotherm was of the "Langmuir" (i.e. linear or Henrian) type.

We believe that due to the complex nature of graphite and the very strong interaction of cesium with graphite* that the sorption of cesium by graphite involves sites on relatively inaccessible interval regions (i.e. intergranular or intercrystalline areas) as well as sites on pore surfaces which comprise the surface area determined by nitrogen or krypton adsorption (i.e. the BET surface area). Notwithstanding the fact that a simple monolayer, surface adsorption is not the entire mechanism, the variety of sorption sites for cesium (Cs) and similar highly electropositive metals (i.e. Rb, Sr, Ba) may have a number distribution which decreases approximately exponentially with site interaction energy, χ, and certainly would have an upper limit, χ_L. The distribution function

*We note that Holian (12) has theoretically calculated the interaction energy for cesium atoms with an ideal graphite surface to be about 500 kJ/mol and with an ideal graphite with six or more carbon atoms missing to form a hole in the surface, to be a little more than 800 kJ/mol. In a study of the desorption of cesium from matrix A-3 (natural) graphite by the temperature programmed desorption (TPD) technique, Hoinkis and Stritzke (13) found that cesium at very low surface concentration ($\approx 10^{-13}$ monolayers) had a desorption energy spectrum between 1.7 to 4.3 eV which peaked at 3.9 eV or 376 kJ/mol. Internally absorbed cesium atoms would be expected to have still higher interaction energies with graphite. Also, this experimental number is noted to be in good agreement with Holian's theoretical estimates considering the various approximations which had to be made.

then is,

$$n(\chi) = \frac{\exp(- \chi/\chi_M)}{\chi_M \left[1 - \exp(- \chi_L/\chi_M)\right]} \tag{2.5}$$

where

χ_M = the characteristic (mean) energy of sorption.

The fraction of available sites occupied is,

$$\theta_T = \frac{C}{C_m} \tag{2.6}$$

where

C = the sorbate concentration (mmol cesium/kg graphite)

C_m = the sorbate concentration when all available sites are occupied (excluding multilayer sorption or lamellar compound formation)

$f(\chi)$ in Equation 2.4 is given by,

$$f(\chi) = \exp\left[- \Delta S_o/R + H_o/RT + (1 - rT)\ \chi/RT\right], (Pa^{-1}) \tag{2.7}$$

where

ΔS_o = entropy of vaporization when $\chi = 0$ (joule/mol K)

ΔH_o = heat of vaporization when $\chi = 0$ (joule/mol)

r = term for change of entropy with χ (K^{-1})

R = gas constant (joule/mol K)

T = absolute temperature (K)

Let us define the reference state of pressure as,

$$P_o = \exp\left[\Delta S_o/R - \Delta H_o/RT\right], (Pa) \tag{2.8}$$

Then substituting Eq. 2.7 into Eq. 2.6 and the result into Eq. 2.3, we obtain,

$$\theta(\chi) = \frac{(P/P_o)\ \exp\ (1 - rT)\ \chi/RT}{1 + (P/P_o)\ \exp\ (1 - rT)\chi/RT} \tag{2.9}$$

The fraction of available sites (Eq. 2.6) may then be calculated using the postulated distribution of sites and the assumption of independent Langmuir isotherm behavior of sites of a given χ, thus

$$\theta_T = \frac{C}{C_m} = \int_o^{\chi_L} n(\chi)\ \ \theta(\chi)\ d\chi \tag{2.10}$$

We change variables such that,

$$\begin{aligned} \nu &= \chi/\chi_M \\ \nu_L &= \chi_L/\chi_M \end{aligned} \tag{2.11}$$

and let

$$u = (1 - rT)\ \chi_M/RT$$

and substituting Eq. 2.5 and Eq. 2.9 into Eq. 2.10 we obtain theoretical expression which we term the <u>modified-exponential</u> isotherm,

$$C(P) = C_m \frac{(P/P_o)}{1 - \exp(-\nu_L)} \int_o^{\nu_L} \frac{\exp(u - 1)\ \nu}{1 + (P/P_o)\ \exp(u\nu)}\ d\nu \tag{2.12}$$

This isotherm equation has no evident closed analytical form but it may be easily evaluated by a modern computer. It has the property at low C and very low P ($P < P_o \exp(-u\nu)$) of being linear, thus $P = k_H C$ (2.13) with

$$k_H = \frac{P_o(u-1)\ [1 - \exp(-\nu_L)]}{C_m\{\exp[(u-1)\nu_L] - 1\}} \tag{2.14}$$

In this region the modified-exponential isotherm (Eq. 2.12) may be said to be Henrian (i.e. follows Henry's Law); however, Gluekauf (11) terms this the Langmuir region.

At higher pressure but with P appreciably less than P_o the theoretical isotherm becomes an exponential isotherm of the Freundlich type,

thus $P = k_F C^u$ (2.15)

where

$$k_F = \frac{\sin(\pi/u)}{(\pi/u)} \frac{P_o}{(C_m)^u} \tag{2.16}$$

Since Equation 2.16 corresponds to Equation 2.1 we can utilize the empirical Freundlich coefficients A, B, D and E along with preselected or estimated values of C_m and C_L (which is related to ν_L, see below)

$$\ln k_F = A + B\ (10^3/T) \tag{2.17}$$

$$u = D + E\ (10^3/T) \tag{2.18}$$

$$\chi_M = 10^3\ R\ E \tag{2.19}$$

$$r = 10^{-3}(D/E)$$

$$\ln P_o = \ln k_F + u\left[\ln C_m + \ln \frac{(\pi/u)}{\sin(\pi/u)}\right] \tag{2.20}$$

The upper limit of Equation 2.11 is given by

$$\nu_L = \frac{1}{u-1} \ln\left\{(u-1)\left[\frac{(\pi/u)}{\sin(\pi/u)}\right]^u \left(\frac{C_m}{C_L}\right)^{u-1}\left[1-\exp(-\nu)\right] + 1\right\} \tag{2.21}$$

ν_L must be obtained by iteration but as first approximation it may be estimated by the equation $\exp(-\nu_L) = C_L/C_m$ (2.22)

Plots of modified-exponential isotherm in the case of Experiment 41 are shown and discussed in the next section.

3. COMPARISON OF THE CESIUM SORPTION AND DESORPTION BEHAVIOR OF BULK VERSUS PARTICULATE GRAPHITE

A review of the differences in the sorptivity and kinetics inherent in the use of bulk graphite in the pseudo-isopiestic method versus the use of particulate (ground) graphite in the Knudsen cell method of determining the sorption of volatile metals, led us to undertake a comparison of the cesium sorption and desorption behavior of these two kinds of graphite samples as described below:

3.1 Discussion of the Knudsen Cell and Pseudo-Isopiestic Methods

The principal method used for obtaining data on the sorption of cesium, at relatively low concentrations ($\lesssim$10 mmol Cs/kg C), besides the pseudo-isopiestic method--which has been used exclusively in this research--is the Knudsen cell method. Most of the basic data obtained at General Atomic for ultimate use in computer codes for design calculations of the release of cesium from HTGR fuel elements into the primary coolant circuit, has been by the Knudsen method. The results of such work carried out extensively at San Diego (G.A. Co.), California and at Harwell (A.E.R.E.) United Kingdom (11a), have recently been reviewed and summarized by Myers and Bell (6) and compared to the results of other methods. Besides the pseudo-isopiestic method these include the relative sorptivity method used at General Atomic (6) and the cascade method used in France (6).

Despite the extensive use and convenience of the Knudsen cell method for cesium-graphite sorption studies,the authors of this paper are concerned that the time periods of this method are too short to obtain true equilibrium data. This is believed to be likely even though in the Knudsen cell method ground graphite (size range 44 to 74 μm) is used so that the attainment of equilibrium between cesium will be accelerated.

Knudsen cell runs involving several equilibrium points taken over an eight hour period. Additional points may be taken in following days.

Experiment has shown the sorption of cesium by the powdered graphite to be greater than that of the same graphite in the bulk form (i.e. of particle size range 1.65 - 3.33 mm (6) or greater. A correction factor of 2.2 was determined at General Atomic by the relative sorptivity method (6). This is used to reduce the concentration data for given cesium vapor pressures obtained in sorption studies of the powdered graphite to corresponding concentration data expected for bulk graphite.

It is to be noted that in Knudsen cell method, as evolved at General Atomic, "a sample of powdered graphite (44 - 74 μm) is impregnated with cesium normally by evaporating a mixture of the graphite and cesium nitrate to dryness. The impregnated sample is loaded into a tantalum Knudsen cell which is placed in a mass spectrometer and brought to the temperature of the experiment. As the temperature rises, the cesium nitrate is converted to sorbed cesium metal with the evolution of NO and CO. During the experiment the effusion of the cesium vapor, which is taken as a negligible perturbation to the equilibrium of cesium between in the vapor and solid phases, is monitored with a mass spectrometer as a function of time and temperature. The total quantity and the vapor pressure of the cesium in the cell are determined with the aid of, 1) the time profile of this effusing mass, and 2) knowledge of the initial and final quantities of the sorbate" (6). In carrying out the Knudsen cell-mass-spectrometric experiment cesium ion current measurements are made at several cell temperatures at the highest concentration of the sample in the Knudsen cell. Next, the concentration of cesium in the sample is lowered allowing effusion to occur at a high rate for some time, then vapor pressures (via Cs^+ current measurement) are taken at several sample temperatures in succession with

little change. Following this the cesium concentration in the sample is again lowered by allowing effusion to continue from the cell before more ion current data points are taken--again at several cell temperatures.

We see from this technique that the data is taken solely in a desorption mode. Furthermore, the initial concentration was not obtained by a long-term exposure to cesium vapor but by a fairly rapid chemical reaction of cesium nitrate ($CsNO_3$) with the graphite of the sample followed by a relatively short-term exposure of the reduced cesium with the graphite powder sample.

In view of this, two questions arise: (1) Is the cesium initially in true equilibrium with the graphite? and, (2) Does the cesium approach equilibrium with the graphite as the desorption proceeds? Another question arises specifically in the case of H-451 graphite powder versus H-451 bulk graphite: Does the factor of 2.2 determined using H-327 graphite at 1200^{o} C as the equilibrium concentration distribution ratio apply to H-451 graphite,in particular, at lower temperatures (i.e. 1000^{o} C)? In addition, the question arises: How does the kinetics of sorption by bulk graphite compare with that of the powder?

3.2 A Pseudo-Isopiestic Study of Cesium Sorption by Particulate Graphite (H-451)—Experimental Runs by Kevin M. Vaughan

After discussion it was agreed by interested researchers of General Atomic Company and North Carolina State University that it would be highly desirable to do a pseudo-isopiestic study of particulate graphite (H-451) of the same kind used in Knudsen cell studies at General Atomic. Accordingly, B. F. Myers and W. E. Bell of General Atomic, arranged for the provision of H-451 powder (size range 44 to 74 μm) to be placed in a molybdenum container and run in our pseudo-isopiestic sorption apparatus (the

apparatus was similar to those used in previous work (1, 2) and as described by Haire and Zumwalt (5), in a manner similar to runs on bulk H-451 graphite samples).

Molybdenum containers (cans) were fabricated so that the inside walls had the approximate size and shape to simulate a bulk graphite sample. The actual dimensions of the molybdenum can were 12.77 mm outer diamter, 50.8 mm long with approximately 0.51 mm wall thickness. One end of the can had nine approximately 0.5 mm diameter holes with a total surface area of about two square millimeters. The cans were loaded with a weighed quantity (about 4 grams) of the graphite powder, and placed in the sorption apparatus at the position that would have been occupied by a bulk graphite sample (dimension 7.94 mm diameter, 44.5 mm length). Preparation of the ^{137}Cs - tagged cesium source and standards, the tantalum liner in the Inconel section of the apparatus, evacuation and out-gassing were all carried out in the same manner as in the case of an experiment on a bulk graphite sample.

To get the experiment with the molybdenum can - graphite powder sample to work, a technique had to be developed so that great care could be taken to reduce the initial pressure in the sorption apparatus quite slowly. This made it possible to avoid sucking powder particles out of the can into the sorption apparatus and into the adjoining vacuum system.

Experiment 40 was carried out as a successful preliminary run but had to be terminated (due to a leak-failure of the glass-to-copper seal of the apparatus) before a complete set of sorption and desorption points were obtained.

The next experiment (Experiment 41) was carried out quite successfully, sorption and desorption equilibrium points were obtained along with sorption and desorption kinetics data for the periods in between equilibrium points.

The data obtained in Experiment 41 is given in Table 3.1 and the equilibrium points numbered in the order they were obtained are given in the log — log plot of P_{C_s} vs C_{C_s} of Figure 3.1. Figure 3.1 also gives the straight-line, least-squares fit of Experiment 41 desorption points to Equation 2.1 with corresponding constants of

$$\ln k_F = A + B(10^3/T) = -9.682, \qquad u = D + E(10^3/T) = 4.036$$

where T - 1273 $\pm$ 10 K. Also the theoretical equilibrium, modified-exponential isotherms (Eq. 1.11) are plotted (two cases). They employ the empirical values of A, B, D, E from teh straight-line fit and the values of C_L = 1.0 and C_L = 2.0 mmol/kg with C_m = 30 mmol/kg in both cases. Table 3.1 not only gives the equilibrium data but also gives the rate of sorption (or desorption) and also the time to reach a 90% change of concentration, the time at a given cesium vapor pressure and the time the sample was held at a given temperature. It is to be noted that at 'equilibrium' the magnitude of the sorption or desorption rate is about 10^{-7} mmol Cs per kg graphite per second. Thus, there is still a small rate of sorption or desorption at 'equilibrium' and, strictly speaking, equilibrium is never quite reached. On the other hand, the sample (graphite powder in a molybdenum can) was exposed to a given cesium vapor pressure, P_{Cs}, for the order of 100 to 400 hours at each temperature (longer times being used at lower P_{Cs}). Thus, much more time was allowed for the attainment of equilibrium than in the typical Knudsen cell experiment where several points are taken in a few hours.

The size of the openings into the molybdenum can (total area about 2 mm^2) limits the flow of Cs vapor to the graphite powder and thus requires a finite time to attain near equilibrium, i.e. to be within 1% saturation.

TABLE 3.1

EXPERIMENT 41: CESIUM SORPTION ON H-451 GRAPHITE POWDER
(44 TO 77 μm SIZE) AT 1272 K.

Run Sequence Number	Sample Temp. (± 10 K.)	Source Temp. (± 2 K.)	Cesium Vapor Pressure at Sample (Pa)	Cesium Concentration[a] (mmol Cs kg graphite)	Rate at Equilibrium (10^{-7}mmol kg-s)	Time to 90% Change in concentration (hours)	Time at Vapor Pressure (hours)	Estimated Effusion Time (hours)	Time at Sample Temp. (hours)
R01	1273	301.5	5.19(-4)[b]	0.52	<1.2	(c)	404.4	91.5	404
R02	1273	335.5	9.46(-3)	3.01	4.1	131	223.8	30.1	628
R03	1272	364.5	7.06(-2)	5.86	5.9	73	185.1	5.33	813
R04	1272	384.0	2.13(-1)	7.80	<1.2	39	312.7	1.79	2126
R05	1272	410.0	7.12(-1)	10.49	<1.2	16	219.7	0.778	1346
R06	1272	430.5	1.75	12.30	<1.2	6	67.9	0.287	1414
R07	1272	413.0	8.13(-1)	10.54	<-1.2	(d)	184.4	0.444	1598
R08	1272	371.5	1.07(-1)	6.58	<-1.2	27	172.3	2.76	1770
R09	1272	337.0	1.08(-2)	3.51	-1.2	69	243.1	15.16	2013
R10	1273	297.0	3.31(-4)	0.92	-2.5	227	457.6	136.4	2471
Sample Tube Background				0.29					

H-451 Sample Weight: before experiment = 4.049g

(a) In situ equilibrium concentration corrected for sample tube background contribution
(b) Read as 5.19×10^{-4}
(c) Not characteristic of the equilibrium approach
(d) Not observed due to temporary malfunction of counting system

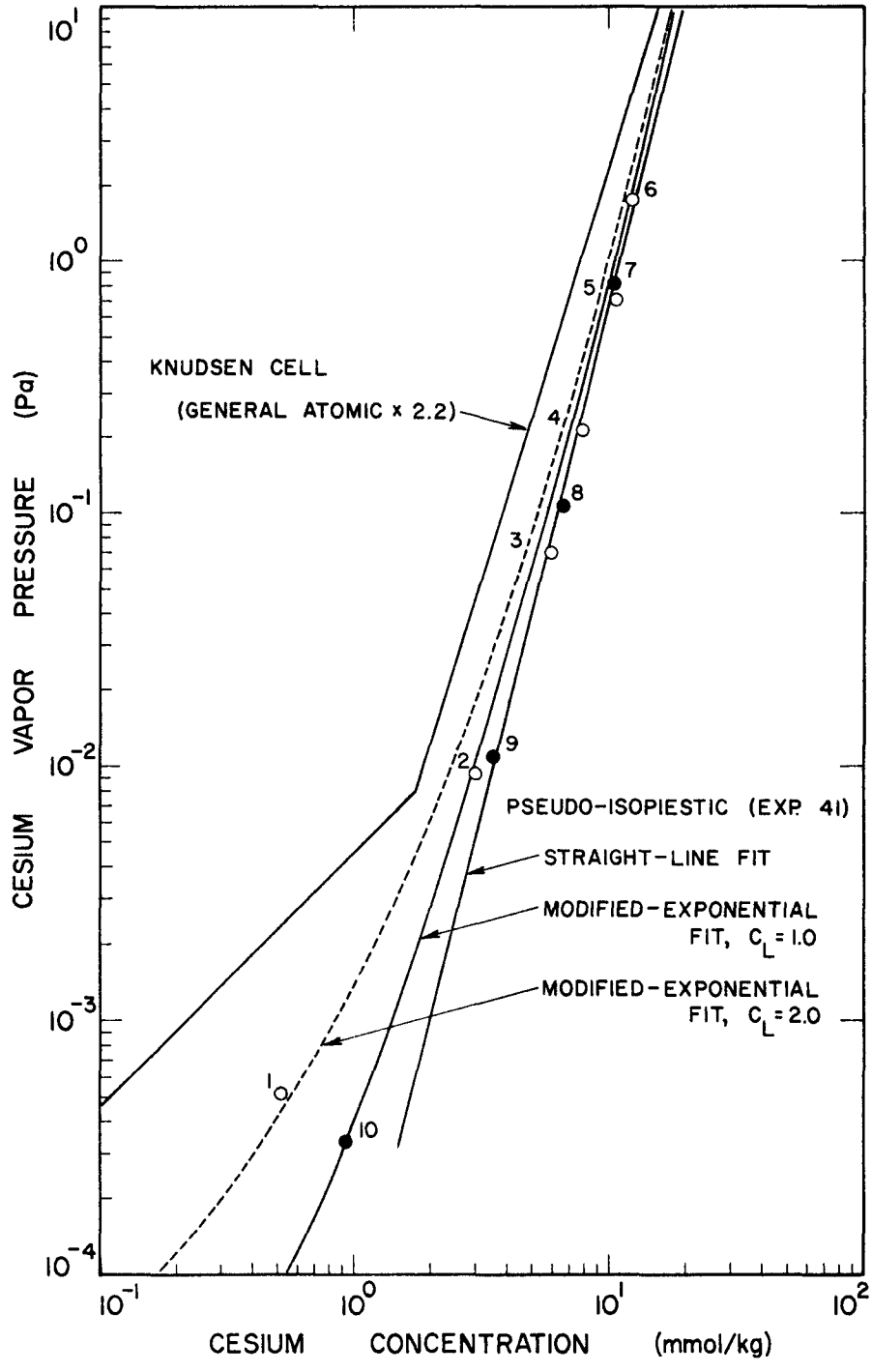

Figure 3.1. Cesium-Graphite (H-451), Powder Sorption Isotherms with Experiment 41 Data Points

Once the cesium-graphite powder isotherm is known and assuming the graphite in the cell (can) is always very close to equilibrium with graphite powder, the Knudsen equation for flow through a thin small orifice can be applied to estimate the time required for 99% saturation (upon sorption) or 101% saturation (upon desorption) as limited by flow of cesium vapor through the holes of the can. These estimated effusion times are given in the next to last column of Table 3.1.

It may be seen in Table 3.1 that the estimated effusion time is always several times less than the time the sample was at a given vapor pressure and at higher vapor pressures ($P_{Cs} > 10^{-2}$ Pa) many times less. Thus, the rate of sorption or desorption of cesium by the graphite powder is determined by the interaction of cesium atoms with the graphite itself. The kinetics data is given and a theoretical model for the kinetics based on activated sorption or desorption of cesium atoms on graphite sorption sites is presented in Section 4. A comparison of Knudsen cell and pseudo-isopiestic equilibrium sorption data follows.

3.3 Comparison of Results Obtained with Graphite Powder

Myers and Bell report in their review of cesium transport data (6) that the Knudsen cell mass spectrometer method was used at General Atomic to obtain most of the cesium sorption data on H-451 graphite. The equilibrium concentration data obtained using graphite powder (44 - 74 μm) was divided by the factor 2.2 to correct for the lower sorptivity of solid graphite. They treated sorption isotherms as consisting of two segments, with the Freundlich isotherm serving as an adequate description in the higher sorbate concentration range and with the Henrian (linear or Langmuir) isotherm being appropriate for the lower sorbate concentration range. At intermediate sorbate concentrations the combination of these two isotherms is

used. The Freundlich isotherm is as given above by Equation 2.1. The Henrian isotherm is given by

$$\ln P = (A + B/T) + (D - 1 + E/T) \ln C_t + \ln C \qquad (3.1)$$

where C_t (mmol/kg) is the transition concentration which corresponds to the C at which P is equal for two isotherms (Equation 2.1 and 3.1). It is approximately equal to C_L of Section 2.5.

For comparison, the Freundlich-Henrian isotherm for solid H-451 graphite given by Myers and Bell is multiplied by the factor 2.2 and shown in Figure 3.1. This is believed to represent a best fit to the General Atomic, Knudsen cell experimental (before correction) data. Comparing the Freundlich portion of the General Atomic data with the Freundlich empirical straight-line, least-squares fit of Experiment 41 data (points numbered 6 thru 9 were fit) shows fair agreement, with the latter having equilibrium cesium concentrations about a factor of 1.3 to 1.8 higher. Assuming the graphite powders to be substantially equivalent, the higher values of the pseudo-isopiestic powder data of Experiment 41 relative to the General Atomic, Knudsen cell data is attributed to the circumstance that the pseudo-isopiestic method permits a closer approach to equilibrium and thus, shows higher equilibrium sorption concentration for a given cesium vapor pressure.

The data and curves of Figure 3.1 show the theoretical modified-exponential isotherm (Eq. 2.11) with C_L =1.0 mmol/kg to fit Experimental data points* best. The theoretical isotherm with C_L = 2.0 mmol/kg has Freundlich-to-Henrian break (or transition) closer to that of the General

*The data points (Fig. 3.1) are numbered on the order taken. Open circles indicate points taken in the absorption mode, and closed circles indicate desorption points.

Atomic, Knudsen cell data (C_t = 1.8 mmol/kg). However, the modified-exponential isotherm would appear to approach the Henrian (linear) portion of the curve at low cesium concentrations at equilibrium vapor pressures which are about an order of magnitude lower than does the General Atomic isotherm.

3.4 Comparison of Bulk Graphite vs Particulate Graphite Equilibrium Cesium Sorption

We compare bulk graphite vs particulate graphite (size range 44 - 77 μm) equilibrium cesium sorption in Figure 3.2. The actual cesium concentration of the particulate graphite has been divided by a factor 2.2 as recommended by General Atomic (6). The curves do not show actual data points but represent best fits of experimental data.

In Figure 3.2 with T = 1273 ± 10 K the curve to the left represents the best General Atomic data for H-451 graphite which is presented as having Freundlich region and a Henrian region. The next curve to the right is the curve of Experiment 41 (pseudo-isopiestic, H-451 powder). Crossing over this curve is the curve representing the pseudo-isopiestic, bulk graphite sorption data of Experiment 36 discussed above (Section 2.4) and finally, the curve farthest right (having the highest C at a given P) is the curve representing the data of Experiments 5, 7 and 9 discussed above (Sections 2.1 and 2.2). We see that the bulk graphite isotherm curves have about the same slope (value of u) which is somewhat greater than the slope (u) of the powder graphite isotherm. The Experiment 41 isotherm, corrected for the greater sorptivity of powdered graphite (using the factor 2.2) agrees fairly well with the isotherm of Experiment 36(3), although their slopes are significantly different (which would appear to indicate the correction factor is not constant). As discussed

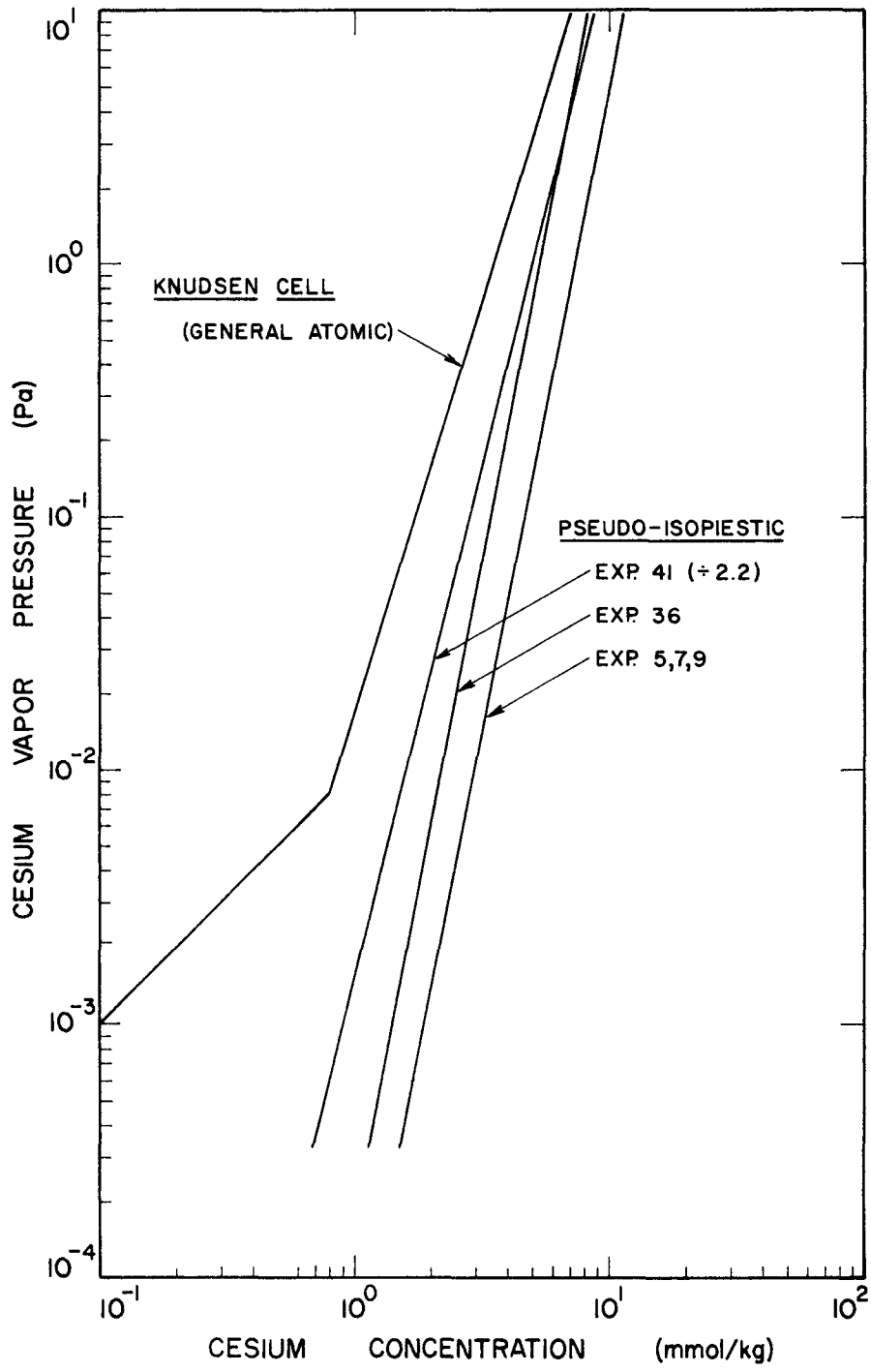

Figure 3.2. Cesium-Graphite (H-451) Solid, Sorption Isotherms-Comparison of Knudsen Cell and Pseudo-Isopiestic Results

above, the General Atomic isotherm is believed to be to the left because of non-attainment of equilibrium in the Knudsen cell. A difference in graphite samples as discussed in Section 2.4 may account for the isotherm curve representing Experiment 5, 7 and 9 being significantly to the right, showing the highest sorptivity.

It is to be noted Faircloth and Pummery of Harwell A.E.R.E.(U.K.)(11a) have obtained cesium sorption data for a Gilsonite graphite (BAR-675). The data were obtained by a Knudsen cell-total collection method using bulk samples (7 mm diameter and 2 mm thick). The Harwell data is in fair agreement with the General Atomic, Knudsen cell, H-451 graphite isotherm (6). This data may, however, not represent true equilibrium for kinetics reasons,as apparently is the case for other Knudsen cell data.

4. KINETICS OF CESIUM-GRAPHITE SORPTION AND DESORPTION

The theory and result of the kinetics of cesium-graphite sorption and desorption are given in this Section.

4.1 Kinetic Theory of an Exponential (Freundlich) Sorption System

As mentioned above, the two most used means of determining cesium vapor pressure, P, vs cesium concentration, C, are 1) Knudsen cell method (6) and, 2) pseudo-isopiestic (or isopiestic) method (5,6). The first method uses graphite powder, to help obtain cesium-graphite equilibrium within the Knudsen cell, while the latter method uses bulk samples. However, we carried out some studies using graphite powder samples with the pseudo-isopiestic method wherein long periods were taken to reach a state close to equilibrium. This resulted in the kinetics data which is modelled here and gave isotherm results for direct comparison with those obtained by the Knudsen cell method at General Atomic.

Our sorption kinetics model assumes the principal process is one of activated sorption by sites (traps) whose activation energy, ε, for a given site is proportional to the energy of sorption of the site, χ. These trapping sites in accordance with the derivation of the Freundlich isotherm by Halsey and Taylor (10), are assumed to be non-uniformly distributed and to have a number which decreases exponentially with interaction (sorption) energy, χ. Accordingly, we assume $\varepsilon = f\chi$ where f = a constant for the system. The model also assumes first order kinetics and that the annealing function $\Theta_1(\varepsilon, t) = \exp\left[-A_s t \exp(-\varepsilon/RT)\right]$ for sorption or desorption may be approximated by a step function which goes from 0 to 1 at $\varepsilon_o = RT \ln (A_s t)$, where A_s = characteristic frequency of the system and t = time of annealing (14,15).

With the assumption that the activation energy for sorption and desorption are about equal, when the cesium vapor pressure is changed stepwise from P_1 to P_2 at t = 0, the concentration of cesium as a function of time is given by the sorption kinetics equation,

$$C(t) = C_m \frac{P_1}{P_o[1-\exp(-\nu_L)]} \int_{\nu_o}^{\nu_L} \frac{\exp[(u-1)\nu]}{1+\frac{P_1}{P_o}\exp(u\nu)} d\nu + C(P_2) - C_m \frac{P_2}{P_o[1-\exp(-\nu_L)]} \int_{\nu_o}^{\nu_L} \frac{\exp[(u-1)\nu]}{1+\frac{P_2}{P_o}\exp(u\nu)} d\nu \quad (4.1)$$

with the lower limit of the integral defined as,

$$\nu_o = \frac{1 - rT}{fu} \ln(A_s t + 1) \quad (4.2)$$

and $\nu_L = \chi_L/\chi_m$ (4.3)

where χ_L = the upper limit of sorption site interaction energy,

χ_m = the mean energy characteristic of the sorption site distribution,

C_m = the estimated concentration if all sorption sites are occupied.

$C(P_2)$ = the equilibrium concentration at cesium partial pressure P_2.

Theoretically, per the modified-exponential isotherm derived in Section 2.5,

$$C(P_2) = C_m \frac{P_2}{P_o[1-\exp(-\nu_L)]} \int_o^{\nu_L} \frac{\exp[(u-1)\nu]}{1+\frac{P_2}{P_o}\exp(u\nu)} d\nu \quad (2.11)$$

We will now derive the kinetics equation (eq. 4.1). It is assumed that $\chi = 0$ is the lower bound of the interaction energy. The total absorption energy for an atom in sorption traps is equal to: the

interaction energy (χ) + energy needed to remove the cesium atom from the average surface (ϕ_s), thus the surface energy of atoms relative to atoms in the dilute vapor state is,

$$E = -(\chi + \phi_s) \tag{4.4}$$

It is to be noted that for cesium sorption on an idealized graphite surface, Holian (12) estimated ϕ_s to be about equal to 60 kK or about 500 J/mol. For a six atom hole, the energy of sorption is estimated to be 102 kK or about 850 J/kg. In our theory, χ is considered to be the interaction energy for "activated" sorption by trapping sites involving greater energies than ϕ_s. The energy of activation for transfer of atoms from holes to traps is taken to be $f\chi$ as indicated in Figure 4.1 and for desorption from traps it is χ. A possible physical explanation for the potential energy diagram (Figure 4.1) is given in Figure 4.2 where the cesium atoms on free surfaces connected to holes are in equilibrium with each other. Here the cesium atoms initially in the vapor phase condense on free surfaces and migrate into holes. Therefore, the cesium atoms in the vapor phase are in equilibrium not only with atoms on free surfaces but also with atoms in the holes. The absorption process involving the transfer of cesium atoms from the holes to the traps will be a time dependent function with an energy of activation of absorption of $f\chi$. Similarly, cesium desorbing from the traps to surface holes will have the energy of activation of desorption of χ. The equilibrium density distribution function of sites (traps) of energy χ is (as given in Section 2.5),

$$n(\chi) = \frac{\exp(-\chi/\chi_M)}{\chi_M[1-\exp(-\chi_L/\chi_M)]} \tag{2.4}$$

with χ_L = upper limit of χ (maximum)

and χ_M = mean value of χ (characteristic of the density distribution).

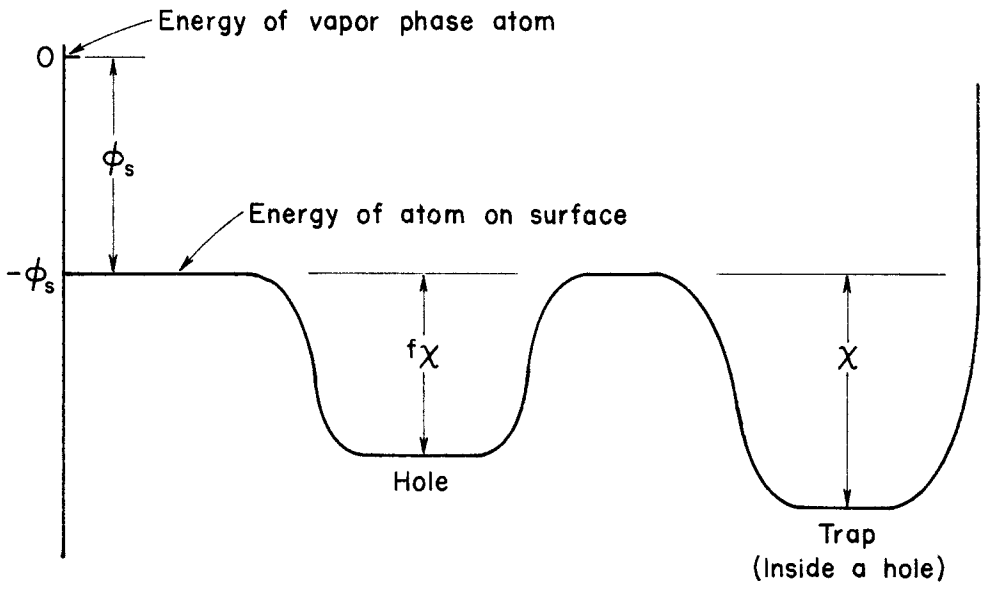

Figure 4.1 Potential Energy Diagram of a Hole and a Trap.

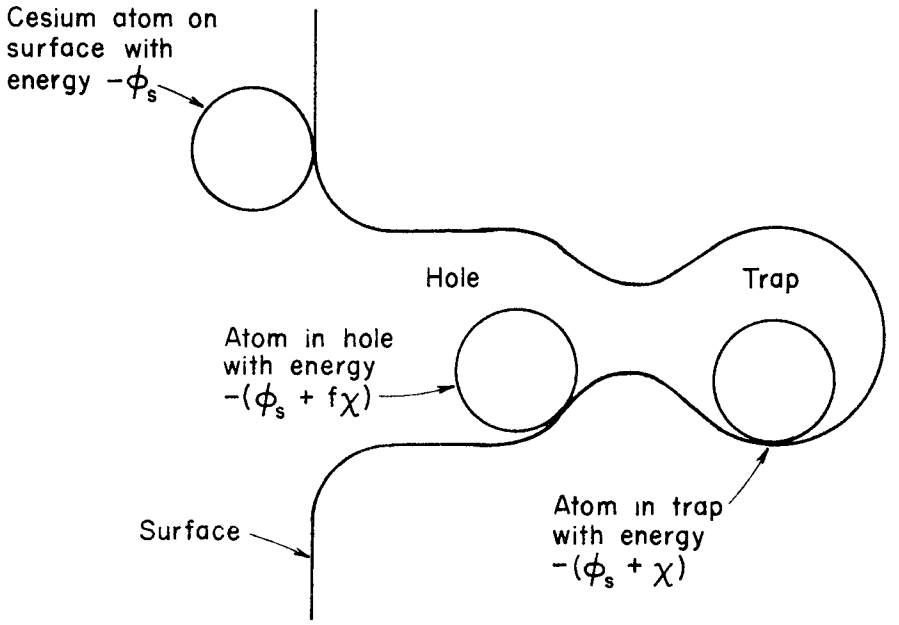

Figure 4.2 A Possible Physical Concept of Potential Energy Diagram (Figure 4.1) with Cesium Atom on Surface, in Hole and in Trap.

Vand (14) introduced the concept of a group of processes distributed in activation energy in order to explain the kinetics of certain reactions occurring in heating evaporated metal deposits. Whereas Primak (15) studied the kinetic behavior of systems in which processes occurred which were distributed over a range of activation energies. In view of these investigations, the Vand-Primak (14,15) formulation of the kinetics of activated (annealing) processes is applied to treat the kinetics of absorption-desorption processes to a system showing exponential or Freundlich isotherm behavior. In this case, the order of reaction is assumed to be 1. It is also assumed that no interaction exists between the sorbed cesium atoms. First, consider the desorption case under isothermal annealing, where the cesium atoms are in traps of various energies χ. They possess sorption energy relative to the vapor phase of

$$E = -(\phi_s + \chi), \tag{4.4}$$

and they are released to the free graphite surface of energy,

$$E = -\phi_s \tag{4.5}$$

but also some atoms reside in surface holes of energy,

$$E = -(\phi_s + f\chi) \tag{4.6}$$

Thus, the cesium atoms are either on the free surface or are in surface holes and they are in equilibrium with atoms in the vapor phase of pressure P. The Freundlich or modified-exponential sorbers are assumed to have an absorption activation energy, ε, which is proportional to the interaction energy χ and equal to $f\chi$. The fractional coverage of trapping sites of energy χ is given by Eq. 2.9 and applies to

the case where final equilibrium pressure has not been attained,

$$\theta(\chi,P) = \frac{(P/P_o)\ \exp[(1 - rT)\ \chi/RT]}{1 + (P/P_o)\ \exp[(1 - rT)\ \chi/RT]} \tag{2.9}$$

with the variables being defined as in Section 2.5.

When cesium partial pressure is changed from P_1 to P_2, from the atomic point of view the process of the interaction of cesium atoms with graphite can be considered as a combined, dynamic desorption-absorption process where atoms are desorbed from activated sites at P_1 and absorbed onto sites at P_2. In the derivation of the kinetics when $P_1 > P_2$ we have a "net desorption" process, and when $P_1 < P_2$ we have a "net absorption" process. Now applying the Vand-Primak kinetic treatment which was originally developed for a desorption process,

$$q = q(\varepsilon_d) \tag{4.8}$$

where q is the property or property change propotional to the number of processes (i.e., desorption which can occur at the activation energy ε_d). The first order reaction for the desorption process is

$$-\left(\frac{dq}{dt}\right) = Kq$$
$$= A_s\ [\exp(-\varepsilon_d/RT)]q \tag{4.9}$$

where A_s = characteristic frequency.

Then if $q = q_1$, at $t = 0$

$$q = q_1\ \exp(-\ Kt)$$
$$= q_1\ \exp[-A_s t \cdot \exp(-\varepsilon_d/RT)] \tag{4.10}$$
$$= q_1\theta_1(\varepsilon_d,\ t)$$

where $\theta(\varepsilon,\ t)$ is the characteristic isothermal annealing function, thus defining

$$\theta_1(\varepsilon, t) = \exp\left[-A_s t \exp(-\varepsilon/RT)\right] \tag{4.11}$$

For a desorption process, Equation 4.11 becomes

$$\theta_1(\varepsilon_d, t) = \exp\left[-A_s t \exp(-\varepsilon_d/RT)\right] \tag{4.12}$$

This is known as the annealing function. Using the Vand-Primak treatment for an absorption process, the rate equation is,

$$\frac{dq}{dt} = Kq_2 - Kq$$

$$= Kq_2 - A_s\left[\exp(-\varepsilon_a/RT)\right]q \tag{4.13}$$

where ε_a is the activation energy of absorption. If $q = 0$ at $t = 0$ and

$$q = q_2 \text{ as } t \to \infty, \text{ then}$$

$$q = q_2\left[1 - \exp(Kt)\right]$$

$$- q_2\left|1 - \theta_1(\varepsilon_a, t)\right| \tag{4.14}$$

where $\theta_1(\varepsilon_a, t) = \exp\left[-A_s t \exp(-\varepsilon_a/RT)\right]$ (4.15)

which is the "annealing function" for absorption.

As discussed by Primak (15) and Vand (14) in the case of annealing, if there is a distribution of activation energies, q corresponds to the distribution function and its measured value of the quantity (or property) is,

$$Q(t) = \int_o^\infty q_o(\varepsilon)\theta_1(\varepsilon, t)d\varepsilon \tag{4.16}$$

where $q_o(\varepsilon)$ is the initial value as a function of ε. Having obtained the relationships for absorption and desorption equations separately,

these equations can be treated to find a net effect of sorption, i.e. the desorption-absorption process, with the final outcome being desorption when pressure P_1 changes to P_2 with $P_1 > P_2$. This quantity is derived as

$$Q(t) = \int_o^\infty q_1 \theta_1(\varepsilon_d, t)d\varepsilon + \int_o^\infty q_2[1 - \theta_1(\varepsilon_a, t)]d\varepsilon \qquad (4.17)$$

Treating for the modified-exponential (Freundlich-Henrian) sorber,

$$q_1 = \frac{\exp(-\chi/\chi_M)}{\chi_M[1 - \exp(-\chi_L/\chi_M)]}\,\theta(\chi, P_1)C_m \qquad (4.18)$$

$$q_2 = \frac{\exp(-\chi/\chi_M)}{\chi_M[1 - \exp(-\chi_L/\chi_M)]}\,\theta(\chi, P_2)C_m \qquad (4.19)$$

where $\theta(\chi, P)$ is defined by Equation 2.9. Here the quantity $\theta(t)$ is the concentration of cesium sorbed C(t), and with the assumption that the activation energies for sorption and desorption are about equal, then

$$\varepsilon_d \simeq fX \qquad (4.20)$$

and $$\varepsilon_a \simeq fX \qquad (4.21)$$

Substituting quantities from the above and Section 2.5 into Equation (4.17), the concentration is given by

$$C(t) = C_m \frac{P_1'}{P_o[1-\exp(-\nu_L)]} \int_o^{\nu_L} \frac{\exp((u-1)\nu)\exp[-A_s t \exp(-fu\nu/(1-rT))]}{1 + \frac{P_1}{P_o}\exp(u\nu)}\,d\nu$$

$$+ C_m \frac{P_2}{P_o[1-\exp(-\nu_L)]} \int_o^{\nu_L} \frac{\exp((u-1)\nu)}{1 + \frac{P_2}{P_o}\exp(u\nu)}\,d\nu - C_m \frac{P_2}{P_o[1-\exp(-\nu_L)]}$$

(equation continued to next page)

$$\cdot \int_o^{\nu_L} \frac{\exp((u-1)\nu)}{1 + \frac{P_2}{P_o}\exp(u\nu)} \exp\left[-A_s t \exp(-fu\nu/(1-rT))\right] d\nu \qquad (4.22)$$

Equation (4.22) applies to a net desorption process, however for a net absorption process where the pressure changes for P_1 to P_2 with $P_1 < P_2$, the equation remains exactly the same. It is to be noted that the second term in Equation (4.22) is the theoretical modified-exponential equation for equilibrium concentration C(P) at P_2,

$$C(P_2) = C_m \frac{P_2}{P_o\left[1-\exp(-\nu_L)\right]} \int_o^{\nu_L} \frac{\exp\left[(u-1)\nu\right]}{1 + \frac{P_2}{P_o}\exp(u\nu)} d\nu \qquad (4.23)$$

If we substitute into Equation (4.23) the equilibrium concentration, i.e. $C(P_2)$ and the annealing function then, then the equation can be simplified to,

$$C(t) = C_m \frac{P_1}{P_o\left[1-\exp(-\nu_L)\right]} \int_o^{\nu_L} \frac{\exp\left[(u-1)\nu\right]}{1 + \frac{P_1}{P_o}\exp(u\nu)} \theta_1(\varepsilon_d, t) d\nu$$

$$+ C(P_2) - C_m \frac{P_2}{P_o\left[1-\exp(-\nu_L)\right]} \int_o^{\nu_L} \frac{\exp\left[(u-1)\nu\right]}{1 + \frac{P_2}{P_o}\exp(u\nu)} \theta_1(\varepsilon_a, t) d\nu \qquad (4.24)$$

where the annealing function varying from 0 to 1 with ε and $\theta_1(\varepsilon,t)$ is given by Equation (4.11). It is found that at

$$t = 0, \ \theta_1(\varepsilon, t) = 1$$

$$t = \infty, \ \theta_1(\varepsilon, t) = 0.$$

thus, at

$$t = 0, \ C(t) = C(P_1)$$

$$t = \infty, \ C(t) = C(P_2)$$

The annealing function is described in Figure 4.3. If the distribution of activation energies is large compared to RT, Vand (14) and Primak (15) have shown that the annealing function $\theta_1(\varepsilon, t)$ may be approximated by a step function with the step at $\varepsilon_o = RT \ln(A_s t)$ as indicated in Figure 4.4. This approximation simplifies Equation (4.16) to

$$Q(t) = \int_{\varepsilon_o}^{\infty} q_o d\varepsilon \tag{4.25}$$

The sorption kinetics equation becomes

$$C(t) = C_m \frac{P_1}{P_o\left[1-\exp(-\nu_L)\right]} \int_{\nu_t}^{\nu_L} \frac{\exp\left[(u-1)\nu\right]}{1 + \frac{P_1}{P_o}\exp(u\nu)} d\nu$$

$$+ C(P_2) - C_m \frac{P_2}{P_o\left[1-\exp(-\nu_L)\right]} \int_{\nu_t}^{\nu_L} \frac{\exp\left[(u-1)\nu\right]}{1 + \frac{P_2}{P_o}\exp(u\nu)} d\nu \tag{4.26}$$

with the lower limit of the integral defined as

$$\nu_t = \frac{1 - rT}{fu} \ln(A_s t) \tag{4.27}$$

It can be shown that as $t \to \infty$, $\nu_t \to \nu_L$, so that the integrals $\to 0$, at the end of the sorption run, thus $C(\infty) = C(P_2)$. Appropriate A_s values are found by trial. In initial trial calculations, the A_s frequency was indicated to be 10^{-5} sec^{-1} or greater.

In order that this treatment give the proper answer at $t = 0$, the lower limit is modified by putting $\nu_t = \nu_o$, where

$$\nu_o = \frac{1 - rT}{fu} \ln\left[A_s\left(t + \frac{1}{A_s}\right)\right] = \frac{1 - rT}{fu} \ln\left[A_s t + 1\right] \tag{4.28}$$

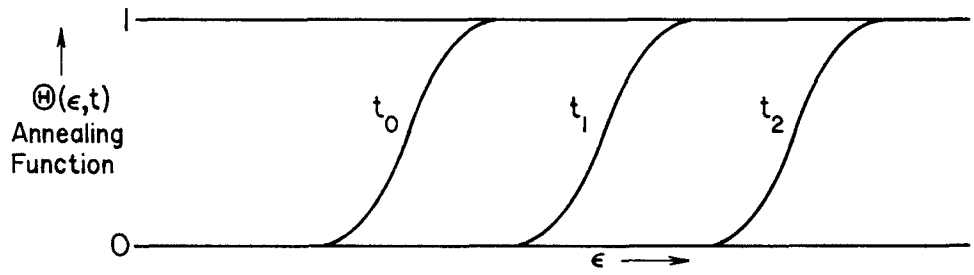

Figure 4.3. Annealing Function Diagram Plot. As the Isothermal Annealing Progresses, the Curve is Displaced along ε but Does Not Alter in Shape.

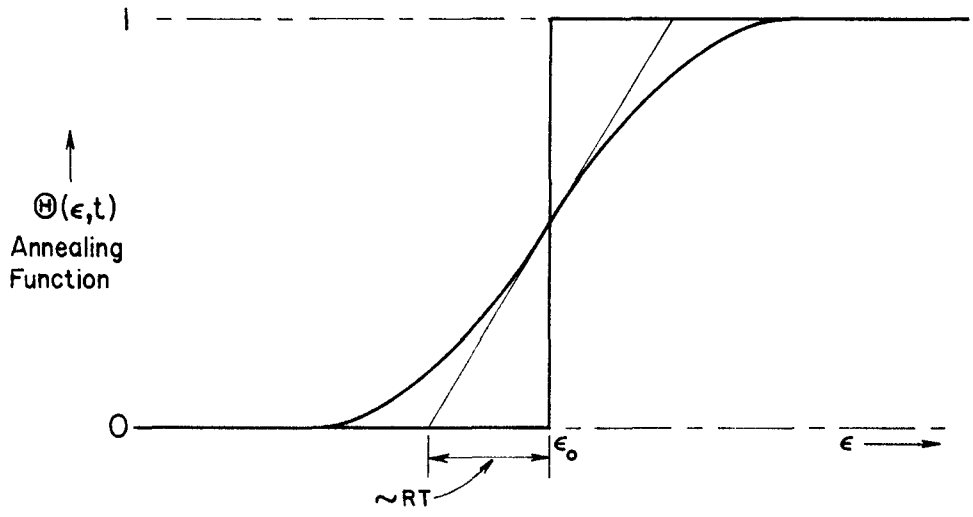

Figure 4.4. Annealing Function Approximated by a Step Function. Step Function is Assumed Because Most of the Processes Occurring Simultaneously Lie in a Narrow Band of Activation Energies of the Magnitude RT.

This gives a value $\nu_o = 0$ at $t = 0$ which is to be expected for the equilibrium condition - prior to the pressure change from P_1 to P_2. The approximate but useful sorption kinetics equation is then

$$C(t) = C_m \frac{P_1}{P_o[1-\exp(-\nu_L)]} \int_{\nu_o}^{\nu_L} \frac{\exp[(u-1)\nu]}{1 + \frac{P_1}{P_o}\exp(u\nu)} d\nu$$

$$+ C(P_2) - C_m \frac{P_2}{P_o[1-\exp(-\nu_L)]} \int_{\nu_o}^{\nu_L} \frac{\exp[(u-1)\nu]}{1 + \frac{P_2}{P_o}\exp(u\nu)} d\nu \qquad (4.1)$$

where $C(P_2)$ is given in Equation (4.23). Computer calculations using Equation (4.1) are described in Appendix I.

4.2 Comparison Theoretical with Observed Kinetics in the Case of Graphite Powder

In carrying out the pseudo-isopiestic experiment on powdered graphite (particle size range 44 - 74 μm) in Experiment 41, six sets of kinetics data were obtained in the process of going from equilibrium points 2 to 3, 3 to 4, 4 to 5, 5 to 6, 7 to 8, 8 to 9, respectively. The equilibrium points are shown in Figure 3.1. The kinetics data points are shown in Figures 4.5, 4.6, 4.7, 4.8, 4.9 and 4.10, respectively, with their trend indicated by a dashed line (labelled, experimental curve). The theoretical "best" fit to these data points is given as a solid line in Figures 4.5 through 4.10.

An inspection of the figures indicates that the theoretical curves fit the data very well and thus Equation 4.1 provides quite a satisfactory model for the kinetics or variation of sorbate concentration with time, for the case of cesium vapor sorbed by H-451 graphite powder.

A "best" fit curve represents the choice made by two individuals of the curve that fits best from a number of curves which were calculated using,

1) the parameters a & b obtained by a least-squares fit of the Freundlich desorption curve of Experiment 41, 2) the parameters C_L = 1.0 and C_m = 30mmol/kg selected as best for the modified-exponential isotherm of Experiment 41, 3) the appropriate values of P_1 and P_2 corresponding to a given experimental data set, and 4) arbitrarily selected values of the kinetics parameters A_s (the characteristic frequency) and f (the ratio of activation energy, ε to interaction energy, χ). With the other parameters fixed by the nature of the sorbate and sorbent and the conditions of the experiment, we have only A_s and f as variables for fitting a theoretical curve to a set of experiment data for a run when vapor pressure is changed from P_1 to P_2 at t = 0, to go to a new equilibrium data point.

The values of the "best" fit kinetics parameters A_s and f are shown on Figures 4.5 through 4.10 and also listed in Table 4.1.

The average together with the standard deviation of the kinetics parameters are $A_s = (7.7 \pm 2.0) \times 10^{-4}$ sec^{-1} and f = 0.92 ± 0.11. Thus, we see that for the absorption or desorption of cesium by graphite (H-451) powder $A_s \simeq 10^{-3}$ sec^{-1} and f ≃ 1 (unity). The good fit of the kinetic curves seems to indicate the sorption of cesium by graphite powder, aside from adsorption on outer surface planes and holes is primarily an activated absorption process with the activation energy ε approximately equal to the interaction energy χ.

4.3 Kinetics of Cesium-Graphite Sorption and Desorption for Bulk H-451 Graphite

4.3.1 Comparison of Theoretical with Observed Kinetics for Experiment 36.

Experiment 36 pertains to pure cesium sorption by H-451 bulk graphite and the isotherm is displayed in Figure 2.9. This figure shows that the equilibrium data points denoted by R08 and onwards fall on the Freundlich

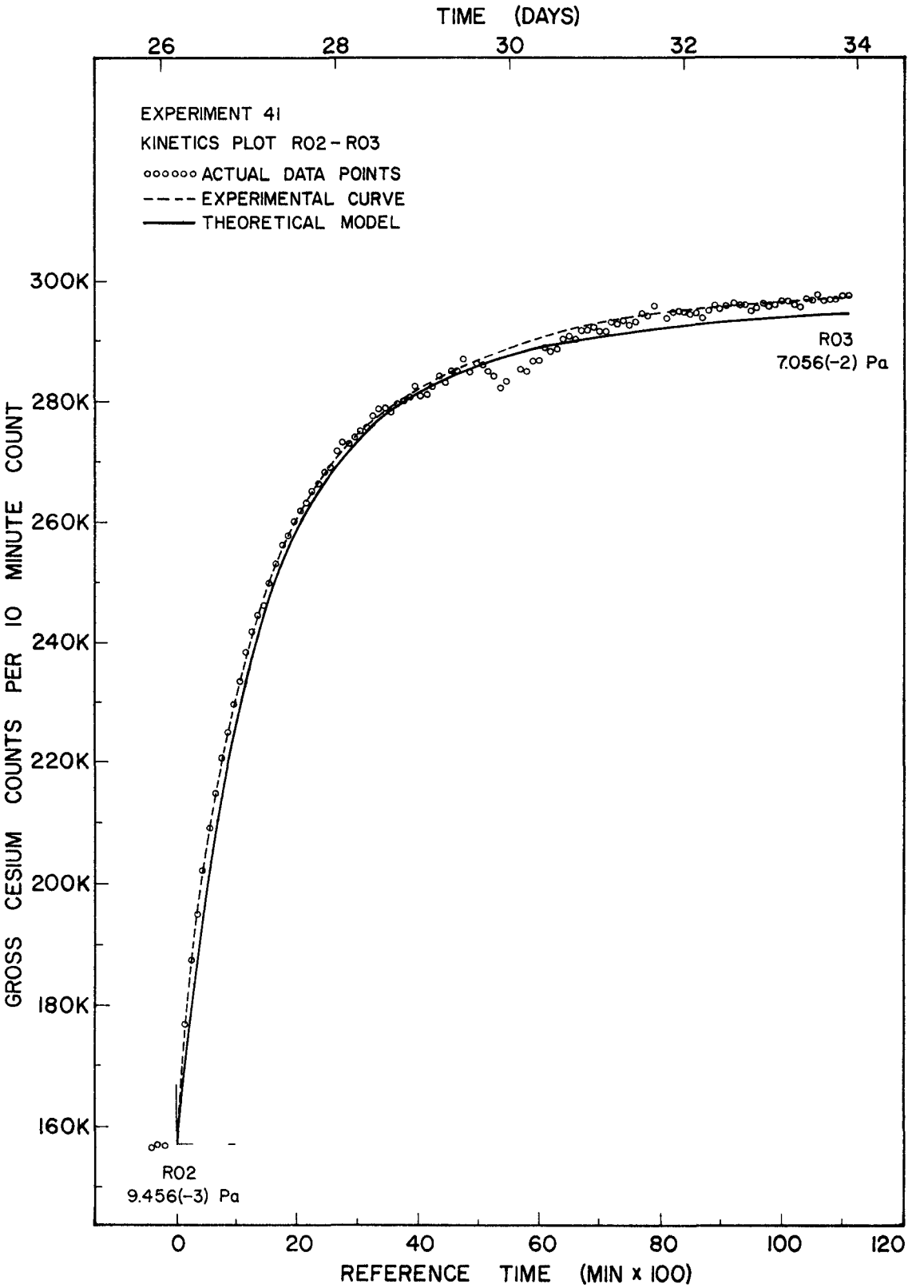

Figure 4.5. Kinetics Data and Curves for Going from Point 2 to Point 3 -- Experiment 41 ($A_s = 5 \times 10^{-4}\ s^{-1}$, f = 1.00)

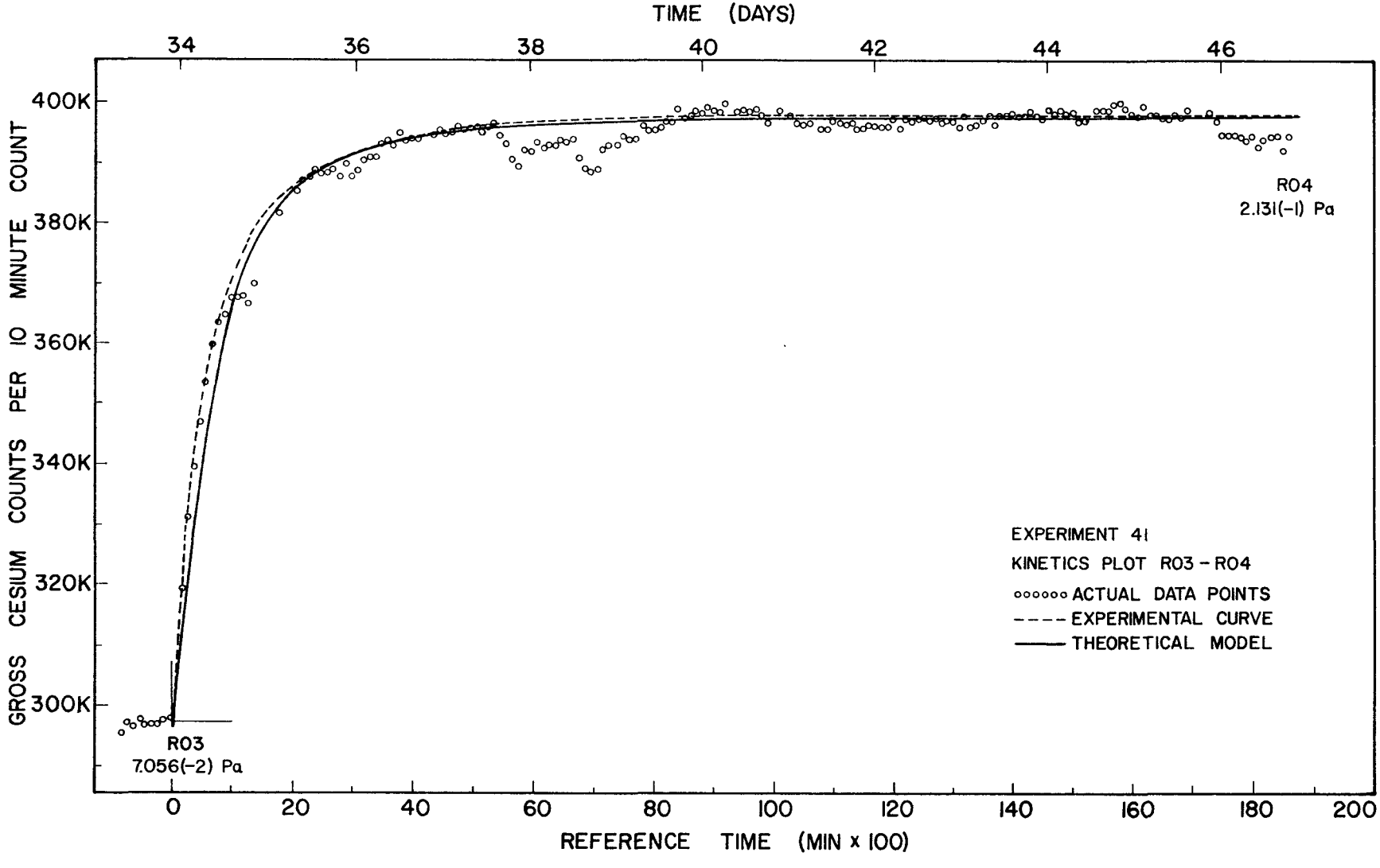

Figure 4.6. Kinetics Data and Curves for Going from Point 3 to Point 4 -- Experiment 41 ($A_s = 7 \times 10^{-4} s^{-1}$, f = 0.95)

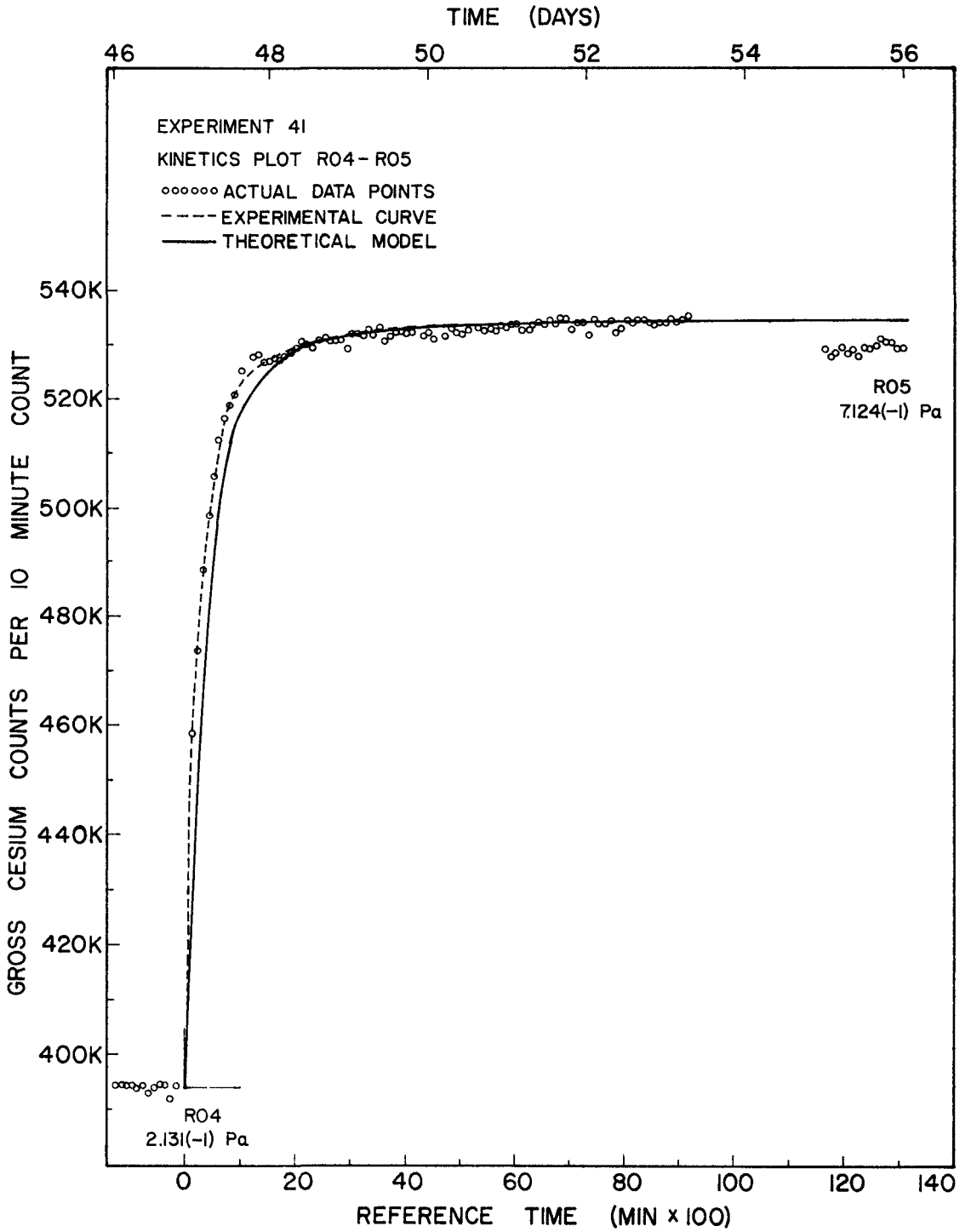

Figure 4.7. Kinetics Data and Curves for Going from Point 4 to Point 5 -- Experiment 41 (A_s 10 x 10^{-4}, s^{-1}, f - 1.00)

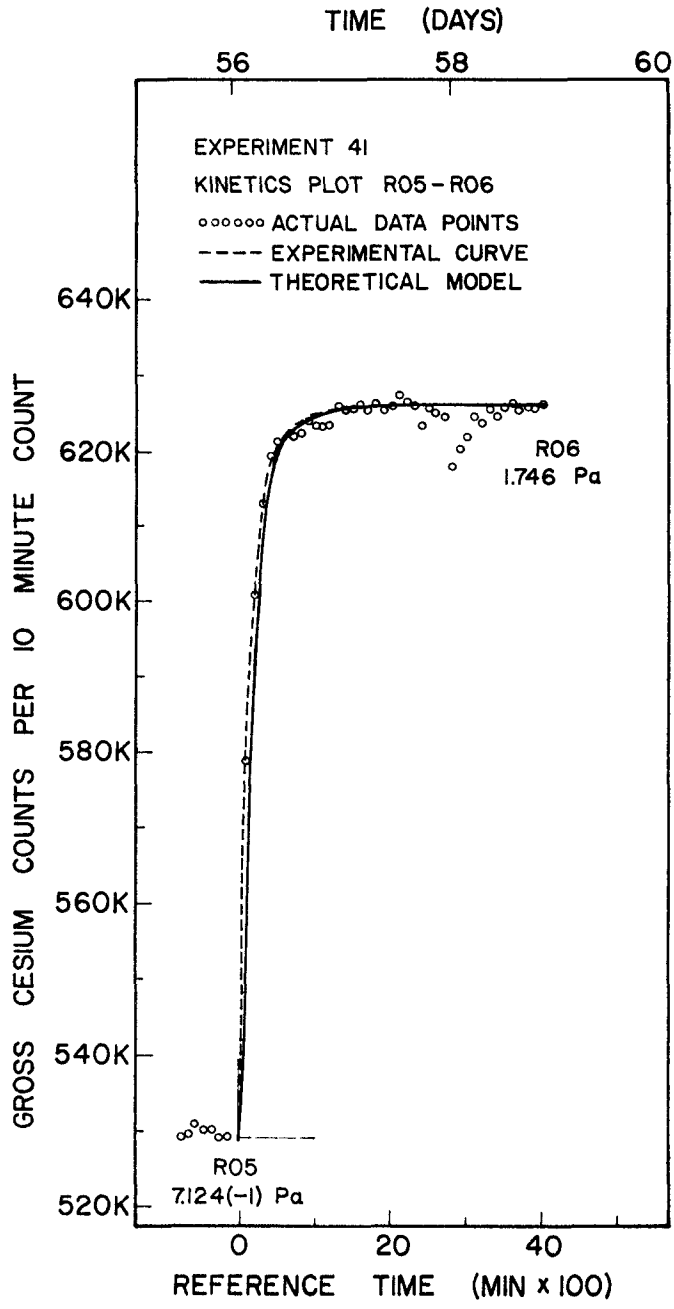

Figure 4.8. Kinetics Data and Curves for Going from Point 4 to Point 5--Experiment 41 (A_s = 10 x 10^{-4} s^{-1}, f = 0.70)

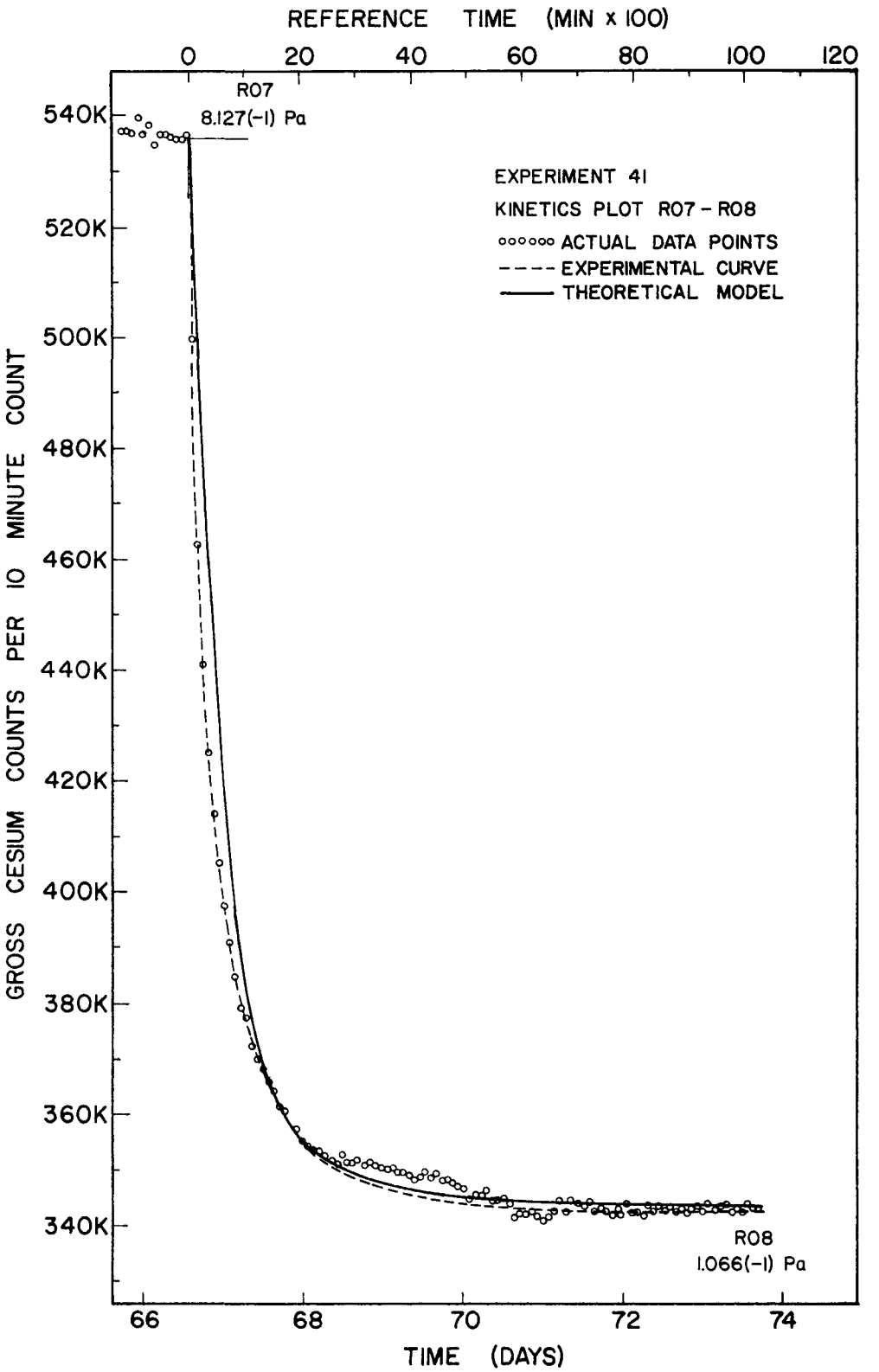

Figure 4.9. Kinetics Data and Curves for Going from Point 7 to Point 8 -- Experiment 41 ($A_s = 7 \times 10^{-4} s^{-1}$, f = 0.90)

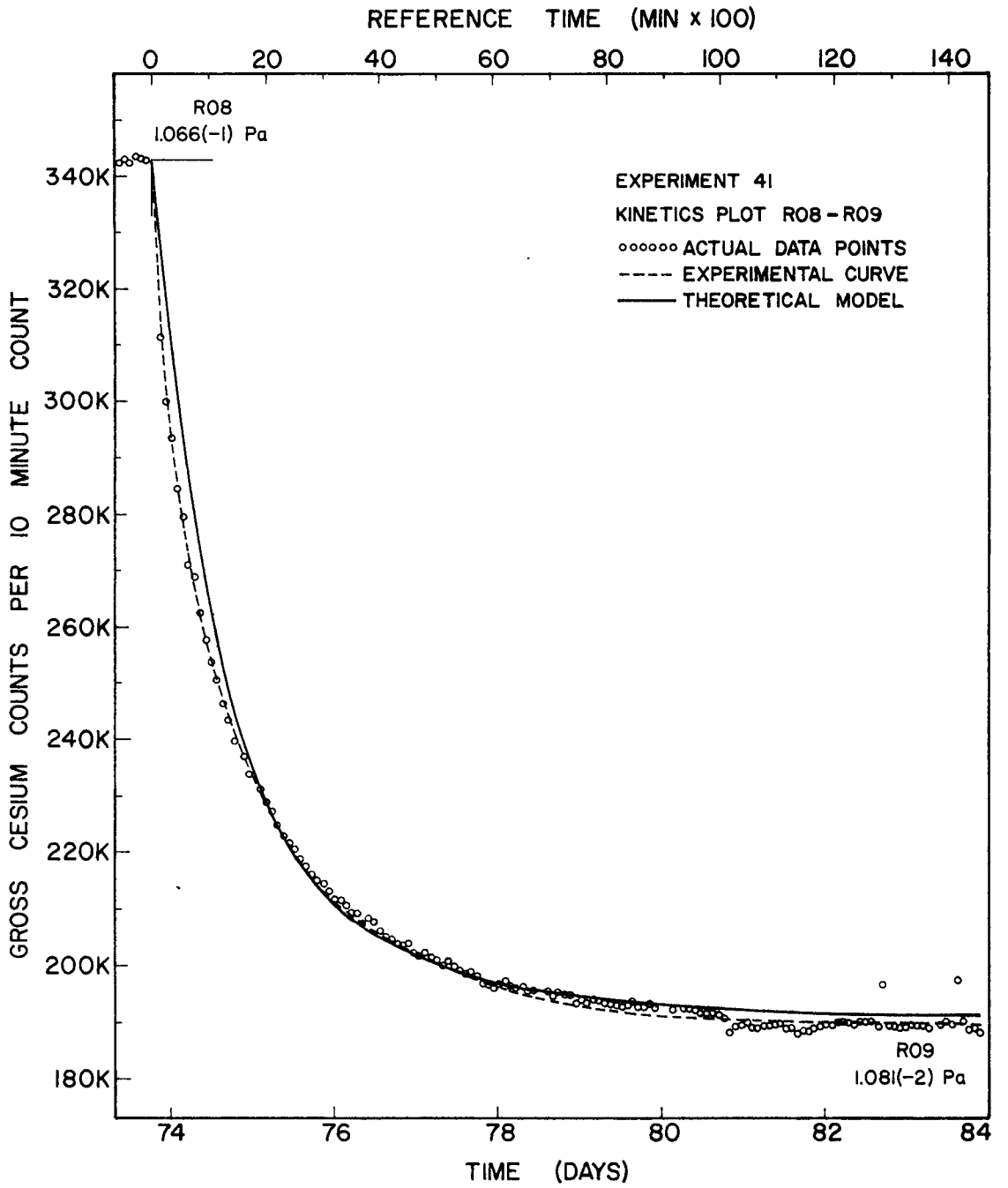

Figure 4.10. Kinetics Data and Curves for Going from Point 8 to Point 9--Experiment 41 ($A_s = 7 \times 10^{-4} s^{-1}$, f = 0.95)

TABLE 4.1

Kinetics Best Fit Parameters for

Cesium Sorption by H-451 Graphite Powder

Equilibrium Data Points	P_1 (Pa)	P_2 (Pa)	A_s (s^{-1})	f
2 → 3	9.5 (-3)*	7.1 (-2)	5 (-4)	1.00
3 → 4	7.1 (-2)	2.13 (-1)	7 (-4)	0.95
4 → 5	2.13 (-1)	7.1 (-1)	10 (-4)	1.00
5 → 6	7.1 (-1)	1.75	10 (-4)	0.70
7 → 8	8.1 (-1)	1.07 (-1)	7 (-4)	0.95
8 → 9	1.07 (-1)	1.08 (-2)	7 (-4)	0.95

* Exponential notation: 9.5 (-3) = 9.5×10^{-3}

isotherm, indicating a linear log P - log C relationship. The kinetic behavior was studied for these points. Information for the kinetic behavior was routinely collected after every 100 minutes by the single channel analyzer counting system. An example is illustrated in Figure 4.11, which shows a plot of sample counting rate versus time for R08 - R09 kinetics. After the cesium source temperature was changed from 132.2° C to 145.5° C, an initial rapid rise in the cesium activity subsequently took place within a couple of hours. Physical adsorption is probably the primary mechanism of retention of cesium by graphite at the early stage with activated absorption by sorption site (trap) taking over at longer times. The data indicates that for a 90% change in the concentration, the time taken is 73 hours as compared to the total run time of 166 hours for the R08 - R09 kinetics. It seems very likely that the diffusion mechanism plays some role in the latter half of the run time, especially at very long times. The diffusion of cesium is a relatively slow process involving cesium transport from the pore surfaces into the bulk of the graphite.

The theoretical relationship used for describing the observed kinetics activated sorption of the cesium by the graphite sample at 1000° C is given by Equation 4.1 . A combination of A_s and f values were chosen so that the theoretical plots determined from Equation 4.1 could be compared with the experimental kinetic results. Some difficulty was involved in getting good fits to the data because the A_s value tended to make the kinetic plot rise faster and the f value tended to spread the "bend" of the kinetics plot. In addition, an increase in the f value caused the right portion of the predicted concentration curve to fall below the experimental kinetics data. Visual estimation was used in selecting the most appropriate combination of A_s and f values - the emphasis being placed on obtaining a

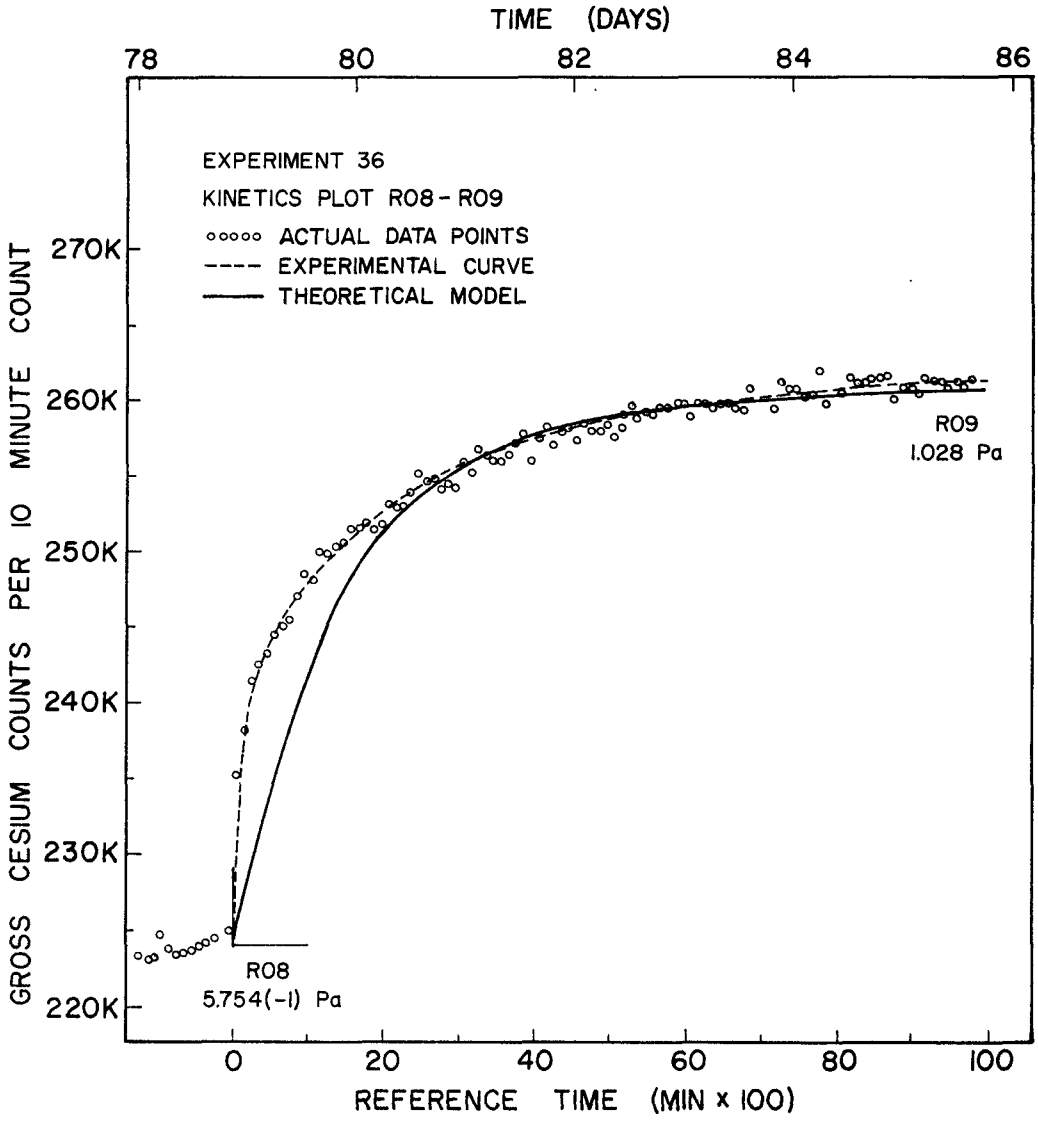

Figure 4.11. Experiment 36: Kinetic Behavior of Cesium on H-451 Graphite at 1273 K. R08 - R09 Kinetics Plot.

good fit in the vicinity of the bend in the kinetics plot. The A_s value was typically on the order of 10^{-4} sec^{-1}. The value of f was limited to a maximum of unity. From Figure 4.1 it is reasoned that the maximum energy of activation of sorption is equal to the interaction energy for activated sorption (trapping). In Figure 4.11, the best fit was obtained for an A_s/f combination of 3×10^{-4} $s^{-1}/0.95$. The second best values are 5×10^{-4} $s^{-1}/1.00$. In Figures 4.11 through 4.17, solid lines represent the theoretical model and dashed lines represent the experimental curve according to the recorded activity counts. The cesium background contribution was considered to be negligible. Table 4.2 indicates the values of A_s (typically in the vicinity of 10^{-4} s^{-1}) and f (in most cases in the range from 0.9 to 1.00) for various kinetics plots. An unusually low value of f (about 0.5) is noted for the last kinetics plot, Figure 4.17 of R14 - R15. No ready explanation is available for this unexpectedly low value of f. Analysis of the kinetics behavior indicated that the theoretical prediction does not adequately deal with the initial rapid gain or loss of cesium. A plausible explanation is that the kinetics model does not account for the surface (physical adsorption) phenomena which does not involve activated sorption.

The assumptions made in the kinetics model are that a transition to Langmuir or Henrian linear concentration dependence occurs at about 0.7 mmol/kg and that the monolayer concentration is limited to 20 mmol/kg. The conclusion reached is that the characteristic frequency, A_s, for the kinetics behavior in Experiment 36 is in the mid 10^{-4} to 10^{-3} per second range with the f value close to unity. Correction factors may need to be included in the kinetics model to account for both initial evaporation surface (physical adsorption) effects and the bulk diffusion phenomena,

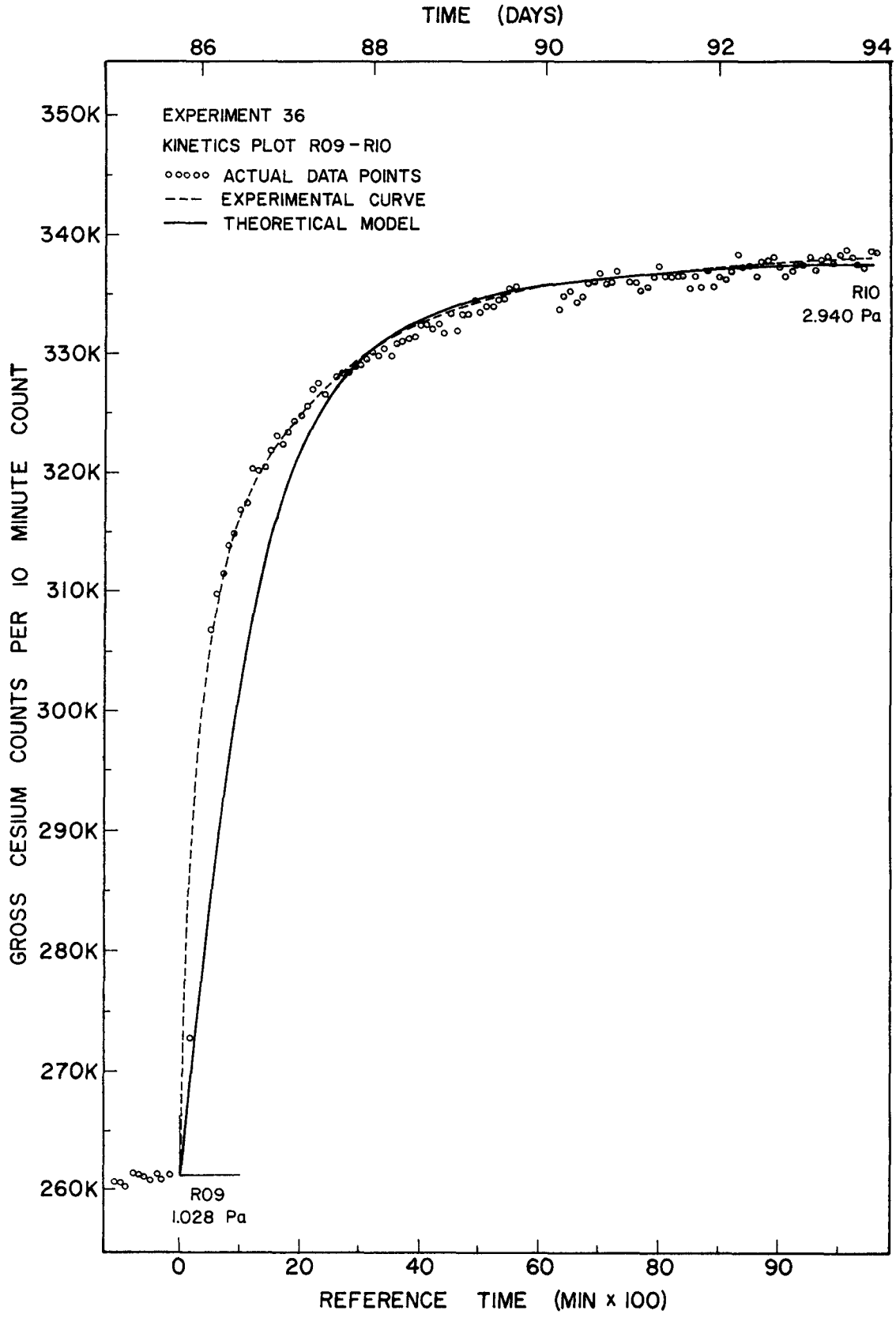

Figure 4.12. Experiment 36: Kinetic Behavior of Cesium on H-451 Graphite at 1273 K. R09-R10 Kinetics Plot.

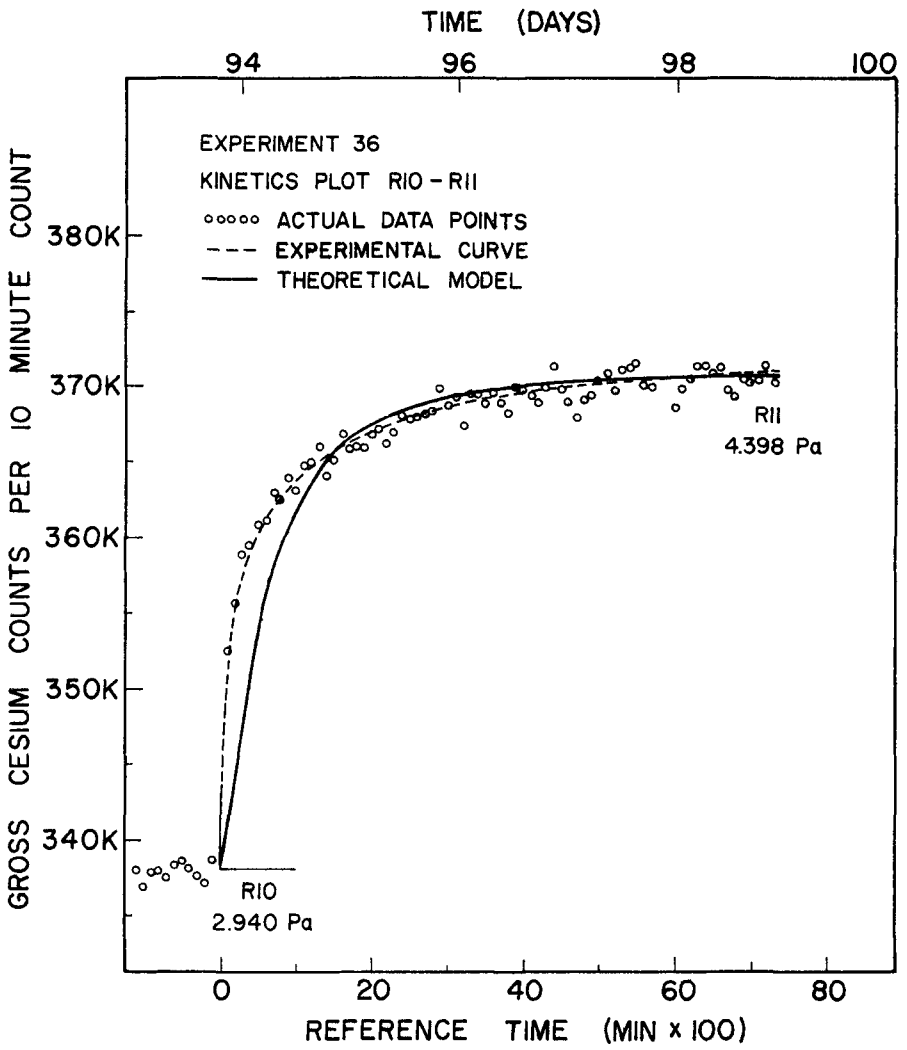

Figure 4.13. Experiment 36: Kinetic Behavior of Cesium on H-451 Graphite at 1273 K. R10 - R11 Kinetics Plot.

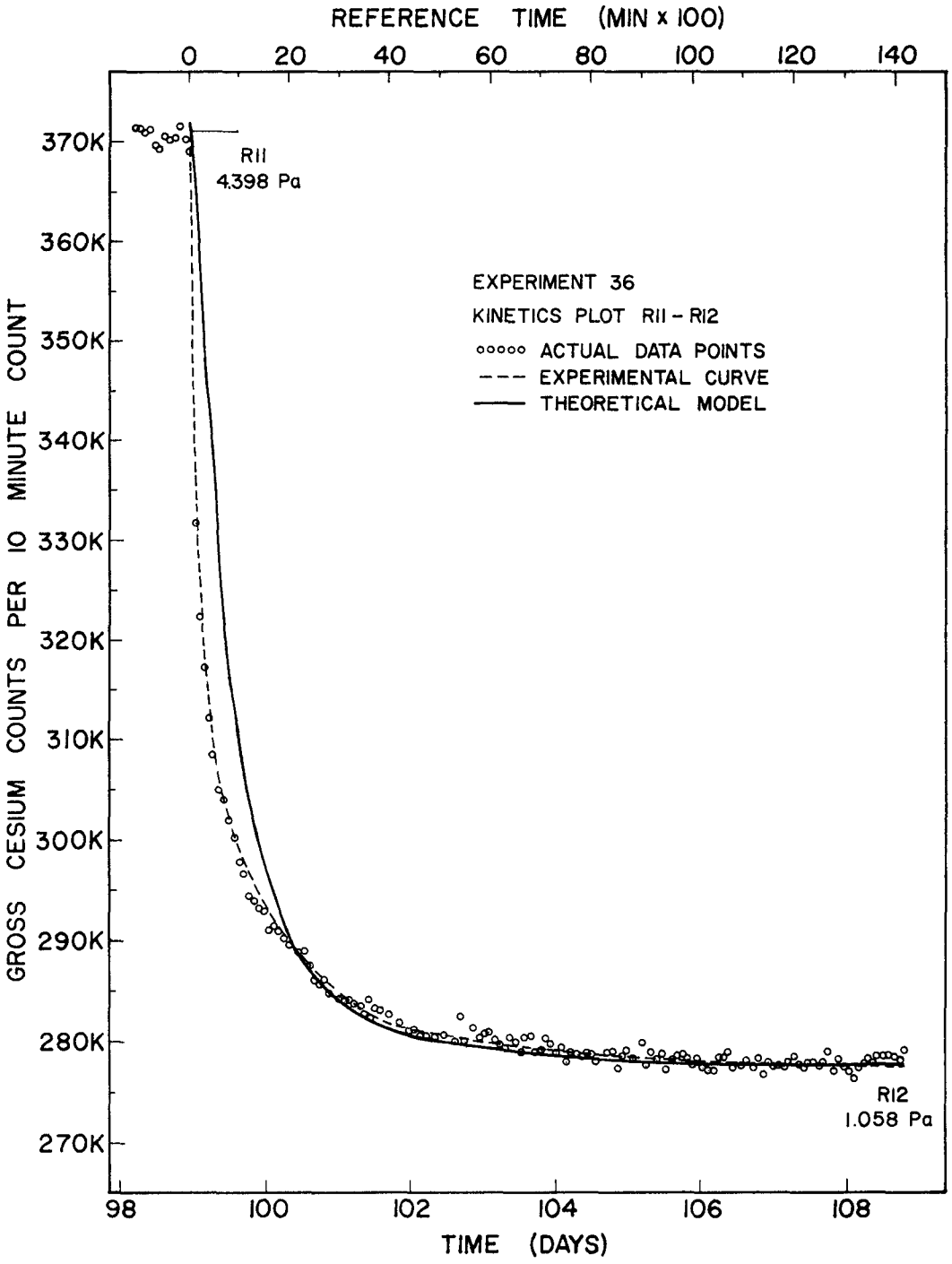

Figure 4.14. Experiment 36: Kinetic Behavior of Cesium on H-451 Graphite at 1273 K. R11 - R12 Kinetics Plot.

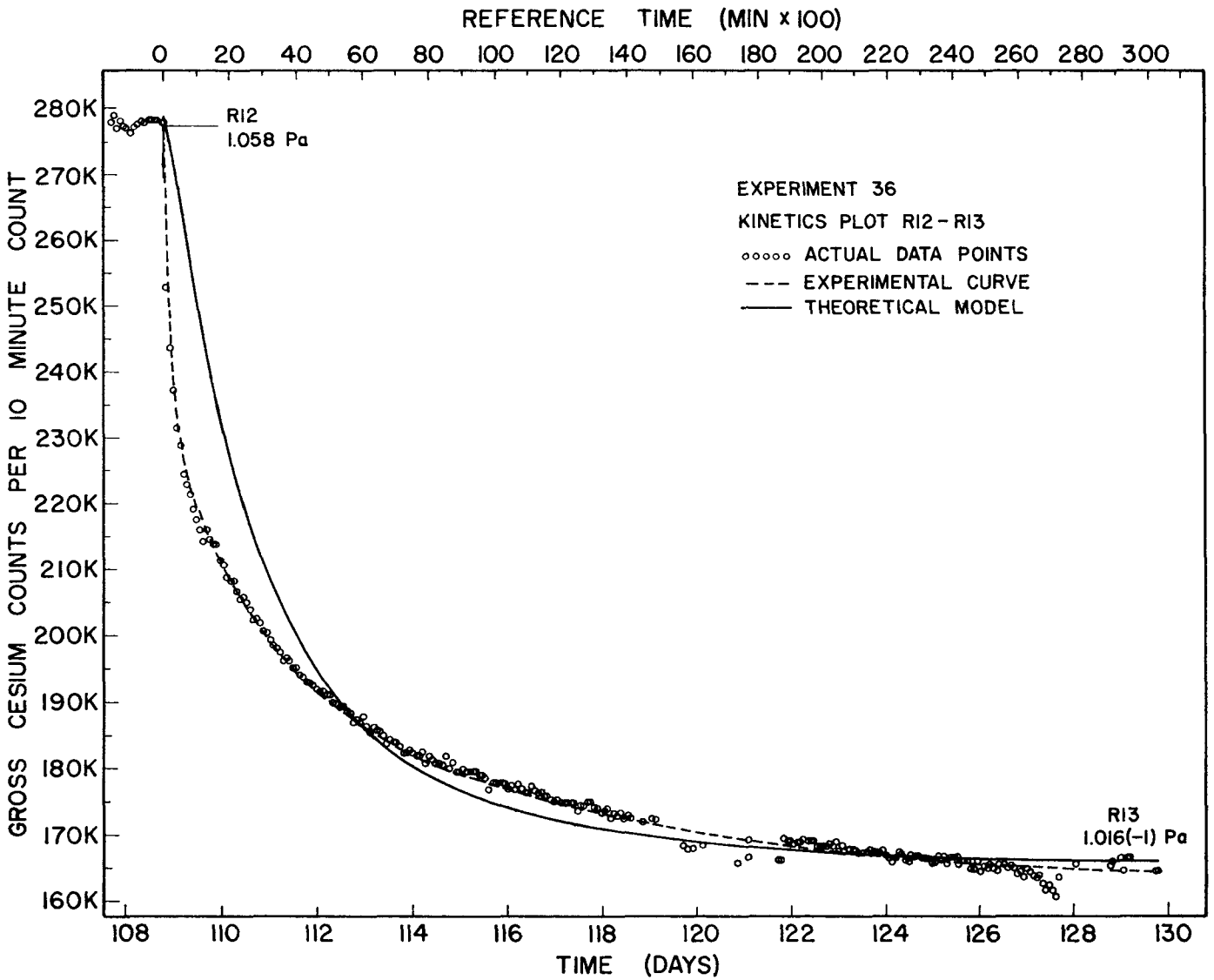

Figure 4.15. Experiment 36: Kinetic Behavior of Cesium on H-451 Graphite at 1273 K. R12 - R13 Kinetics Plot.

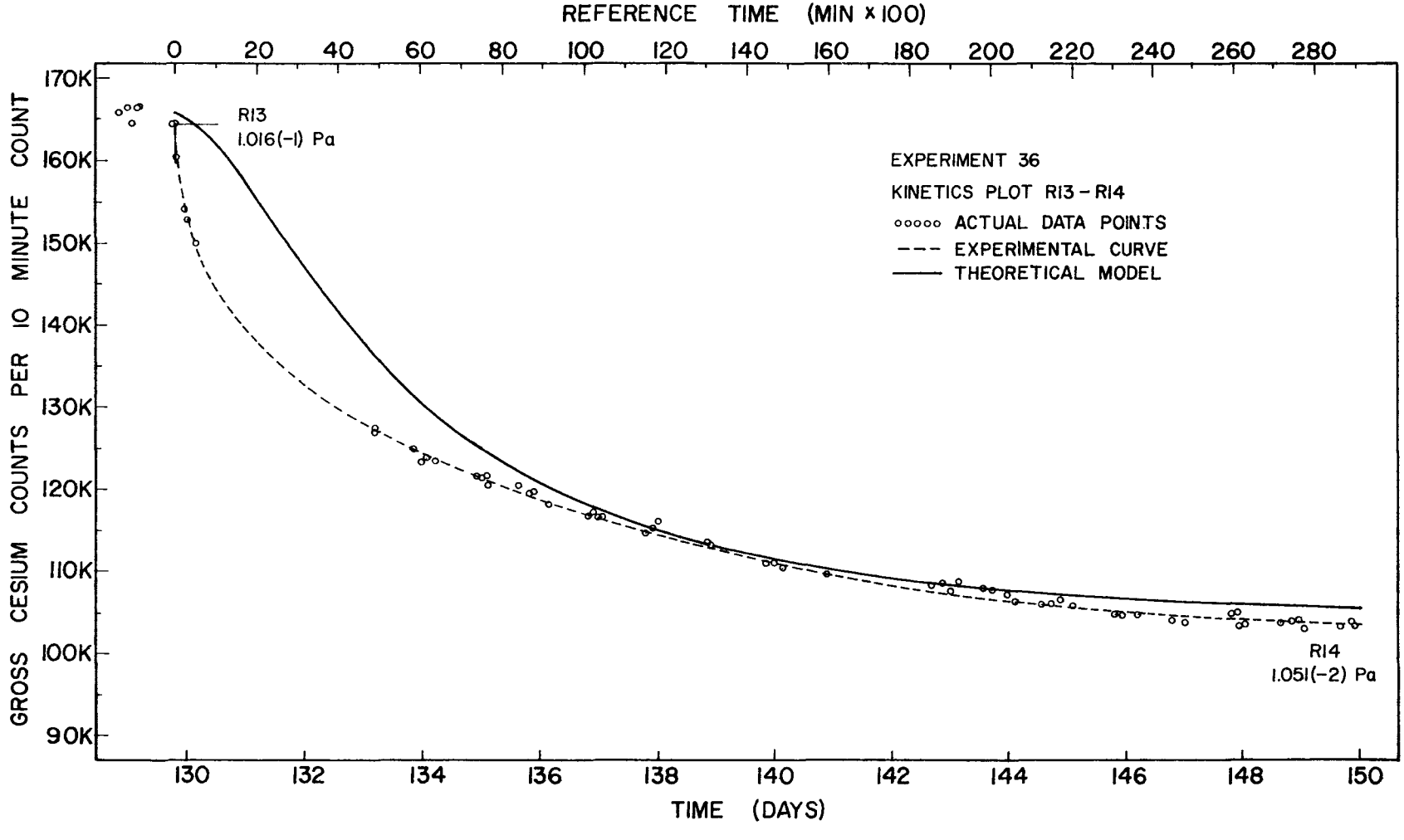

Figure 4.16. Experiment 36: Kinetic Behavior of Cesium on H-451 Graphite at 1273 K. R13 - R14 Kinetics Plot.

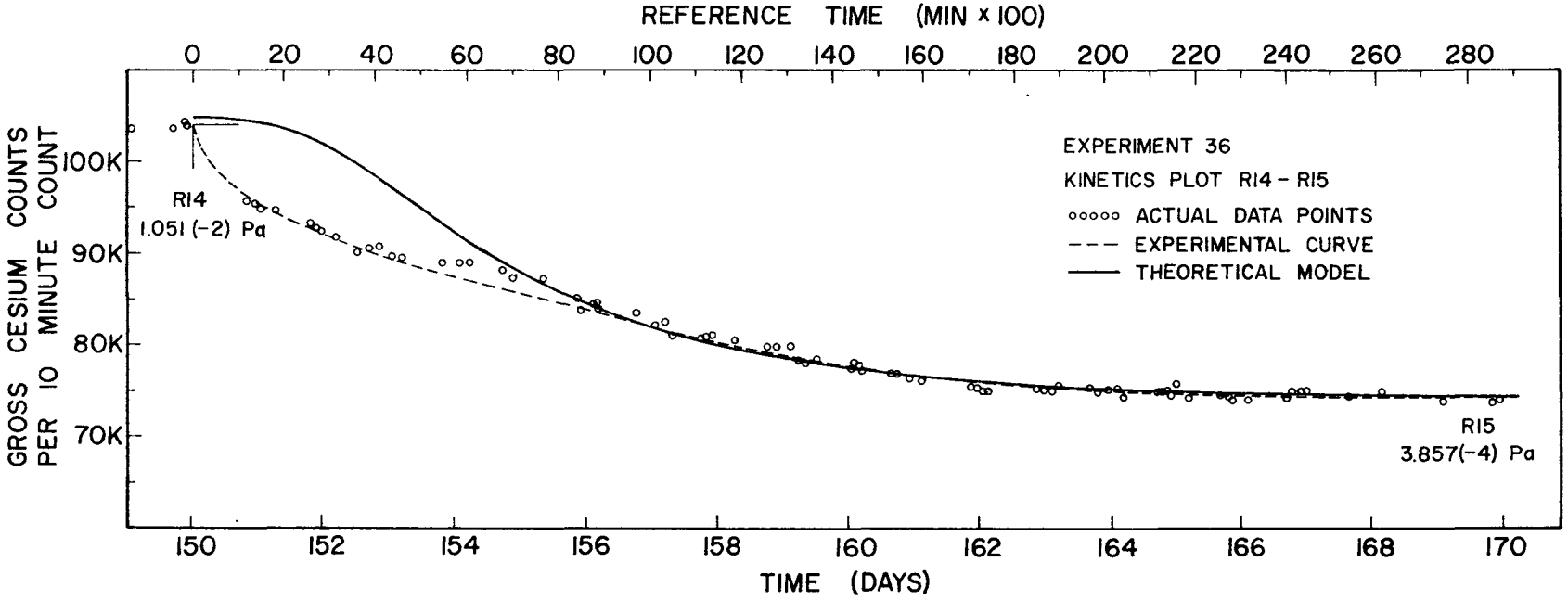

Figure 4.17. Experiment 36: Kinetic Behavior of Cesium on H-451 Graphite at 1273 K. R14 - R15 Kinetics Plot.

TABLE 4.2: EXPERIMENT 36

Data Points and Best Choice and Next Best Choice for the Kinetics Parameters A_s and f.

Equilibrium Data Points	Best Choice		Next Best Choice	
	$A_s (s^{-1})$	f	$A_s (s^{-1})$	f
R08 - R09	3×10^{-4}	0.95	5×10^{-4}	1.00
R09 - R10	3×10^{-4}	0.90	5×10^{-4}	1.00
R10 - R11	5×10^{-4}	1.00	3×10^{-4}	0.90
R11 - R12	5×10^{-4}	0.90	3×10^{-4}	0.80
R12 - R13	3×10^{-4}	0.95	5×10^{-4}	1.00
R13 - R14	5×10^{-4}	0.80	10×10^{-4}	0.875
R14 - R15	10×10^{-4}	0.50	5×10^{-4}	0.425

which plays a role when near-equilibrium sorption is attained. Nevertheless, it would appear that the activated sorption kinetics model in its present state is useful for approximating the kinetics of the sorption process.

4.3.2 Comparison of Theoretical with Observed Kinetics for Experiment 16.

Pyecha and Zumwalt made a kinetics analysis of sorption Experiment 16 in which the H-451 graphite sample at 1000^{o} C was exposed to a constant cesium vapor pressure of 1.3 Pa for 450 hours. The initial equilibrium pressure before changing to this value was 1.6×10^{-4} Pa. Their approach was based on the coupled diffusion model formulated by Zumwalt and Phelps (1975). The parameters determined from this model indicated transport of cesium by in-pore diffusion with a coefficient on the order of 10^{-7} cm^2/sec, and the slow diffusion phenomenon with a coefficient of 10^{-10} cm^2/sec. The slope towards equilibrium did not level off - indicating that equilibrium in which the bulk diffusion process was dominant was not attained.

Another approach that can be used to model the kinetic behavior involves the use of Equation 4.1 which is based on the theory of sorption given in Section 4.1. As indicated in Figure 4.18, the best A_s value obtained is 50×10^{-4} s^{-1} with f as 0.975. The next best parameter for A_s is 70×10^{-4} s^{-1} with a unity f value. In the latter half of the run, the theoretical prediction falls slightly below the experimental kinetics data, evidently due to the fact that the slow bulk diffusion process is not considered in the kinetics model. This would indicate that the bulk diffusion plays a role in the sorption process at long times.

Although the characteristic frequency (A_s) for this experiment is an order of magnitude higher than that of Experiment 36, it can be concluded that the kinetics theory can be applied to the sorption kinetic behavior with a fair degree of accuracy. However, some account must be taken of diffusion in bulk graphite at longer times (>200 hours).

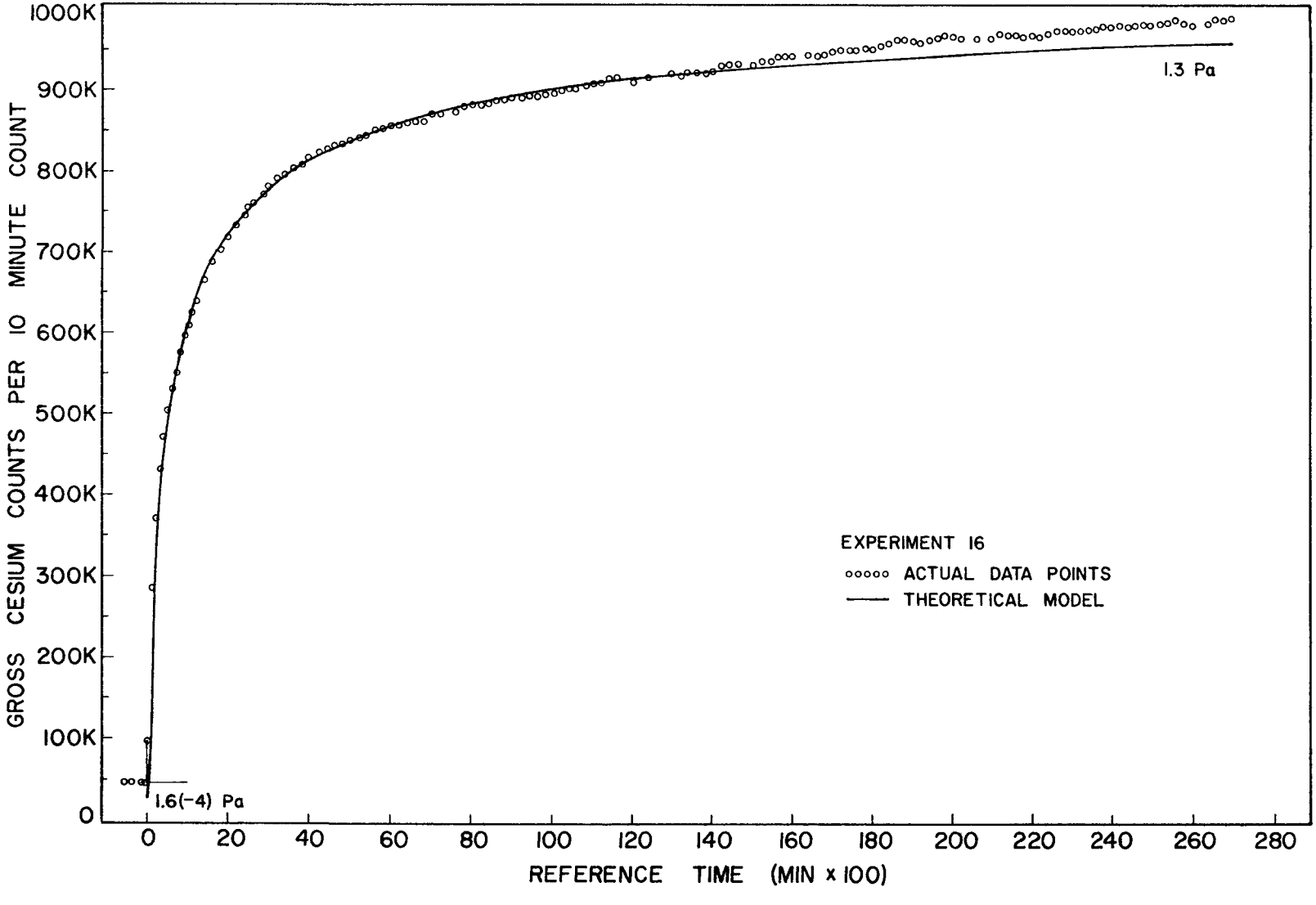

Figure 4.18. Experiment 16: Kinetic Behavior of Cesium on H-451 Graphite at 1273 K.

5. BINARY SORPTION

A study of the effect of barium on cesium sorption by H-451 nuclear graphite is reported and the previously reported study of the effect of strontium on sorption is presented with corrected data and revised results. The application of thermodynamic and FREVAP models are reviewed and the thermodynamic model with activity coefficients is applied to the binary sorption data.

5.1 Cesium Sorption Isotherms of Barium-Impregnated H-451 Graphite

Graphite samples were impregnated with barium in order to study the effect of barium on the sorption of cesium by graphite. Four isotherms obtained for barium-impregnated graphite at 1000° C in Experiments 33, 32, 31 and 35 are shown as log-log plots in Figures 5.1, 5.2, 5.3 and 5.4, respectively, the order being in increasing barium content of the graphite samples. Figure 2.9 gives the isotherm for zero barium concentration, Experiment 36. Tables 5.1, 5.2, 5.3 and 5.4 list the data from Experiments 33, 32, 31 and 35, respectively. Table 5.5 gives the data at zero barium concentration for comparison with the other barium-cesium sorption experiment data (Tables 5.1 thru 5.4). Generally, the binary sorption process took a shorter time to reach equilibrium than did the single component (cesium alone) sorption process. It is believed that the reason for this is that barium atoms could be expected to be homogeneously distributed in the graphite and would occupy some of the high energy sites leaving fewer sites with high activation energies for the cesium atoms to occupy at a slow rate.

During the absorption process, the loss of barium was high, especially for large loadings of barium in the graphite sample. The loss was as high as 35%. The barium loss could have resulted from a combination of two

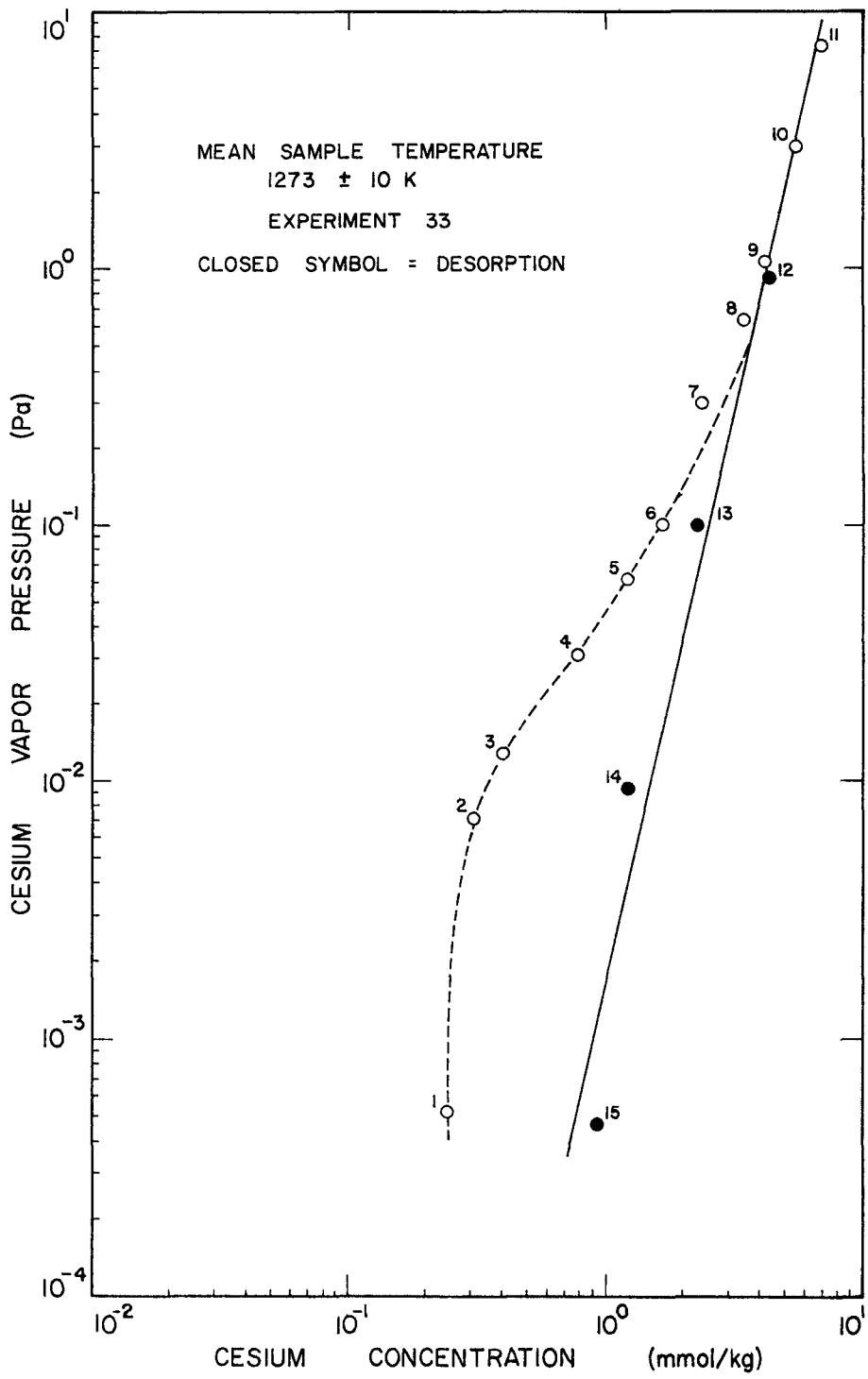

Figure 5.1. Experiment 33: Cesium Sorption by Barium-Impregnated H-451 Graphite at 1273 K. Average Barium Concentration for Desorption is 4.86 mmol Ba/kg.

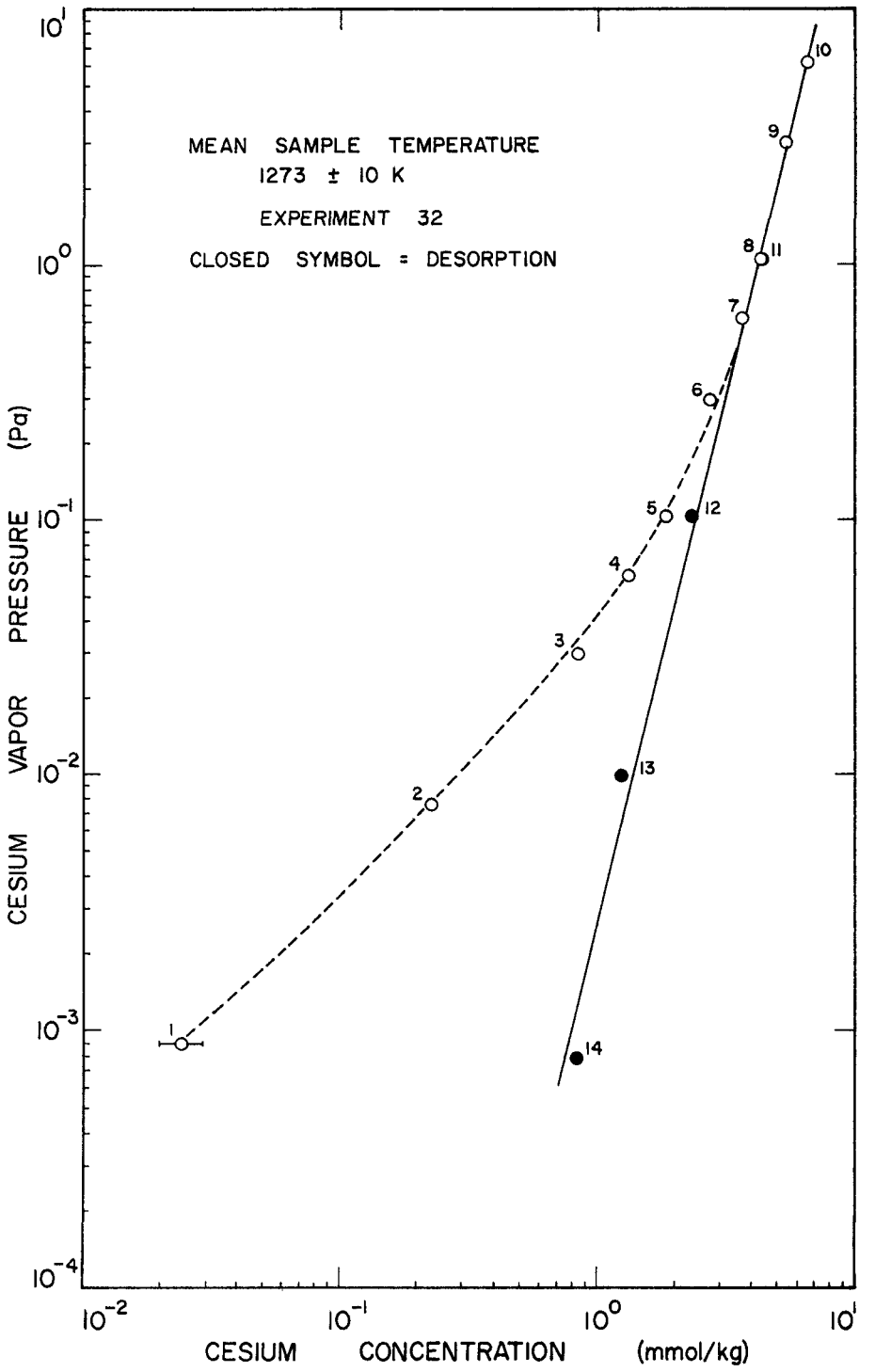

Figure 5.2. Experiment 32: Cesium Sorption by Barium-Impregnated H-451 Graphite at 1273 K. Average Barium Concentration for Desorption is 5.08 mmol Ba/kg.

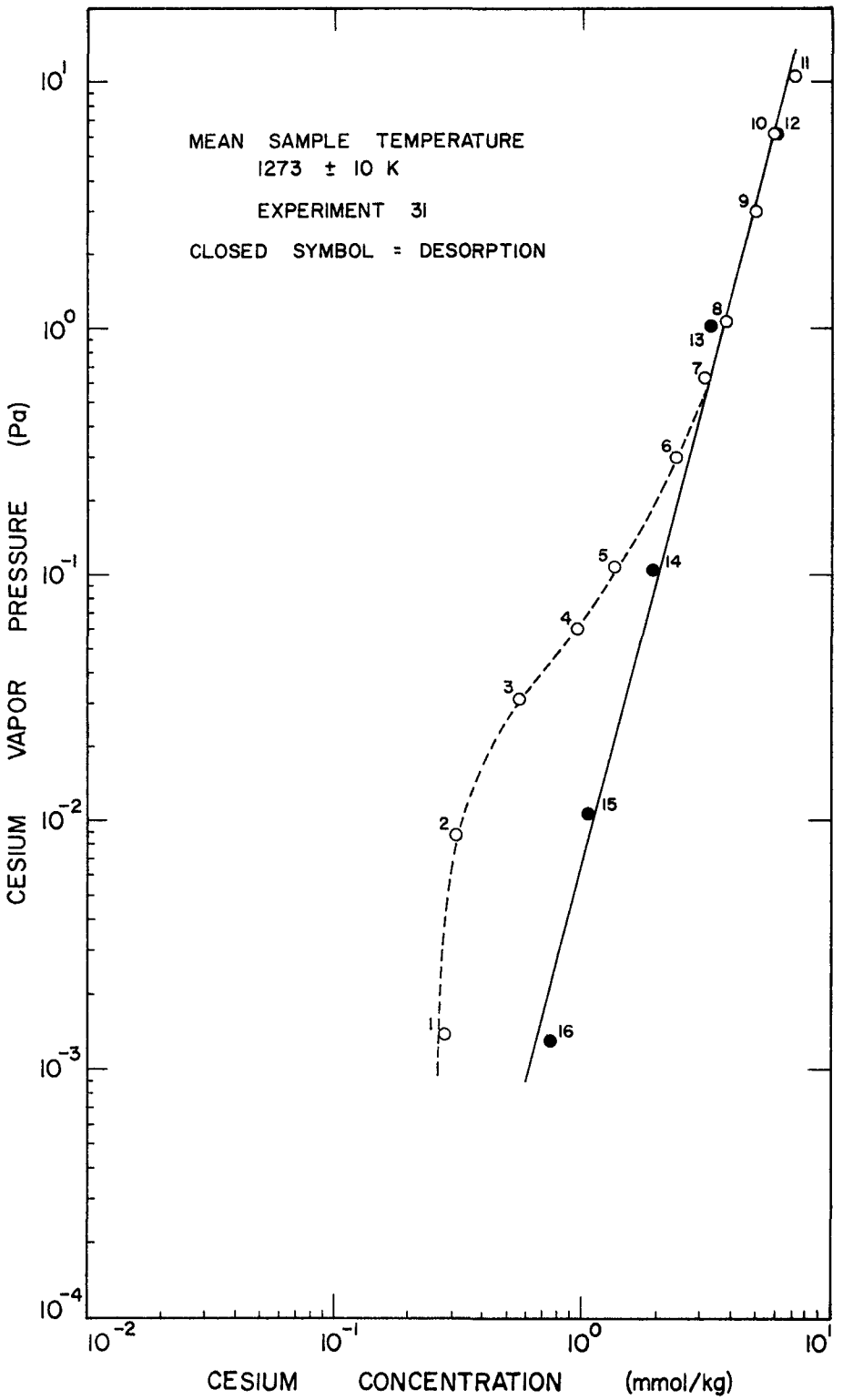

Figure 5.3. Experiment 31: Cesium Sorption by Barium-Impregnated H-451 Graphite at 1273 K. Average Barium Concentration for Desorption is 6.76 mmol Ba/kg.

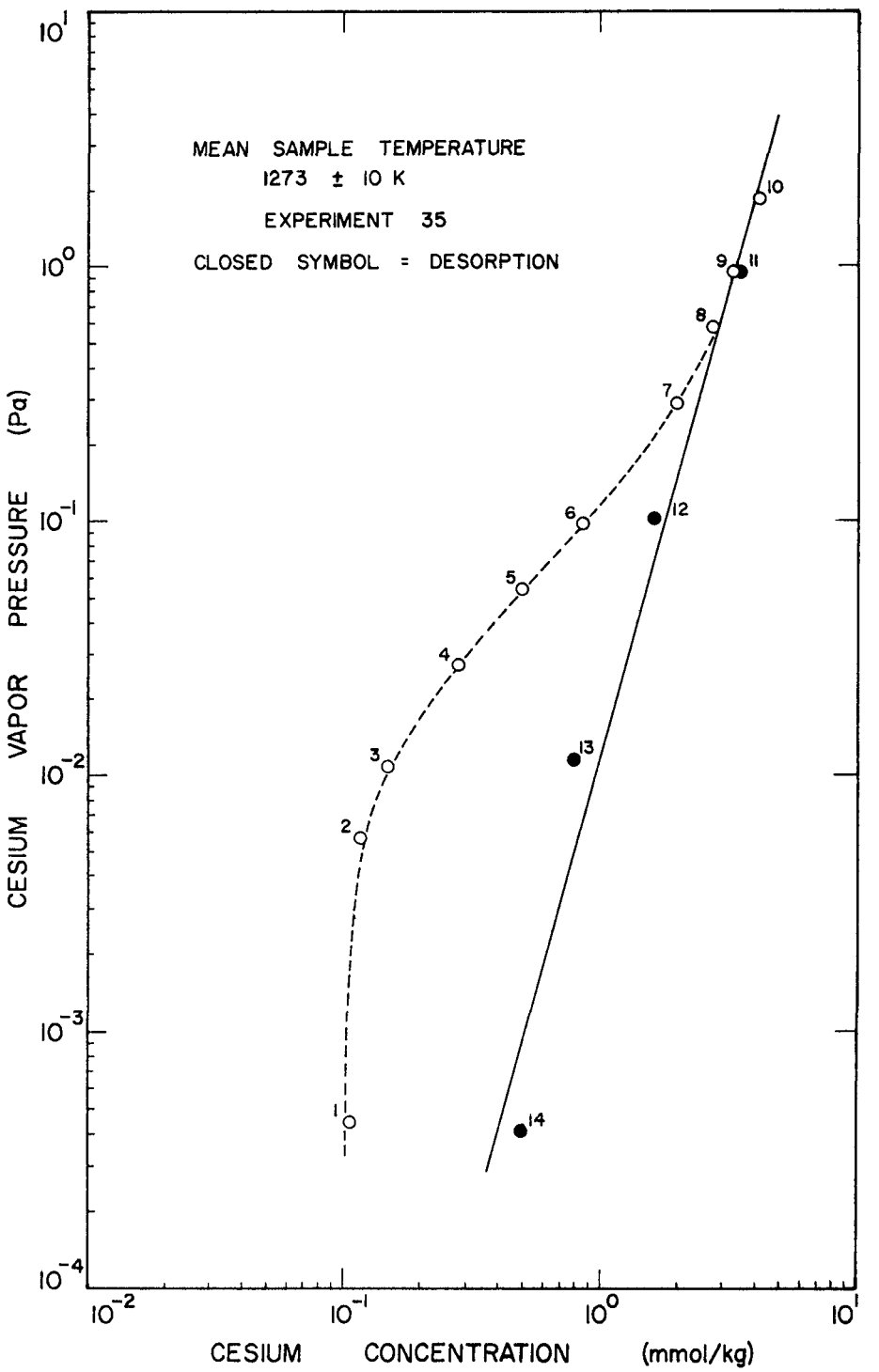

Figure 5.4. Experiment 35: Cesium Sorption by Barium-Impregnated H-451 Graphite at 1273 K. Average Barium Concentration for Desorption is 9.18 mmol Ba/kg.

TABLE 5.1

EXPERIMENT 33: Cesium Sorption on Barium Impregnated H-451 Graphite
H-451 Sample Weight: Before Impregnation = 3.7342 g

Run Sequence Number	Sample Temperature (10 K)	Source Temperature (2 K)	Sample Cesium Vapor Pressure(Pa)	Time at Vapor Pressure (hours)	Gross(a) Cesium Concentration (mmol Cs/kg C)	Net(b) Cesium Concentration (mmol Cs/kg C)	Gross(a) Barium Concentration (mmol Ba/kg C)	Net(b) Barium Concentration (mmol Ba/kg C)
R00	294	294	1.174(-4)(c)	815.7	1.262		9.859	
R01	1273	301.8	5.265(-4)	67.5	0.250	0.247	9.537	
R02	1273	331.7	7.138(-3)	49.9	0.317	0.310	9.604	
R03	1272	339.3	1.283(-3)	47.4	0.412	0.403	9.790	
R04	1273	351.8	3.126(-2)	97.0	0.698	0.686	9.689	
R05	1273	362.2	6.164(-2)	215.5	1.242	1.227	9.698	
R06	1273	370.4	1.014(-1)	143.6	1.693	1.675	9.724	
R07	1273	391.2	3.020(-1)	259.2	2.388	2.363	7.571	
R08	1273	407.5	6.346(-1)	146.9	3.462	3.429	8.165	
R09	1273	419.4	1.071	141.5	4.196	4.158	8.099	
R10	1273	443.0	3.003	124.5	5.505	5.450	7.992	
R11	1273	464.4	7.349	97.5	6.942	6.867	8.008	5.051
R12	1273	416.0	9.199(-1)	193.3	4.354	4.280	8.016	5.058
R13	1273	370.2	1.000(-1)	191.2	2.359	3.285	7.887	4.930
R14	1272	335.2	9.354(-3)	262.6	1.307	1.232	7.770	4.812
R15	1273	300.6	4.665(-4)	163.0	1.014	0.940	7.413	4.455
EOR(d)					0.995	0.920	7.801	4.843
Tube(e)					0.074		2.957	
Sample	(sample only - in situ but clean tube)				0.767		4.032	

(a) Not corrected for tube background contribution
(b) Corrected for tube background contribution
(c) Read as 1.174×10^{-4}
(d) End of run in situ(sample and tube)-cesium oxidized
(e) End of run tube background (sample removed)

TABLE 5.2

EXPERIMENT 32: Cesium Sorption on Barium Impregnated H-451 Graphite
H-451 Sample Weight: Before Impregnation = 3.7375 g

Run Sequence Number	Sample Temperature (10 K)	Source Temperature (2 K)	Sample Cesium Vapor Pressure(Pa)	Time at Vapor Pressure (hours)	Gross(a) Cesium Concentration (mmol Cs/kg C)	Net(b) Cesium Concentration (mmol Cs/kg C)	Gross(a) Barium Concentration (mmol Ba/kg C)	Net(b) Barium Concentration (mmol Ba/kg C)
R00	297	297	1.597(-4)(c)	503.8	0.019		8.609	
R01	1273	307.6	9.068(-4)	91.3	0.030	0.020	8.295	
R02	1275	332.5	7.626(-4)	141.2	0.249	0.229	8.062	
R03	1273	351.2	2.993(-2)	361.4	0.884	0.853	7.859	
R04	1273	362.0	6.095(-2)	260.2	1.360	1.320	7.549	
R05	1273	370.9	1.042(-1)	292.1	1.891	1.844	7.238	
R06	1273	391.0	2.992(-1)	237.3	2.794	2.727	6.841	
R07	1273	407.1	6.232(-1)	194.8	3.708	3.621	6.823	
R08	1273	419.3	1.064	190.1	4.398	4.293	6.698	
R09	1273	443.1	3.012	169.7	5.503	5.355	6.456	
R10	1273	460.2	6.174	161.2	6.713	6.525	6.394	
R11	1273	419.3	1.058	150.7	4.585	4.396	6.408	5.124
R12	1273	370.9	1.042(-1)	233.8	2.514	2.327	6.325	5.040
R13	1273	335.9	9.872(-3)	360.1	1.437	1.249	6.497	5.213
R14	1273	306.2	7.931(-4)	241.1	1.033	0.845	6.240	4.956
EOR(d)					1.047	0.859	6.228	4.944
Tube(e)					0.188		1.284	
Sample	(sample only - in situ but clean tube)				0 910		4.816	

(a) Not corrected for tube background contribution
(b) Corrected for tube background contribution
(c) Read as 1.597×10^{-4}
(d) End of run in situ (sample and tube)-cesium oxidized
(e) End of run tube background (sample removed)

TABLE 5.3

EXPERIMENT 31: Cesium Sorption on Barium Impregnated H-451 Graphite
H-451 Sample Weight: Before Impregnation = 3.7227 g

Run Sequence Number	Sample Temperature (10 K)	Source Temperature (2 K)	Sample Cesium Vapor Pressure(Pa)	Time at Vapor Pressure (hours)	Gross(a) Cesium Concentration (mmol Cs/kg C)	Net(b) Cesium Concentration (mmol Cs/kg C)	Gross(a) Barium Concentration (mmol Ba/kg C)	Net(b) Barium Concentration (mmol Ba/kg C)
R00	297	297	1.597(-4)(c)	1702.8	1.180		11.860	
R01	1274	312.3	1.393(-3)	90.6	0.288	0.280	11.274	
R02	1274	334.3	8.777(-3)	122.4	0.327	0.312	10.880	
R03	1274	351.8	3.138(-2)	164.7	0.585	0.563	10.583	
R04	1274	361.8	6.045(-2)	285.7	0.982	0.955	10.053	
R05	1273	371.4	1.075(-1)	190.1	1.385	1.352	9.786	
R06	1274	391.0	3.000(-1)	337.1	2.418	2.371	9.225	
R07	1273	407.3	6.271(-1)	192.4	3.132	3.072	8.725	
R08	1273	419.3	1.064	194.8	3.843	3.771	8.625	
R09	1273	443.1	3.012	189.6	5.068	4.966	8.360	
R10	1274	460.0	6.138	122.2	5.992	5.863	8.190	
R11	1273	473.3	1.040(+1)	165.4	7.298	7.143	8.219	6.946
R12	1274	459.8	6.071	110.2	6.303	6.149	8.137	6.864
R13	1273	418.2	1.014	126.9	3.391	3.236	8.128	6.855
R14	1274	371.0	1.050(-1)	314.6	2.070	1.915	7.847	6.575
R15	1273	337.0	1.074(-2)	287.4	1.210	1.055	8.044	6.771
R16	1273	311.6	1.304(-3)	190.7	0.904	0.749	7.807	6.534
EOR(d)					0.901	0.746	7.676	6.404
Tube(e)					0.154		1.272	
Sample	(sample only - in situ but clean tube)				0.758		6.322	

(a) Not corrected for tube background contribution
(b) Corrected for tube background contribution
(c) Read as 1.597×10^{-4}
(d) End of run in situ (sample and tube)-cesium oxidized
(e) End of run tube background (sample removed)

TABLE 5.4

EXPERIMENT 35: Cesium Sorption on Barium Impregnated H-451 Graphite
H-451 Sample Weight: Before Impregnation = 3.7326 g

Run Sequence Number	Sample Temperature (10 K)	Source Temperature (2 K)	Sample Cesium Vapor Pressure(Pa)	Time at Vapor Pressure (hours)	Gross(a) Cesium Concentration (mmol Cs/kg C)	Net(b) Cesium Concentration (mmol Cs/kg C)	Gross(a) Barium Concentration (mmol Ba/kg C)	Net(b) Barium Concentration (mmol Ba/kg C)
R00	294	294	1.174(-4)(c)	304.1	1.039		21.069	
R01	1272	300.1	4.458(-4)	88.1	0.109	0.107	18.057	
R02	1273	328.9	5.723(-3)	40.5	0.122	0.118	16.450	
R03	1273	337.1	1.082(-2)	52.5	0.155	0.150	15.810	
R04	1274	349.9	2.737(-2)	69.8	0.289	0.283	16.098	
R05	1273	360.2	5.436(-2)	99.3	0.514	0.506	15.103	
R06	1273	369.9	9.847(-2)	115.1	0.877	0.868	14.747	
R07	1273	390.5	2.920(-1)	246.9	2.017	2.003	14.007	
R08	1273	405.5	5.790(-1)	186.8	2.756	2.739	12.505	
R09	1273	416.8	9.511(-1)	96.9	3.330	3.309	12.185	
R10	1274	432.0	1.856	167.2	4.206	4.180	11.875	
R11	1273	416.7	9.482(-1)	88.2	3.553	3.527	11.819	9.631
R12	1273	370.5	1.020(-1)	216.7	1.672	1.646	11.540	9.352
R13	1273	338.0	1.156(-2)	219.6	0.830	0.805	11.149	8.961
R14	1274	299.3	4.130(-4)	213.2	0.525	0.500	10.951	8.762
EOR(d)					0.525	0.500	10.909	8.721
Tube(e)					0.026		2.188	
Sample	(sample only - in situ but clean tube)				0.445		7.660	

(a) Not corrected for tube background contribution
(b) Corrected for tube background contribution
(c) Read as 1.174×10^{-4}
(d) End of run in situ (sample and tube)-before oxidizing cesium
(e) End of run tube background (sample removed)

TABLE 5.5 EXPERIMENT 36: Cesium Sorption on Barium-Free H-451 Graphite

Run Sequence Number	Sample Temperature (10 K)	Source Temperature (2 K)	Sample Cesium Vapor Pressure(Pa)	Time at Vapor Pressure (hours)	Gross(a) Cesium Concentration (mmol Cs/kg C)	Net(b) Cesium Concentration (mmol Cs/kg C)
R00	297	297	1.597(-4)(c)	841.9	2.172	
R01	1273	298.1	3.649(-4)	115.1	0.566	0.565
R02	1273	328.0	5.314(-3)	94.8	0.740	0.737
R03	1273	336.2	1.008(-2)	124.7	0.894	0.890
R04	1273	350.2	2.807(-2)	430.6	1.426	1.422
R05	1272	360.9	5.681(-2)	211.3	1.821	1.815
R06	1274	370.4	1.014(-1)	218.6	2.384	2.377
R07	1273	389.9	2.844(-1)	359.9	3.631	3.621
R08	1273	405.3	5.754(-1)	337.0	4.571	4.559
R09	1272	418.6	1.028	166.2	5.331	5.316
R10	1272	442.5	2.940	193.2	6.779	6.757
R11	1272	452.0	4.398	123.2	7.409	7.385
R12	1272	419.2	1.058	236.7	5.546	5.521
R13	1272	370.5	1.016(-1)	504.4	3.195	3.171
R14	1272	336.8	1.051(-2)	485.2	2.034	2.009
R15	2173	298.7	3.857(-4)	484.0	1.327	1.302
EOR(d)					1.339	1.314
Tube(e)					0.024	
Sample	(sample only - in situ but clean tube)				1.279	

(a) Not corrected for tube background contribution
(b) Corrected for tube background contribution
(c) Read as 1.597×10^{-4}
(d) End of run in situ (sample and tube)-cesium oxidized
(e) End of run tube background (sample removed)

factors: the time dependent loss, and the displacement of barium atoms sorbed onto the sites by cesium atoms. Figure 5.5 shows the absorption and desorption kinetic behavior in the high cesium vapor pressure region. In observing the approach towards equilibrium, it is noted that the cesium concentration appears to be following a somewhat erratic pattern of sorption behavior with respect to the run time - in contrast to the smooth approach to equilibrium observed in barium-free sorption experiments. This is possibly due to the fact that cesium and barium atoms are in the process of being exchanged on various sorption sites at different rates. For high barium loadings, an equilibrium data point was taken to have been reached when a change of 0.02 - 0.03 mmol Cs/kg occurred in one day instead of the usual rate of 0.01 - 0.015 mmol Cs/kg per day. This was done to minimize the time dependent loss of barium so that a better estimate could be made of the effect of barium on cesium sorption. In the desorption process the total loss of barium was found to be less than 10%, which is low compared to the initial loss of barium (up to 35%) in the absorption stage (see Tables 5.1, 5.2, 5.3 and 5.4).

The sorption isotherms show a distinct hysteresis occurring in the range between 0.5 and 1 Pa pressure. No definite conclusion can be made for the effect of barium on the magnitude of the hysteresis effect. Cesium sorption Experiments 12, 13, 17 and 18 performed by Pyecha and Zumwalt (1) on strontium-impregnated graphite indicate an apparent tendency for the hysteresis to disappear as the strontium content in a graphite sample is increased. In the case of barium-impregnated graphite, the hysteresis did not disappear.

The desorption isotherms derived with parameters obtained by an unweighted, linear least-squares fit are shown in Figure 5.6 for barium-

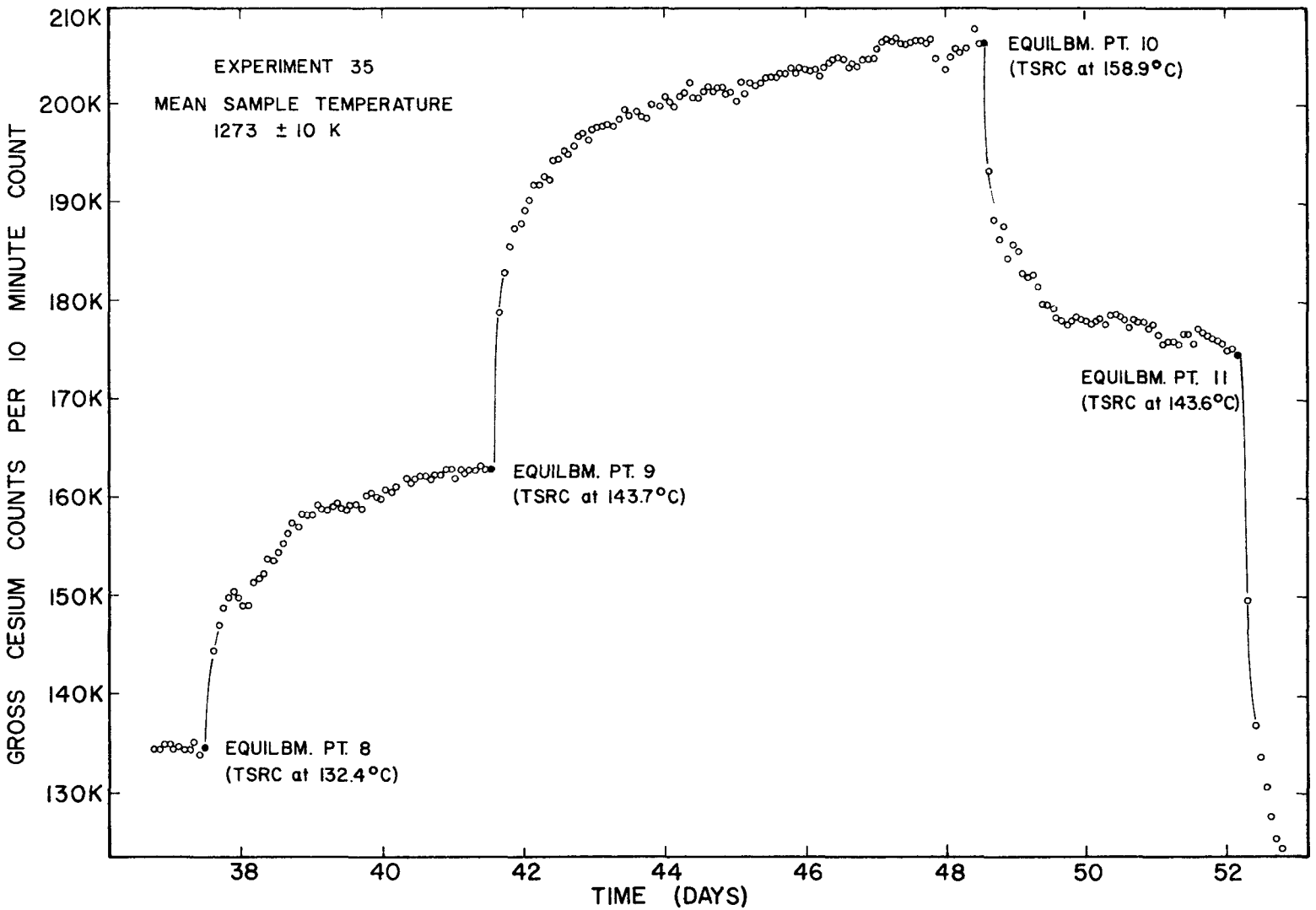

Figure 5.5. Experiment 35: Kinetic Behavior of Cesium in Barium-Impregnated H-451 Graphite at 1273 K.

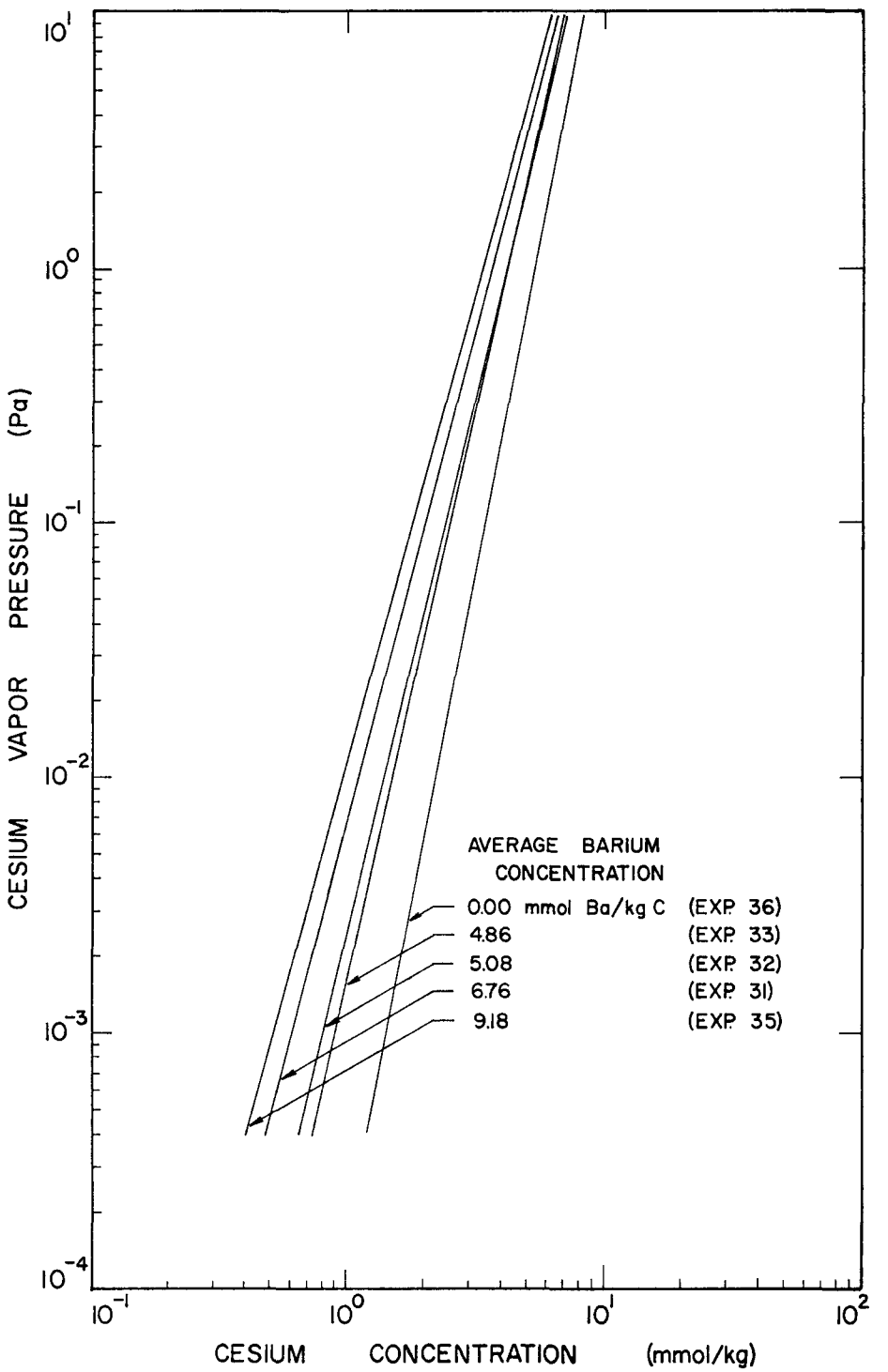

Figure 5.6. Least-Squares Fit for Cesium Desorption Isotherms over Barium-Impregnated H-451 Graphite at 1273 K.

impregnated H-451 graphite. The empirical constants in the relationship

$$\ln P = (A + B \frac{10^3}{T}) + (D + E \frac{10^3}{T}) \ln C \qquad (2.1)$$

lead to the expression for parameters $a = A + B \frac{1}{1.273}$ and $b = D + E \frac{1}{1.273}$. These parameters are presented in Table 5.6. Determination of a and b rather than the constants A, B, D and E was necessary because the experimental study was carried out at a single temperature (1000° C).

Table 5.6. Cesium Desorption Isotherm Parameters for Barium-Impregnated H-451 Graphite at 1273 K

Unweighted Linear Least-Squares Fit of Data to:

$$\ln P(Pa) = a + b \ln C \text{ (mmol/kg)} \qquad (5.1)$$

where $a = (A + B\ 10^3/T)$ (5.2a)

$b = (D + E\ 10^3/T)$ (5.2b)

Experiment Number	a	b	Average Barium Concentration mmol/kg
36	- 8.681	5.193	0.00
33	- 6.454	4.487	4.86
32	- 6.001	4.198	5.08
31	- 5.006	3.866	6.76
35	- 4.471	3.681	9.18

Figure 5.7 shows the cesium vapor pressure plotted as a function of barium concentration at various cesium concentrations. The barium concentrations obtained were averaged over the desorption stages of the experiments and the cesium vapor pressures were determined from a least-squares

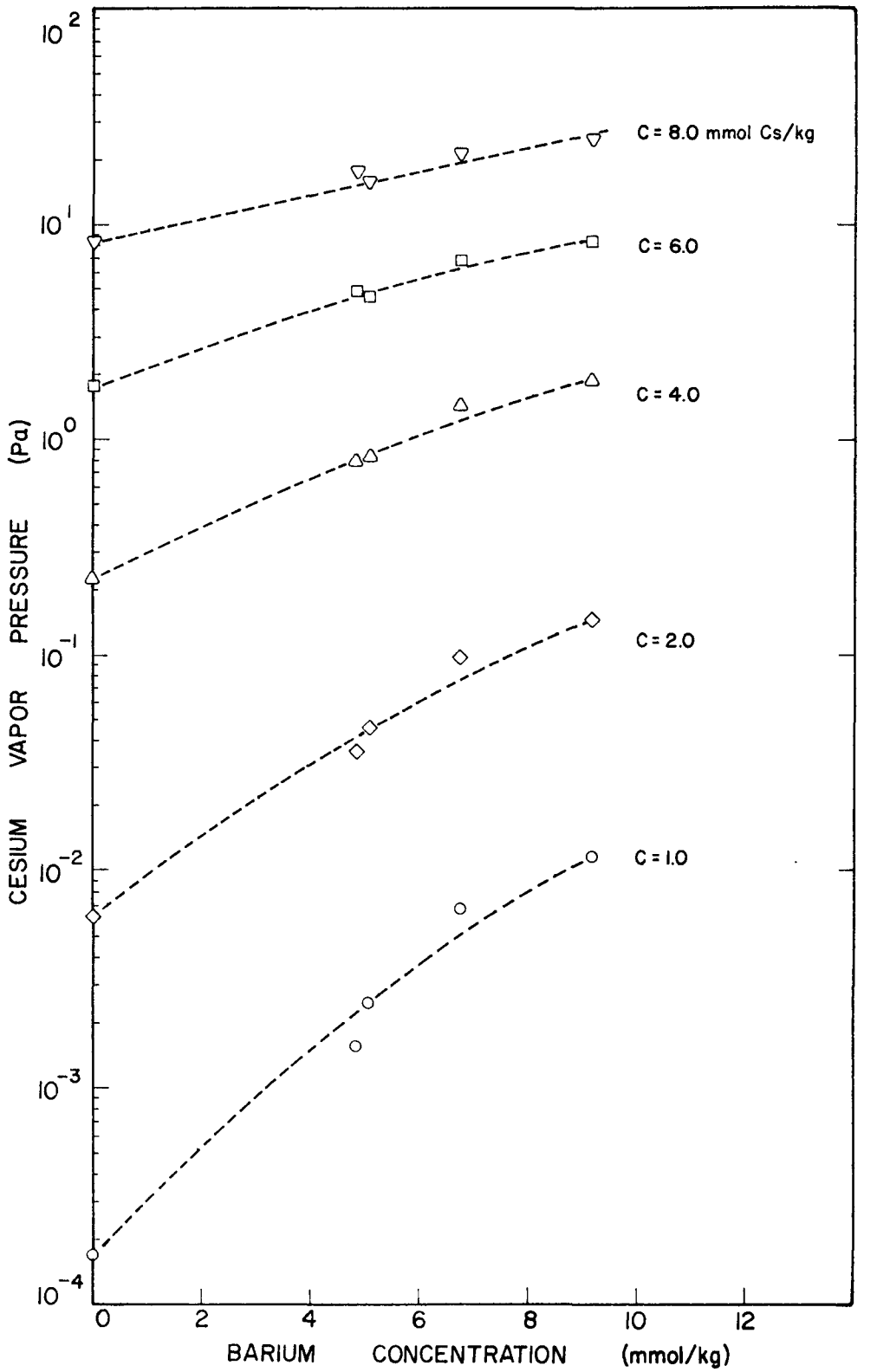

Figure 5.7. Cesium Desorption Isotherms for Barium-Impregnated H-451 Graphite at 1273 K.

fit of the desorption isotherms. Background activity correction as discussed in Appendix V was applied. As shown in Figure 5.7, the log of cesium vapor pressure is approximately linear with an increase in barium concentration. The slope of the log of cesium vapor pressure decreases with an increased loading of barium. As predicted by the sorption theory for constant cesium content, the cesium vapor pressure increases with greater concentration of barium. This corresponds to a decrease in the number of available higher-energy sorption sites; in other words, a decrease in the effective interaction energy of the sites. As concluded from Figure 5.7 the log of cesium vapor pressure as a function of barium concentration is approximately a linear relationship and there is no indication of a maximum. This strongly suggests that the coverage of barium and cesium atoms is indeed that of sub-monolayer and that no multi-layer sorption is to be expected. It is concluded that the presence of barium in graphite does have a substantial effect on the sorption of cesium. The data is treated thermodynamically in Section 5.3.

5.2 Cesium Sorption Isotherms on Strontium-Impregnated H-451 Graphite

As reported previously (1) but with revised, corrected data and revised standard international units (SI), four cesium sorption isotherms on H-451 graphite samples initially impregnated to various known levels of strontium concentration were obtained at approximately 1273 K. Two of these utilized finned cylindrical graphite samples (Experiments 12 and 13) and two utilized solid cylindrical samples (Experiments 17 and 18). The samples were impregnated as described previously (1). Although the loss of strontium continued throughout each experiment, the strontium concentrations were within 10% of the final equilibrium strontium values after approximately 1100 hours, or less, of exposure at the experimental sample temperature and accordingly,

little loss occurred during the desorption phase of each isotherm. The average concentration of strontium for each isotherm was obtained by averaging the strontium concentration, corrected for the sample tube background, observed at each equilibrium cesium sorption or desorption point used in the linear least-squares fit to the Freundlich relation

$$\ln P = a + b \ln C \qquad (5.1)$$

where P is the cesium vapor pressure in pascals, C is the cesium concentration sorbed in mmol Cs/ kg graphite, and a and b are the desorption coefficients.*

The estimated values of the coefficients a and b of Equation (5.1) and the statistical results of the fit are tabulated in Table 5.7 for each isotherm obtained at the indicated average strontium concentrations. Also included in the table are the results of the strontium-free 1271 K isotherm data obtained in Experiments 5, 7 and 9 and similarly fitted to Equation (5.1). All of the equilibrium data points of the strontium-impregnated experiments and those points included in the strontium-free 1271 K isotherm fit are summarized in Figure 5.8. The fitted relation is represented by the solid lines over the range of vapor pressures studied. The significant effect of the presence of strontium is apparent. Although there is no <u>a priori</u> reason for the sorption of cesium in the presence of strontium to follow the Freundlich relation, the equilibrium point data clearly show this to be the case. Figure 5.9 shows cesium vapor pressure as a function of strontium concentration with cesium

---

*Note: $a = A + B\left(\frac{10^3}{1273}\right)$ (5.2a), $b = D + E\left(\frac{10^3}{1273}\right)$ (5.2b)
where A, B, D, & E are the empirical Freundlich coefficients of Equation 2.1.

TABLE 5.7. Cesium Desorption Isotherm Coefficients for Strontium Impregnated H-451 Graphite

Non-weighted, linear-least-squares set of

$$\ln P = a + b \ln C \qquad (5.1)$$

where: P = cesium vapor pressure (pascals)
C = cesium equilibrium concentration mmol Cs/kg graphite)

Average Strontium Concentration (mmol/kgC	Sample Temperature (± 10K)	Experiment Number	Coefficient Estimates a ± σ	Coefficient Estimates b ± σ	Linear Correlation Coefficient Squared	Mean Square Error (b)	Number of data Points Fitted
0.00	1271	5,7 and 9	-10.140 ± 0.345	5.084 ± 0.176	0.985	0.0818	17
0.59	1271	13(c)	- 8.511 ± 0.244	4.684 ± 0.141	0.985	0.1378	7
2.00	1270	13(c)	- 6.622 ± 0.173	4.217 ± 0.131	0.994	0.0396	8
2.46	1273	18	- 6.690 ± 0.213	4.264 ± 0.172	0.994	0.0682	6
3.38	1273	17	- 5.091 ± 0.137	3.301 ± 0.129	0.986	0.832	11

σ = standard (root mean square) deviation

(b) mean square error = $\left(\frac{1}{n-k-i} \right) \sum_{i=1}^{n} (y_i - g_i)^2$

(c) finned cylindrical sample

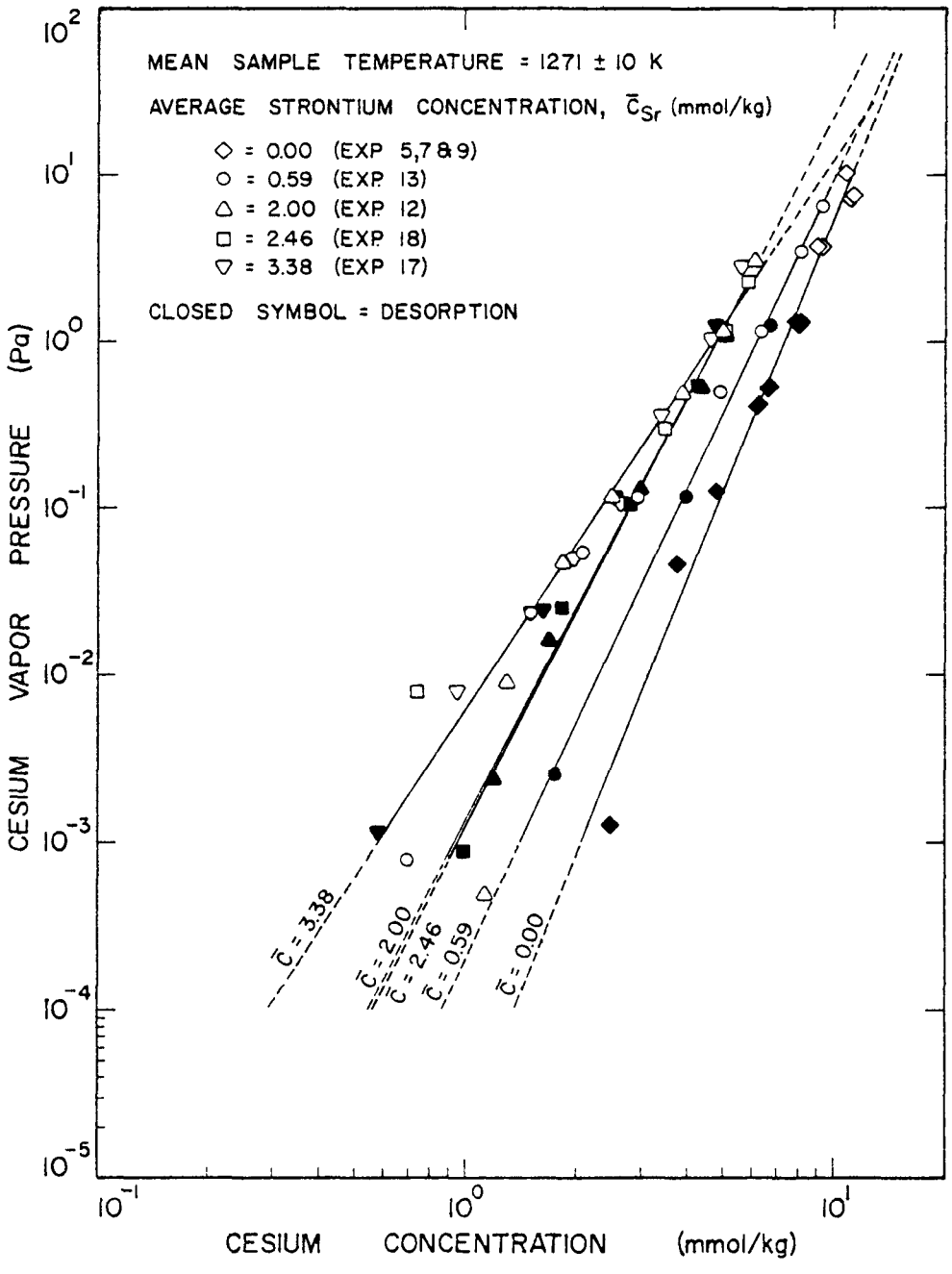

Figure 5.8. Freundlich fit of Cesium Sorption on Strontium Impregnated H-451 Graphite

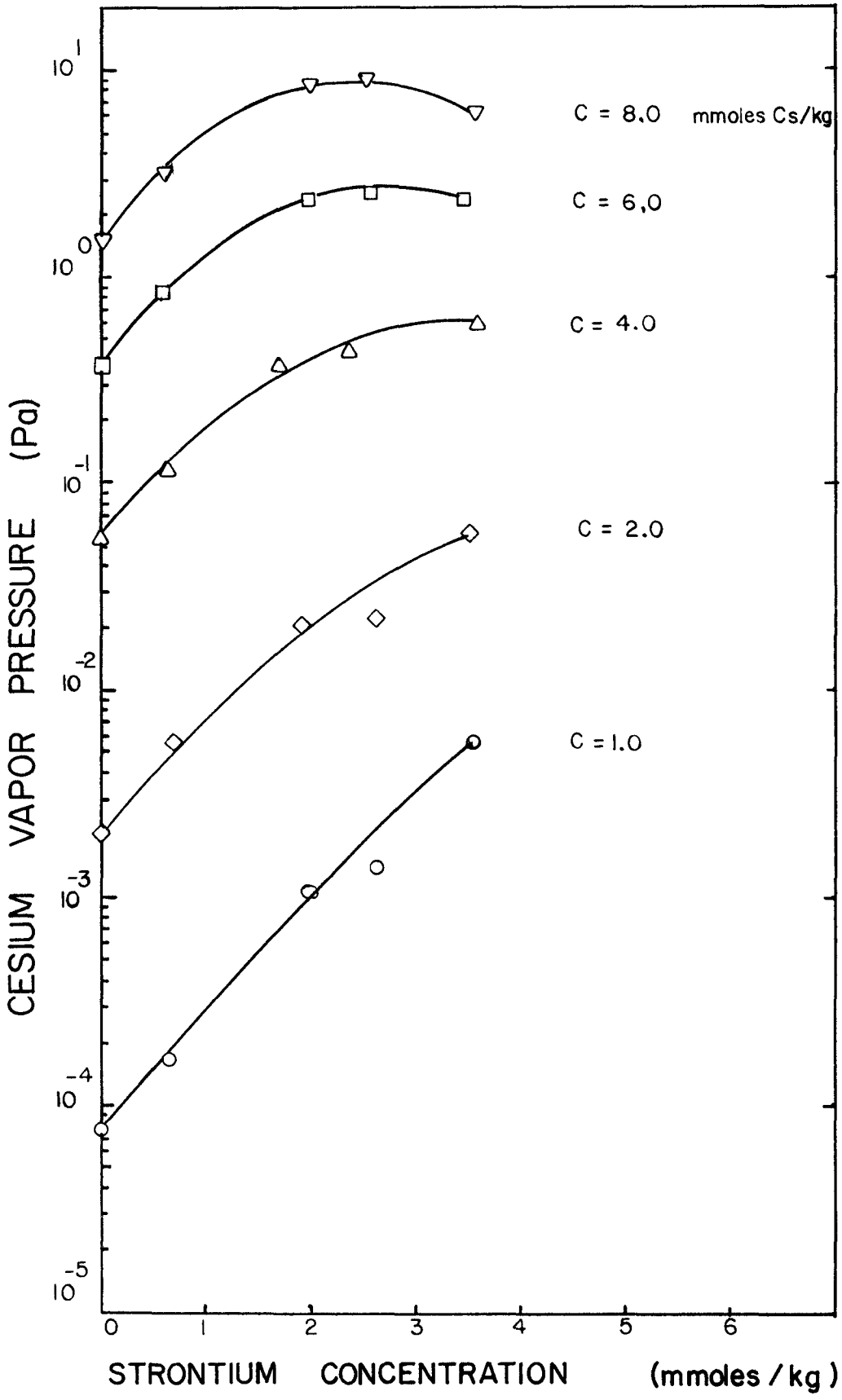

Figure 5.9. Cesium Vapor Pressure as a Function of Strontium Concentration at Various Cesium Concentrations

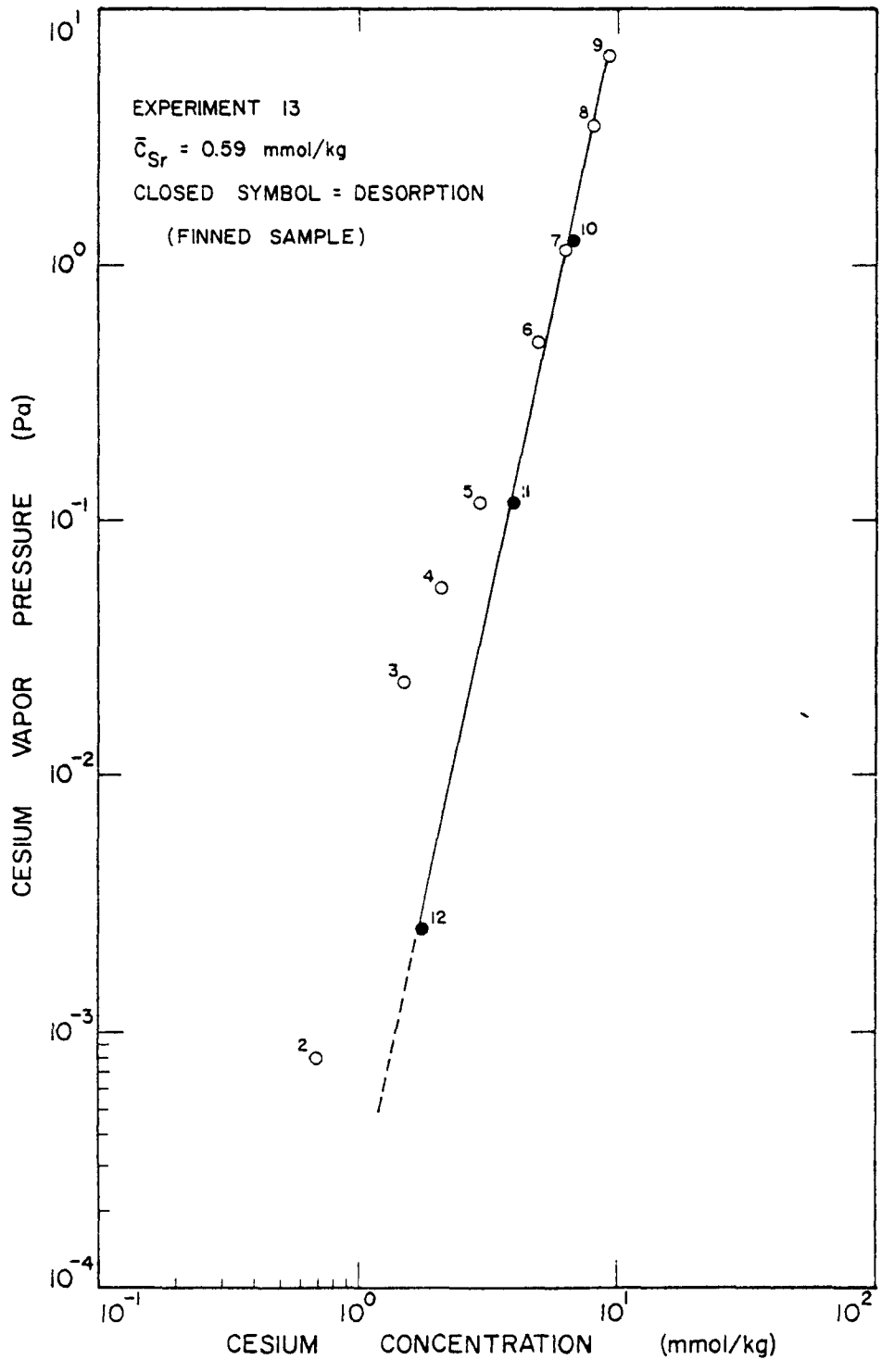

Figure 5.10. Cesium Sorption at 1271 K on H-451 Graphite with an Average of 0.59 mmol Sr/kg graphite (Experiment 13)

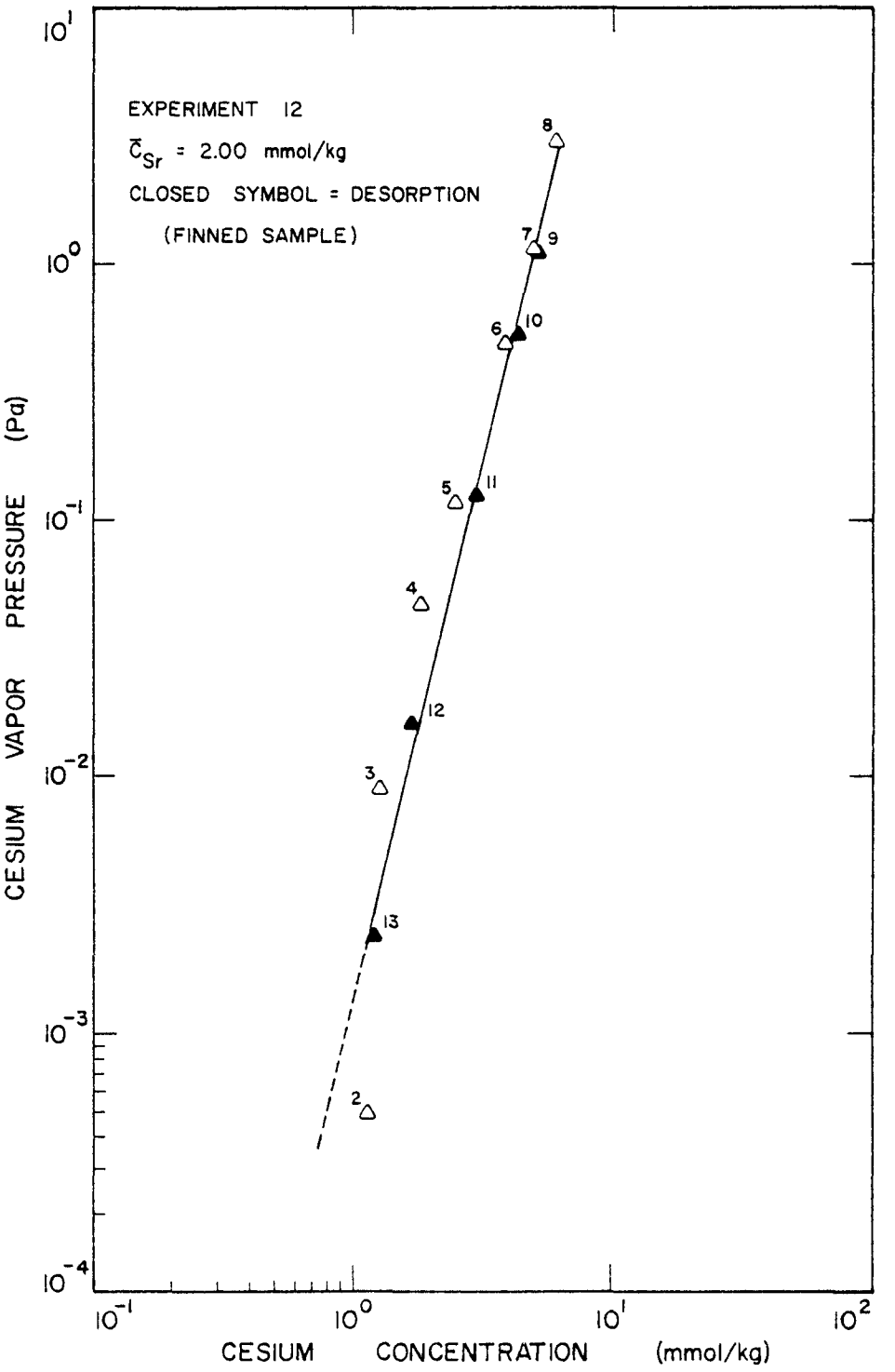

Figure 5.11 Cesium Sorption at 1269 K on H-451 Graphite with an Average of 2.00 mmol Sr/kg graphite (Experiment 12)

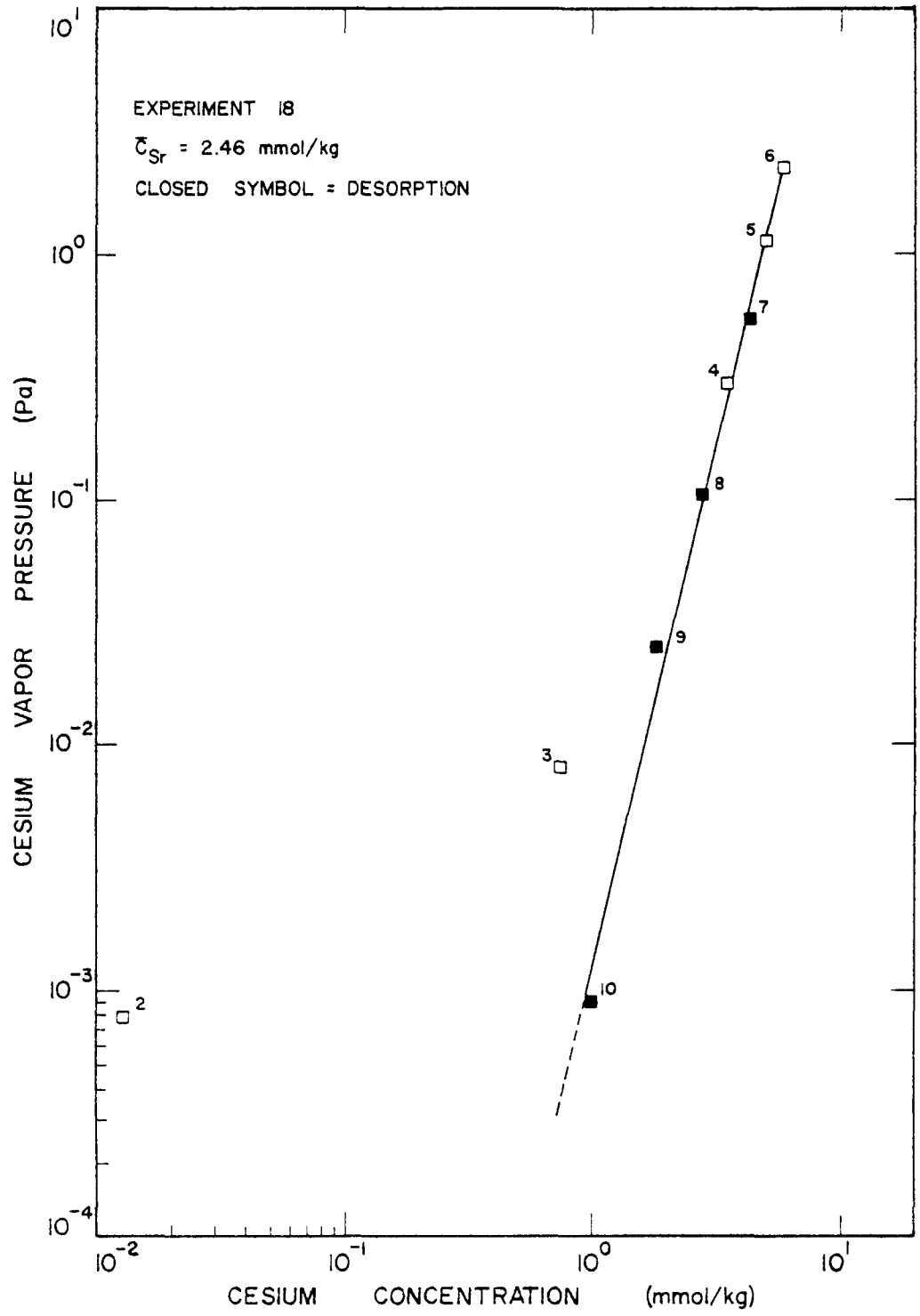

Figure 5.12 Cesium Sorption at 1273 K on H-451 Graphite with an Average of 2.46 mmol Sr/kg graphite (Experiment 18)

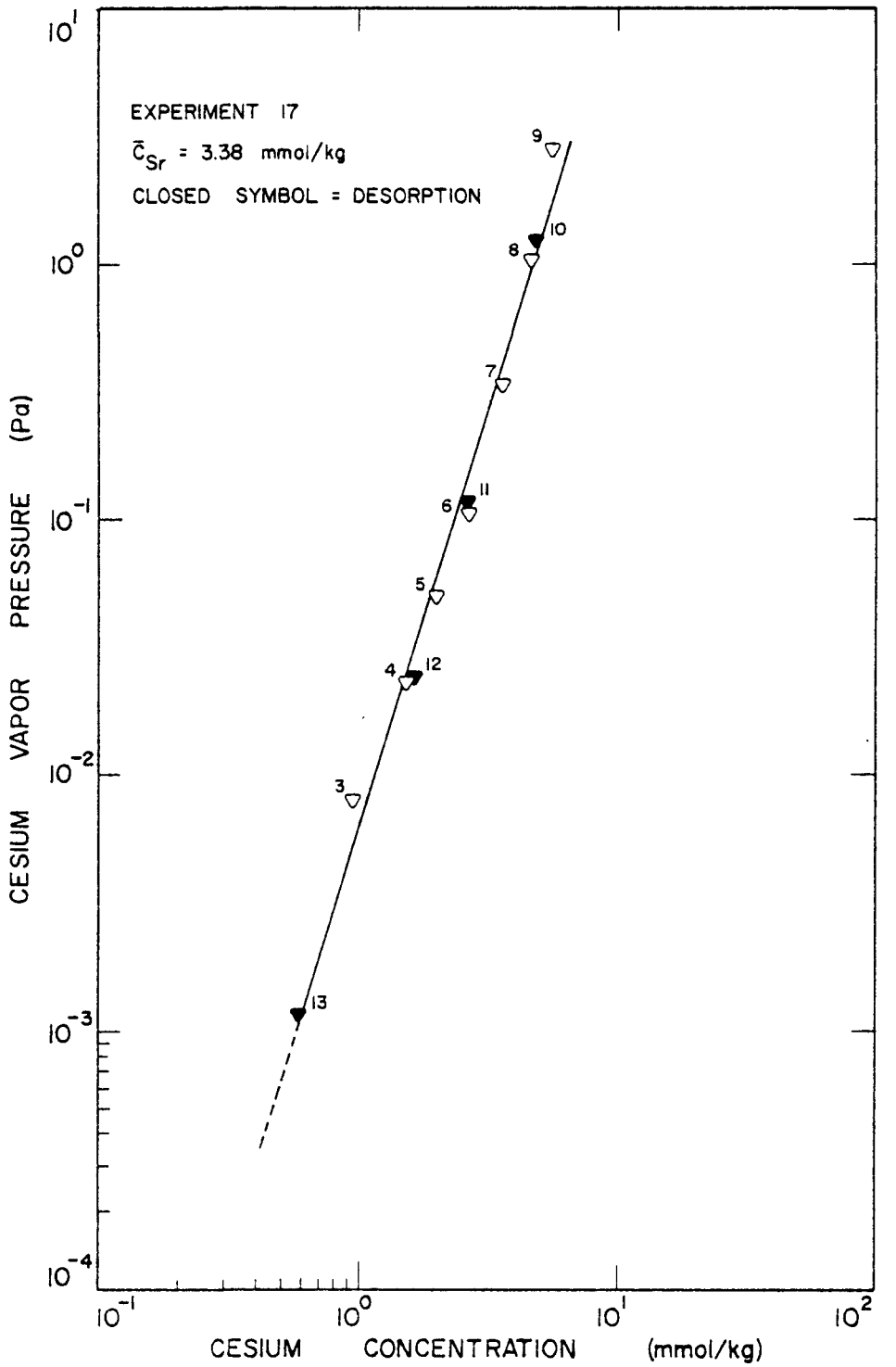

Figure 5.13. Cesium Sorption at 1273 K on H-451 Graphite with an Average of 3.38 mmol Sr/kg graphite (Experiment 17)

Table 5.8. EXPERIMENT 13: Cesium Sorption at 1271° K on H-451 Graphite (Finned Sample) Impregnated to 0.924 mmol Sr/kg Graphite

Sample Temp. (± 10 K)	Source Temp. (± 2 K)	Cesium Vapor Pressure at Sample (Pa)	Cesium Concentration[a] (mmol Cs/kg C)	Rate at Equilibrium (10^{-7} mmol Cs/kg C-s)	Time to 90% Change in Concentration (hours)	Time at Vapor Pressure (hours)	Time at Sample Temp. (hours)	Strontium Concentration[a] (mmol Sr/kg C)
293[e]	293	1.06(-4)[b]	0.081	(c)	(c)	1327	1330	0.924
1270[e]	306	7.88(-4)	0.691	1.6	(c)	156.0	186	0.827
1271[e]	347.5	2.33(-2)	1.500	4.9	76.7	121.4	359	0.775
1271[e]	360	5.40(-2)	2.072	2.6	154.4	182.8	546	0.759
1270[e]	373	1.18(-1)	2.925	6.0	120.9	154.0	709	0.730
1271	402	4.99(-1)	4.886	4.0	112.6	171.2	908	0.655
1271	421	1.15	6.320	3.8	64.5	142.9	1072	0.630
1272	446.5	3.50	8.128	5.8	37.8	84.0	1191	0.591
1271	461.5	6.48	9.278	2.6	17.6	83.1	1296	0.573
1272	423.5	1.27	6.692	2.7	19.6	159.8	1458	0.559
1271	373	1.18(-1)	3.940	<1.2	98.3	229.0	1696	0.560
1270	319	2.53(-3)	1.751	4.7	388.6	666.4	2368	0.581
300[e]	297.5	1.65(-4)	2.142	(d)	(d)	20.5	(d)	0.584
Sample tube background			0.248					0.107
Sample returned in situ			1.936					0.533
Final sample concentration			2.027					0.527

H-451 sample weight: before impregnation = 2.864 g
end of experiment = 2.802 g

Average strontium concentration = 0.59 mmol/kg

(a) In situ equilibrium concentration corrected for sample tube background contribution as discussed in Section 4.4.
(b) Read as 1.06×10^{-4}.
(c) Not observed or not obtained due to temperature fluctuations early in approach to equilibrium.
(d) Cesium source oxidized.
(e) Not included in the least squares fit to Equation 4.11.

Table 5.9. EXPERIMENT 12: Cesium Sorption at 1269° K on H-451 Graphite (Finned Sample) Impregnated to 3.520 mmol Sr/kg Graphite

Sample Temp. (± 10 K)	Source Temp. (± 2 K)	Cesium Vapor Pressure at Sample (Pa)	Cesium Concentration[a] (mmol Cs/kg C)	Rate at Equilibrium (10^{-7} mmol Cs/kg C-s)	Time to 90% Change in Concentration (hours)	Time at Vapor Pressure (hours)	Time at Sample Temp. (hours)	Strontium Concentration[a] (mmol Sr/kg C)
293[e]	293	1.06(-4)[b]	9.887	(c)	(c)	1415	1415	3.520
1270[e]	301	4.89(-4)	1.133	3.4	23.6	187.2	187	2.721
1267[e]	334.5	8.93(-3)	1.287	1.4	52.8	122.8	361	2.536
1269[e]	358	4.67(-2)	1.830	1.6	118.0	184.5	547	2.453
1267[e]	373	1.18(-1)	2.492	4.4	127.8	153.3	718	2.393
1267	402	4.93(-1)	3.880	3.6	86.2	169.8	906	2.093
1265	421	1.15	4.948	4.7	92.2	142.0	1071	1.907
1268	443	3.01	6.117	<1.2	33.8	106.3	1190	2.009
1269	420	1.10	5.074	2.6	21.3	82.2	1296	2.012
1268	403.5	5.33(-1)	4.355	2.0	39.7	160.8	1458	1.995
1269	374	1.25(-1)	2.965	1.2	137.1	229.6	1697	1.995
1274	342.5	1.60(-2)	1.685	<1.2	412.5	627.0	2329	1.988
1271	318.5	2.37(-3)	1.205	1.7	176.8	254.6	2608	2.000
295[e]	295	1.30(-4)	1.207	(d)	(d)	20.6	(d)	1.910
Sample tube background			0.050					0.119
Sample returned in situ			1.210					1.904
Final sample concentration			1.333					1.898

H-451 sample weight: before impregnation = 3.071 g
end of experiment - 2.976 g

Average strontium concentration = 2.00 mmol/kg

(a) In situ equilibrium concentrations corrected for sample tube background contribution as discussed in Section 4.4
(b) Read as 1.06×10^{-4}.
(c) Not observed.
(d) Cesium source oxidized.
(e) Not included in the least squares fit to Equation 4.11.

Table 5.10. EXPERIMENT 18: Cesium Sorption at 1273° K on H-451 Graphite Impregnated to 5.189 mmol Sr/kg Graphite

Sample Temp. (± 10 K)	Source Temp (± 2 K)	Cesium Vapor Pressure at Sample (Pa)	Cesium Concentration[a] (mmol Cs/kg C)	Rate at Equilibrium (10^{-7} mmol Cs/kg C-s)	Time at 90% Change in Concentration (hours)	Time at Vapor Pressure (hours)	Time at Sample Temp. (hours)	Strontium Concentration[a] (mmol Sr/kg C)
298[e]	296.0	1.45(-4)[b]	0.020	(c)	(c)	563.0	560	5.189
1272[e]	306.0	7.88(-4)	0.013	<1.2	(c)	54.8	55	4.628
1273[e]	333.0	7.96(-3)	0.737	1.7	286.4	375.8	432	3.414
1273[e]	391.0	2.98(-1)	3.467	<2.0	(c)	139.1	574	3.018
1273	421.0	1.14	5.027	<2.0	56.4	151.9	729	2.747
1273	436.5	2.28	5.852	<2.0	(c)	165.9	932	2.458
1273	404.0	5.45(-1)	4.283	1.4	33.1	142.4	1080	2.381
1273	371.0	1.04(-1)	2.787	1.5	92.1	239.3	1323	2.324
1273	348.5	2.47(-2)	1.827	1.3	173.8	383.7	1711	2.479
1273	307.5	9.07(-4)	0.990	2.8	227.0	317.5	2050	2.389
298[e]	298.0	1.77(-4)	0.973	(d)	(d)	18.3	(d)	2.368
Sample tube background			0.377					0.284
Sample returned in situ			1.003					2.240
Final sample concentration			1.016					2.246

H-451 sample weight: before impregnation = 3.716 g
end of experiment = 3.616 g

Average strontium concentration = 2.46 mmol/kg

(a) In situ equilibrium concentration corrected for sample tube background contribution as discussed in Section 4.4.
(b) Read as 1.45×10^{-4}.
(c) Not observed or not obtained due to source temperature fluctuations early in the approach to equilibrium.
(d) Cesium source oxidized.
(e) Not included in the least squares fit to Equation 4.11.

Table 5.11. EXPERIMENT 15: Cesium Sorption at 1273° K on H-451 Graphite Impregnated to 7.810 mmol Sr/kg Graphite

Sample Temp. (± 10 K)	Source Temp. (± 2 K)	Cesium Vapor Pressure at Sample (Pa)	Cesium Concentration[a] (mmol Cs/kg C)	Rate at Equilibrium 10^{-7} mmol Cs/kg C-s)	Time to 90% Change in Concentration (hours)	Time at Vapor Pressure (hours)	Time at Sample Temp. (hours)	Strontium Concentration[a] (mmol Sr/kg C)
298[e]	296.0	1.45(-4)[b]	0.007	(c)	(c)	385.0	385	7.810
1272[e]	312.0	1.37(-3)	<0.001	(c)	(c)	53.4	53	6.298
1271	333.0	7.96(-3)	0.949	1.8	247.7	375.0	432	3.953
1271	347.5	2.33(-2)	1.537	2.3	218.8	294.5	730	3.631
1273	359.0	5.01(-2)	1.969	3.3	133.3	180.5	931	3.315
1273	371.0	1.04(-1)	2.664	1.3	194.6	384.6	1322	3.379
1273	393.5	3.39(-1)	3.562	<1.2	43.3	186.4	1514	3.290
1273	418.5	1.03	4.616	<1.2	61.9	196.3	1712	3.303
1273	441.5	2.84	5.599	<1.2	(c)	142.7	1876	3.273
1273	423.0	1.26	4.754	<1.2	21.8	173.0	2049	3.293
1273	373.0	1.18(-1)	2.600	1.3	44.4	259.4	2311	3.321
1273	348.0	2.42(-2)	1.624	<1.2	83.4	208.3	2521	3.297
1273	310.0	1.14(-3)	0.579	<1.2	128.9	238.1	2760	3.174
339[e]	300.0	2.29(-4)	0.593	(d)	(d)	3.2	(d)	3.234
Sample tube background			0.935					1.006
Sample returned in situ			1.399					3.031
Final sample concentration			1.668					3.083

H-451 sample weight: before impregnation = 3.724 g
end of experiment = 3.658 g

Average strontium concentration = 3.38 mmol/kg

(a) In situ equilibrium concentration corrected for sample tube background contribution as discussed in Section 4.4.
(b) Read as 1.45×10^{-4}.
(c) Not observed or not obtained due to source temperature fluctuations early in approach to equilibrium.
(d) Cesium source oxidized.
(e) Not included in the least squares fit to Equation 4.11.

concentration fixed. The thermodynamic treatment of these curves will be discussed in Section 5.3.

The individual cesium isotherms and the fitted relationship are displayed on Figures 5.10 through 5.13. The number beside each equilibrium point is the ordinal number of the sequence of point which are obtained in each given experiment. The data are also tabulated by experiment in the sequence obtained in Tables 5.8 through 5.11. Included in the tabulations are the rates of change observed in the cesium concentration at the equilibrium points and the times observed for the cesium concentrations to change by 90%. The "Sample returned in situ" and the "Final sample concentration" entries in the tables refer to the concentrations determined at the end of each experiment after returning the graphite sample to its in situ arrangement in a clean sample tube and to the concentration determined on a separate NaI(Tl) scintillation detection system of low background, respectively. The strontium concentration (calculated as mentioned above) is also given for reference.

With reference to Figure 5.8 and Figures 5.10 through 5.13, the desorption branch is quite linear for each isotherm. In all cases, the absorption branch is non-linear below the point of merger with the desorption branch. The tendency of this hysteresis to decrease with increasing strontium concentrations is apparent although not clearly defined. With no strontium present the branches merge at approximately 0.3 Pa and 5.8 mmol Cs/kg C, decreasing to about 0.02 Pa and 1.4 mmol Cs/kg C with 3.38 mmol Sr/kg C present. The initial sorption of cesium at the low vapor pressures is quite variable, as noted previously (Section 2.2) for the strontium-free samples. In Experiments 13, 17 and 18 the amount of cesium desposited on the samples during the experimental preparation stages was relatively low

(≤0.081 mmol Cs/kg C), and the variability in the initial equilibrium sorption behavior is evident. In Experiment 12 a large amount of cesium initially deposited on the sample (9.89 mmol Cs/kg C). Although the majority of this loosely sorbed cesium desorbed rapidly upon heating the sample to 1270 K, the difficulty in desorbing all of it is indicated by the initial sorption branch (see point 2) crossing the desorption branch in Figure 5.11. It is not obvious at this intermediate strontium concentration (2.00 mmol Sr/kg C) whether the resulting narrow hysteresis "loop" above 0.01 Pa is related to this high initial sorbed cesium concentration or to the amount of strontium retained in the sample. The results of Experiment 18 (Figure 5.12) which contained a similar amount of strontium (2.46 mmol Sr/kg C) could not resolve this question because of the lack of a sufficient number of sorption equilibrium points in the low pressure region. At the higher strontium concentration of Experiment 17 (3.38 mmol Sr/kg C), the cesium sorption above approximately 0.02 Pa is reversible (Figure 5.13).

5.3 Application of the Thermodynamic and FREVAP Models to Binary Sorption

The thermodynamic and FREVAP models for binary sorption apply to the Freundlich portions of the desorption isotherms (5). The FREVAP model by itself gives empirical relationships for use in fission product release calculations. On the other hand, the thermodynamic model is based on classical thermodynamic principles with the inherent advantage that no physical model is imposed. Generally, a coefficient or a correction factor is applied when trying to correlate an experimental value with an ideal value.

As shown by Haire and Zumwalt (5) the thermodynamic model gives the ideal pressure, in the case of mixed, binary Freundlich sorption as

$$P_1 \text{ (ideal)} = k_{F1}\, C_1 \frac{\left[C_1 + (u_2/u_1)\, C_2\right]^{u_1}}{(C_1 + C_2)} \tag{5.3}$$

with the equation for P_2 (ideal) given by an interchange of subscripts. The symbols P_i, C_i, k_{F1} and u_i are for a single component (i) as given by Equation 2.3. For the thermodynamic model, the "activity coefficient" is defined as the ratio of the experimental or true pressure value to the predicted value of pressure,

$$\gamma_i = \frac{P_i \text{ (exp)}}{P_i \text{ (ideal)}} \tag{5.4}$$

Similarly for the FREVAP model, a correction factor g_i is used.

As displayed in Figure 5.14, in the case of barium-cesium sorption, the FREVAP model with unit correction factor and the thermodynamic model with unit activity coefficient were applied to the sorption data and found to give poor fits. It is noted that the deviation between the experimental values and those of the models is greater for higher barium concentrations. This implies that the activity coefficient and the correction factor should be determined as a function of barium concentration.

In this study, activity coefficients were determined as a function of barium concentration by least-squares polynomial fit calculations. The activity coefficient determination is discussed in Appendix IV. After applying the activity coefficients to the thermodynamic model, the true partial pressure values obtained were plotted as a function of barium concentration for a constant cesium content. The true pressure curves indicate a good fit to the sorption data as shown in Figure 5.15. The cesium activity coefficients γ_1 were found to be empirically expressed as a function of barium concentration due to strong dependence on the concentration effects of the sorbed species, so that

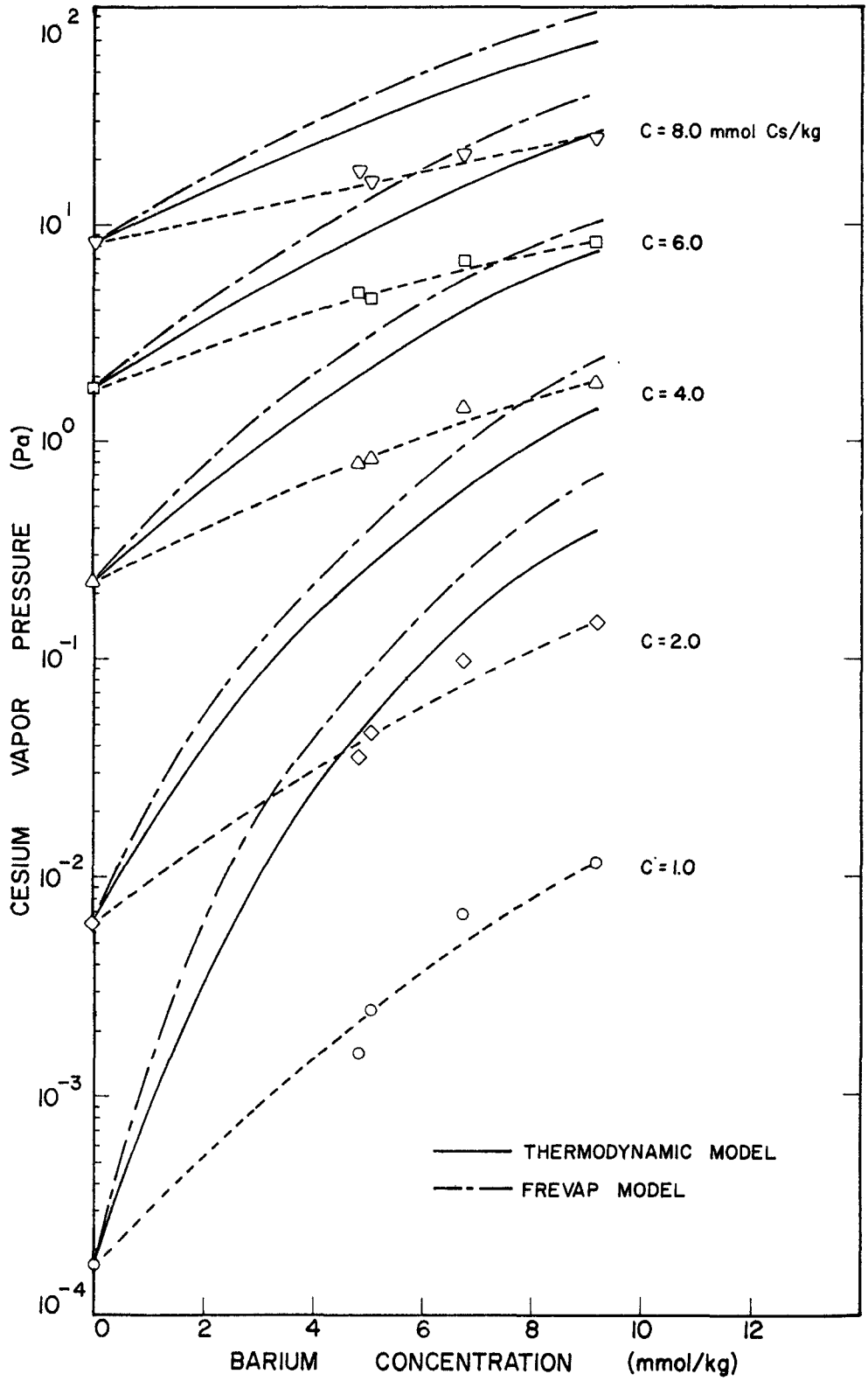

Figure 5.14 Cesium Desorption Isotherms for Barium-Impregnated H-451 Graphite at 1273 K. FREVAP Model with unit Correction Factor and Thermodynamic Model with unit Activity Coefficient.

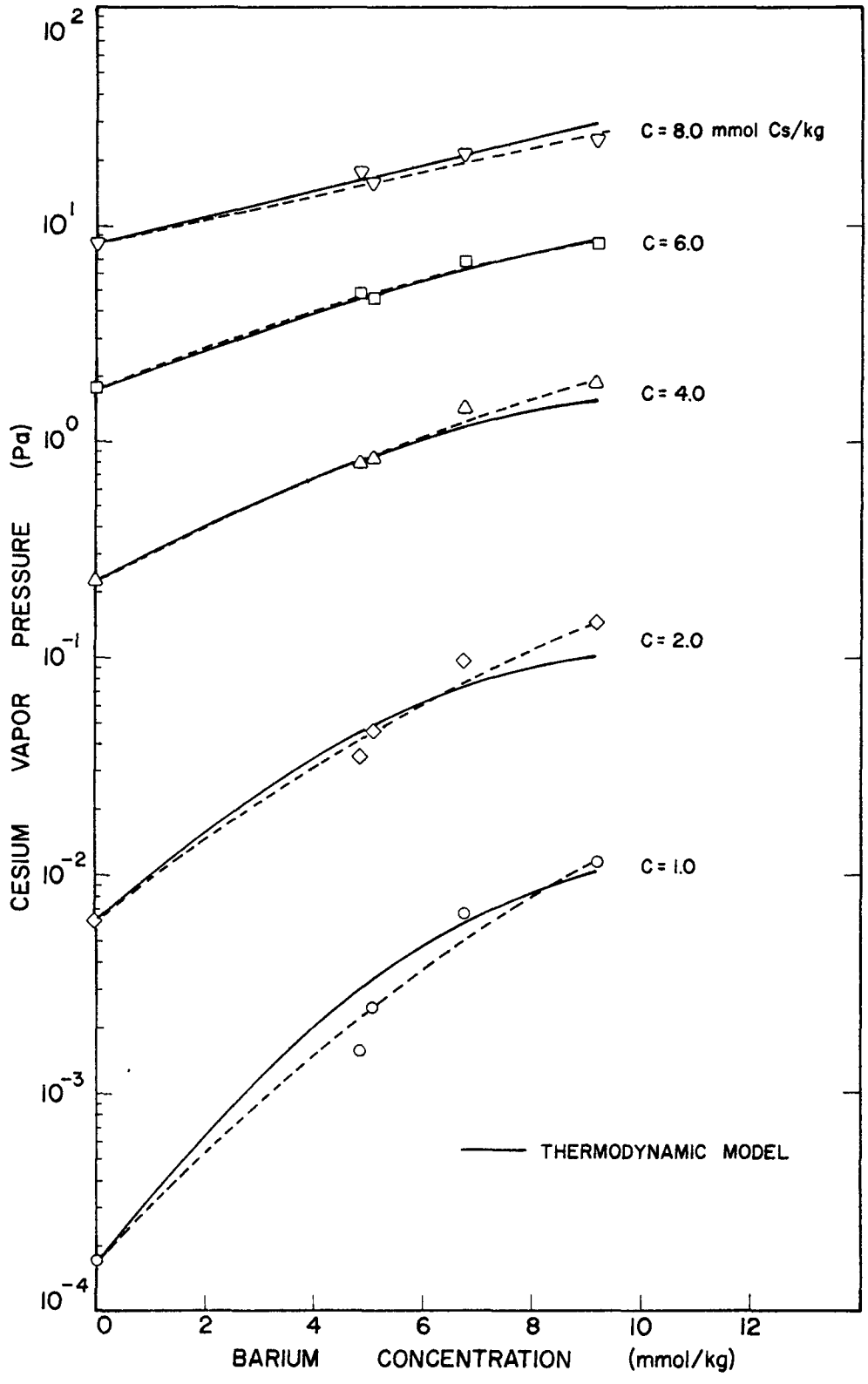

Figure 5.15 Cesium Desorption Isotherms for Barium-Impregnated H-451 Graphite at 1273 K. Thermodynamic Model with Activity Coefficient.

$$\gamma_1 = \exp(-3.78x_2 + 10.15x_2^2 - 11.53x_2^3)$$

where x_2 is mole fraction of barium. Other polynomial expressions were tried but the cubic expression gave the best reduced chi-squared value.

Table 5.12 lists the values of the experimental and predicted points as well as the activity coefficients. After applying the activity coefficients to the experimental values, it is shown that the thermodynamic model seems to be reasonably successful in predicting the cesium-barium sorption behavior.

Application of the thermodynamics model to the cesium-strontium sorption data of Section 5.2 gives the following results. The best fit value for the cesium activity coefficient γ_1 defined as

$$\gamma_1 = P_{Cs}(exp)/P_{Cs}(ideal) \qquad (5.4a)$$

is

$$\gamma_1 = \exp(8.112x_2 - 18.09x_2^2 + 11.31x_2^3)$$

where x_2 = mole fraction of strontium in the cesium-strontium sorbate. The natural logarithm of γ_1 for the data points and the best fit curve are plotted in Figure 5.16. The cesium vapor pressure points, true (experimental) and ideal thermodynamic best fit curves (Eq. 5.3) for several constant values of cesium concentration (C_{C_s}) are plotted against strontium mole fraction (x_2) in Figure 5.17.

TABLE 5.12: Experimental and Predicted Data Points

Cesium Concentration in mmol/kg	Barium Concentration in mmol/kg: Ba = 4.86	Ba = 5.08	Ba = 6.76	Ba = 9.8
Experimental Vapor Pressures of Cesium (Pa)				
Cs = 1.00	0.157E-02	0.248E-02	0.670E-02	0.144E-01
Cs = 2.00	0.353E-01	0.455E-01	0.977E-01	0.147E 00
Cs = 4.00	0.791E 00	0.835E 00	0.142E 01	0.188E 01
Cs = 6.00	0.488E 01	0.458E 01	0.683E 01	0.837E 01
Cs = 8.00	0.177E 02	0.153E 02	0.208E 02	0.241E 02
Vapor Pressures of Cesium (Pa) Predicted by Thermodynamic Model				
Cs = 1.00	0.464E-01	0.533E-01	0.135E 00	0.388E 00
Cs = 2.00	0.244E 00	0.272E 00	0.581E 00	0.142E 01
Cs = 4.00	0.208E 01	0.225E 01	0.390E 01	0.776E 01
Cs = 6.00	0.917E 01	0.974E 01	0.150E 02	0.262E 02
Cs = 8.00	0.289E 02	0.303E 02	0.433E 02	0.690E 02
Values of Fitted Activity Coefficients - γ_1				
Cs = 1.00	0.656E-01	0.614E-01	0.405E-01	0.272E-01
Cs = 2.00	0.187E 00	0.175E 00	0.115E 00	0.716E-01
Cs = 4.00	0.399E 00	0.386E 00	0.294E 00	0.202E 00
Cs = 6.00	0.502E 00	0.493E 00	0.421E 00	0.326E 00
Cs = 8.00	0.549E 00	0.543E 00	0.493E 00	0.416E 00
True Vapor Pressures of Cesium After Applying Activity Coefficients to Thermodynamic Model				
Cs = 1.00	0.305E-02	0.327E-02	0.548E-02	0.106E-01
Cs = 2.00	0.455E-01	0.478E-01	0.666E-01	0.102E 00
Cs = 4.00	0.830E 00	0.867E 00	0.115E 01	0.157E 01
Cs = 6.00	0.460E 01	0.480E 01	0.633E 01	0.855E 01
Cs = 8.00	0.159E 02	0.165E 02	0.213E 02	0.287E 02

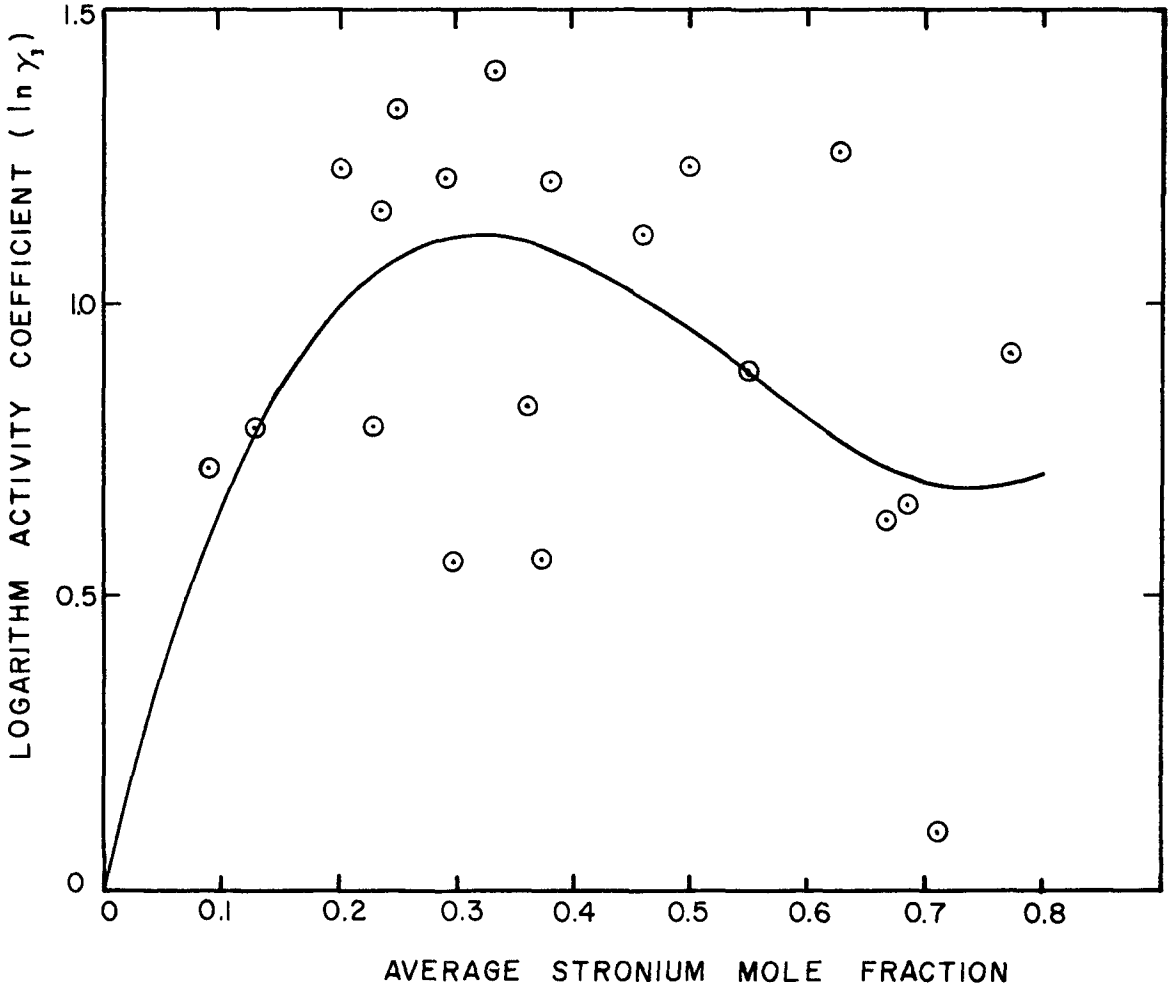

Figure 5.16. Logarithm of Activity Coefficient (γ_1) for Cesium Sorbed by Strontium-Impregnated H-451 Nuclear Graphite

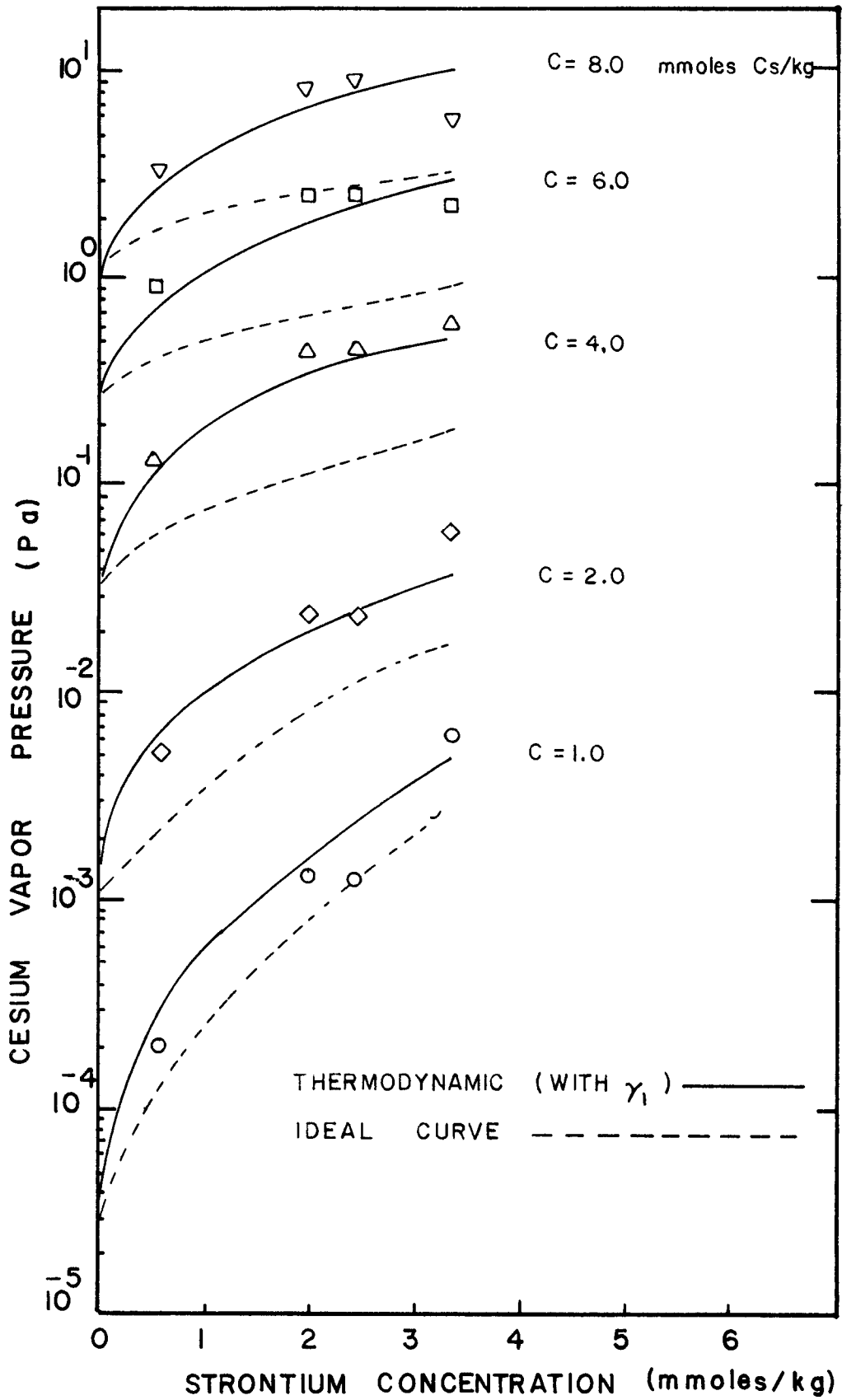

Figure 5.17. Cesium Vapor Pressure as a Function of Strontium Concentration at Various Cesium Concentrations

6. SUMMARY AND CONCLUSIONS

6.1 Summary

This is the final report of a series of four on a study of the sorption of cesium by graphites at high temperatures. The temperature range of the studies was 800 to 1100° C and in the latter part of these studies, work was concentrated on H-451 nuclear-grade graphite (16.) The pseudo-isopiestic method which utilized radioisotope-tagged sorbates (of cesium, cesium and barium or cesium and strontium) was used in all of the experiments - over forty in number.

A primary objective was the study of the effect on cesium sorption equilibrium of the presence of a second sorbate-barium or strontium - in the graphite. A thermodynamic approach was deemed best to treat the binary sorption data.

A second important objective was to compare equilibrium sorption results obtained by the pseudo-isopiestic method and the Knudsen cell method using the same material in particulate form - ground H-451 nuclear-grade graphite (particle size range 44 to 74 μm).

A third objective was to review sorption kinetics data obtained, for both particulate and solid H-451 graphite samples, the course of our work. This led to the development of a kinetics model, mathematical formulation which applies to a system which shows Freundlich equilibrium sorption isotherm behavior. The formulation, in particular, is consistent with the modified-exponential theoretical isotherm discussed (and derived) in this report.

The report also reviews and presents some new data on simple cesium-graphite (H-451) isotherms and includes additional data on isotherm hysteresis which definitely occurs at low cesium pressure (< 0.2 Pa) with graphite samples which, in general, have not been exposed to higher cesium vapor pressures.

6.2 Conclusions

1. The kinetics of absorption and desorption of cesium by bulk nuclear-grade graphite and even by the graphite in particulate form (size range 44 to 74 μm) is such that, in general, several days are required to reach a near equilibrium state. Accordingly, the pseudo-isopiestic method, although time consuming, appears to be the best method to assure the obtainment of equilibrium data in the cesium vapor pressure range of about 10 Pa down to 10^{-3} Pa.*

2. The Knudsen cell method for studying the incongruent vaporization of cesium from nuclear graphite powders (size range 44 to 74 μm), in general, appears to not give equilibrium vapor pressure data. This conclusion was reached by studying the kinetics behavior and equilibrium data of cesium sorption by graphite powder (H-541) using the pseudo-isopiestic method.

3. Hysteresis - where the absorption curve (at apparent equilibrium) falls to the left of the desorption curve - is definitely observed at lower cesium vapor pressures ($\leq$ 0.2 Pa) in the case of solid graphite (H-451) samples, both unimpregnated and impregnated with barium or strontium. It is to be noted that the Knudsen cell method gives desorption data only, so the method would not be expected to show hysteresis - however, at low partial pressure a non-equilibrium effect is shown in Knudsen cell experiments even upon desorption (6).

4. Essentially no hysteresis occurred in the pseudo-isopiestic experiment with graphite powder (Experiment 41). Also, there is some indication that once a solid sample is exposed to a high vapor pressure of cesium ($\geq$ 1 Pa) hysteresis no longer occurs and absorption steps

---

* The Knudsen cell method may not be "kinetics" limited at higher cesium vapor pressures ($P_{Cs} \gtrsim 1$ Pa). The pseudo-isopiestic method is limited by gas flow kinetics at $P_{Cs} \lesssim 10^{-3}$ Pa.

taken after desorption steps follow the Freundlich (exponential) desorption isotherm curve.

5. The pseudo-isopiestic experiment with graphite powder (Exp. 41) gives an equilibrium cesium sorption curve which falls substantially to the right of the General Atomic, Knudsen cell data (see Fig. 3.1). This is believed to be due to the fact that the pseudo-isopiestic method permits a closer approach to equilibrium than does the Knudsen cell method. The kinetic data (variation of cesium sorbate concentration versus time) of the experiments also indicated the sorption process, in general, is too slow to be followed by the Knudsen cell technique.

6. The modified-exponential equation (Equation 2.12) appears to be the most satisfactory mathematical formulation for cesium-graphite sorption behavior. It gives a good approximation to Freundlich behavior in the vapor pressure region 10^{-3} Pa to 10 Pa and at lower vapor pressures tends to become Henrian in behavior.

7. The kinetics data of the pseudo-isopiestic experiment with graphite powder was found to be very well represented mathematically by kinetics Equation 4.1, which is based on the site (trap) activation energy, ϵ, being approximately equal to the site interaction (sorption) energy, χ. In accordance with theory for modified-exponential sorption, the sites are taken to be non-uniformly distributed having a number which decreases exponentially with interaction energy, χ, which has a finite upper limit χ_L.

8. The kinetics data of the pseudo-isopiestic experiments with solid graphite do not fit kinetics Equation 4.1 quite as well as does the data obtained with a powdered graphite sample. The fit, however, is reasonably good and at short times, the data appears to reflect rapid evaporation of cesium from external graphite surfaces while at very long times the

kinetics are believed to be controlled by a slow diffusion of atoms to residual sites within the bulk of the graphite.

9. In binary sorption studies, where data was obtained of the effects of barium or strontium in graphite (H-451) on the equilibrium vapor pressure of cesium, a thermodynamic treatment was found the most useful. The ideal vapor pressure is given by Equation 5.1 which utilizes first component activity coefficient, γ_1, defined as the ratio of true cesium vapor ressure to the ideal vapor pressure. The logarithm of the activity coefficient is expressed by a polynomial,

$$\pm \ln \gamma_1 = c_1 x_2 + c_2 x_2^2 + c_3 x_2^3$$

where x_2 = the mole fraction of the second component, barium or strontium. The right side of the equation is positive. Deviation from the ideal is such that barium yields a negative deviation (- sign) while strontium gives a positive deviation (+ sign) for ln γ. The coefficients, c_j, for barium are $c_1 = 3.78$, $c_2 = -10.15$, $c_3 = 11.53$ and for strontium are $c_1 = 8.112$, $c_2 = -18.09$, $c_3 = 11.31$.

7. ACKNOWLEDGEMENTS - CONTACTS WITH OTHER LABORATORIES

The assistance and interest of W. E. Bell and B. F. Myers of General Atomic Company in connection with our study of cesium sorption by particulate graphite are most appreciated.

Also we wish to acknowledge the excellent experiment work of Kevin M. Vaughn in carrying out a portion of the study.

The interest and theoretical work of B. L. Holian of the Los Alamos Scientific Laboratory on the interaction of cesium with idealized graphite are greatly appreciated. Also the interest of other workers in the field (of Knudsen cell and cesium desorption studies) including, R. L. Faircloth and F. C. W. Pummery of Harwell (A.E.R.E.) and E. Hoinkis of the Hanh-Meitner Institute of Berlin is appreciated.

8. LIST OF REFERENCES

1. Pyecha, T. D. and L. R. Zumwalt. "Sorption of Graphites at High Temperatures". North Carolina State University, ORO-4682-3 (1977).

2. Pyecha, T. D. and L. R. Zumwalt. "Sorption of Graphites at High Temperatures". North Carolina State University, ORO-4682-2 (1976).

3. Pyecha, T. D. and L. R. Zumwalt. "Sorption of Graphites at High Temperatures". North Carolina State University, ORO-4682-1 (1975).

4. Milstead, C. E., A. B. Riedinger and L. R. Zumwalt. "Cesium Graphite Sorption Isotherms Determined by a Static Method". Carbon 4:99-106 (1966).

5. Haire, M. J. and L. R. Zumwalt. "Mixed Sorption Models and Isotherms of the Cesium-Rubidium-Graphite System at High Temperatures". Nucl. Sci. Eng. 50:91-97 (1973).

6. Myers, B. F. and W. E. Bell. "Cesium Transport Data for HTGR Systems". GA-A13990. General Atomic Company (1979).

7. Liang, S. C. "On the Calculation of Thermal Transpiration". J. Phys. Chem. 57:910-911 (1953).

8. J. Zeldowitch, Acta. Phys. Chem. U.R.S.S., 1, 961 (1934).

9. E. Cremer and S. Flugge, Z. physik. Chem. B 41, 453 (1938).

10. G. Halsey and H. Taylor, J. Chem. Physics 15, 624 (1947).

11. E. Gluekauf, Trans. Faraday Soc. 49, 1066-1079 (1953).

11a. R. L. Faircloth and F. C. W. Pummery. "Vapor Pressure of Cesium over Nuclear Graphite". AERE, Harwell, Applied Chemistry Division, Report AERE-R8283, January 1976.

12. B. L. Holian, "The Interaction Between Cesium and Graphite for Use in the Study of Surface Phenomena". Submitted to the Conference on Computer Simulation for Materials Application, NBS, Gaithersburg, Md., Los Alamos Scientific Laboratory Report, LA-UR-76-854 (1976).

13. E. Hoinkis and D. Stritzka. "Cesium Desorption from Graphite in the Presence of Gases". Trans. Amer. Nucl. Soc. 32, 281 (1979).

14. V. Vand. Proc. Phys. Soc. 55, 222 (1943).

15. W. Primak. Phys. Rev. 200, 1677 (1955).

16. G. B. Engle, R. J. Price, W. R. Johnson and L. A. Beron. "Development Status of Near-Isotropic Graphites for Large HTGRs", Report GA-A12944, UC-77 (June 1, 1974).

17. E. Schonfeld, "Alpha-A Computer Program for the Determination of Radioisotopes by the Least-Squares Resolution of Gamma Ray Spectra". Nucl. Inst. Meth. 42, 213-218 (1966).

APPENDIX I Edit of FORTRAN Computer Code KINETICS

```
$JOB      NCS.EZ.NE/KAZI.TIME=0010.PAGES=0020
C$OPTIONS LINES=48
C
C
C  PROGRAM KINETICS:
C
C  PURPOSE:
C  THIS PROGRAM INVOLVES THE KINETICS MODEL BASED ON THE
C     SORPTION THEORY (DERIVED IN EQUATION 3-56) TO
C  DETERMINE  CHARACTERISTIC FREQUENCY AND F VALUE FOR
C  FOR SORPTION OF CESIUM BY H-451 GRAPHITE IN EXPERIMENT
C  NUMBER 16
C
C
C  DESCRIPTION OF PARAMETERS:
C        T - TIME IN MINUTES
C  CINTAL - INITIAL CONCENTRATION (ALSO C1)
C  CFINAL - FINAL   CONCENTRATION (ALSO C2)
C       P1 - INITIAL PRESSURE
C       P2 - FINAL PRESSURE
C     CONC - TOTAL CONC AS A FUNCTION OF TIME
C  CONCLA - CONC(LANGMUIR)
C  CONCMO - CONC(MONOLAYER)
C   CONC1 - FIRST  INTEGRAL CONCENTRATION
C   CONC2 - SECOND INTEGRAL CONCENTRATION
C      A,U - CONSTANTS AS IN EQN LN P = A + U*LN CONC
C      D,E - CONSTANTS AS IN EQN U=(D+E*10**3/TEMP)
C       VL - UPPER LIMIT OF INTEGRALS
C        N - NUMBER OF POINTS
C     TEMP - SAMPLE TEMPERATURE
C       AS - CHARACTERISTIC FREQUENCY
C        R - TERM FOR CHANGE OF ENTROPY WITH
C            INTERACTION ENERGY
C  FVALUE - VALUE OF F (SEE FIGURE 3.1)
C       P0 - REFERENCE PRESSURE
C  TGAP14 - TIME INCREMENT IN FIRST QUARTER RUN TIME
C  TGAP34 - TIME INCREMENT IN  LAST    3/4  RUN TIME
C   YAXIS - Y-AXIS GRAPH SCALING FACTOR FOR CONCENTRATION
C       A1 - LOWER LIMIT OF FIRST  INTEGRAL
C       A2 - LOWER LIMIT OF SECOND INTEGRAL
C
C
C
      IMPLICIT REAL*8(A-H,O-Z)
      DIMENSION Z(24),WEIGHT(24)
      DIMENSION CONC(100),T(100)
      DIMENSION CONC1(100),CONC2(100),YAXIS(100)
      DATA CONCLA,CONCMO/0.7000,20.0000/
```

```
      DATA EP/1.D-06/
      DATA D,E/-6.566,14.498/
      DATA TEMP/1273./
      N=20
C
C
C  READING NODES AND WEIGHTS FOR 24-POINT GAUSSIAN
C  QUADRATURE INTEGRATION
C
      DO 10 I = 1,12
   10 READ(1,20) Z(I),WEIGHT(I)
   20 FORMAT(2F22.21)
C
C READING VALUES OF CONCENTRATION AND PRESSURE
C  AT TWO EQUILIBRIUM POINTS AND DETERMINING VALUES
C  OF A AND U BETWEEN THESE TWO POINTS
C
      READ,SCALE
      END=SCALE
      READ,P1,P2,CINTAL,CFINAL,T(1),T(N)
      READ,AS
      READ,FVALUE
      SCALE=SCALE/(CFINAL-CINTAL)
      U=DLOG(P1/P2)/DLOG(CINTAL/CFINAL)
      A=DLOG(P1)-U*DLOG(CINTAL)
      CALL TRAPS(1,1,50000,1,1)
      PI=4.*DATAN(1.D0)
      R=1.D-03*D/E
       Y=A +U*(DLOG(CONCMO)+DLOG(PI/U/DSIN(PI/U)))
      P0=DEXP(Y)
      THETAL=CONCLA/CONCMO
      UMINUS=U-1.
      X=UMINUS*(PI/U/DSIN(PI/U))**U * (1.D0/THETAL)
     .**UMINUS
      VL=-DLOG(THETAL)
C
C  ITERATION FOR UPPER LIMIT  VL USING NEWTON-
C  RAPHSON'S METHOD
C      EP - EPSILON FOR ITERATION PURPOSES
C
      DO5I=1,35
      FUNVL=1.D0/UMINUS*DLOG(X*(1.D0-DEXP(-VL)) +1.D0) -VL
      DFUNVL=1.D0/UMINUS-1.D0
      DELTA=-FUNVL/DFUNVL
      VL=VL+DELTA
      DELTA=DABS(DELTA)
      IF(DELTA.LE.EP) GO TO 1
    5 CONTINUE
```

```
      1 B=VL
        NN=N/2
        INTVAL=N/2-1
        TGAP14=(T(N)-T(1))/4./DFLOAT(INTVAL)
        TGAP34= (T(N)-T(1))*3./4./DFLOAT(NN)
        X1=1.D0/(P0*(1.D0-DEXP(-VL)))
        XF=X1*P2
        XI=X1*P1
        WRITE(3,99)CONCLA,CONCMO,CINTAL,CFINAL,P1,P2,
       .P0,A,U,R,VL
     99 FORMAT('1','CL =',D15.8/' CM =',D15.8/' C1 =',
       .D15.8/' C2 =',D15.8/' P1 =',D15.8/' P2 =',
       .D15.8/' P0 =',D15.8/'  A =',D15.8/'  U =',
       .D15.8/'  R =',D15.8/' VL =',D15.8/)
        WRITE(3,101) AS,FVALUE
    101 FORMAT('0',4X,'AS = ',D12.5/1X,'FVALUE = ',D12.5,
       .//6X,'TIME(M)',5X,'CONC',4X,'CONC1',4X,'CONC2',
       .4X,'Y-AXIS'/)
C
C   CALCULATING FOR FIRST AND SECOND INTEGRALS
C
        DO 14 J =1,N
        JJ=J-1
        IF(J.NE.1) GO TO 11
        A1=0.
        A2=0.
        GO TO 9
     11 IF(J.GT.NN) GO TO 8
        T(J)=T(1) + TGAP14*DFLOAT(JJ)
        GO TO 7
      8 JJJ=J-NN
        T(J)=T(NN) + TGAP34*DFLOAT(JJJ)
      7 TIME=(T(J)-T(1))*60.
        A1=(1.-R*TEMP)*DLOG(AS*(TIME+1.D0/AS))/FVALUE/U
        A2=A1
        IF(A2.GT.B) GO TO 2
     9  C1=(B+A1)/2.
        C2=(B+A2)/2.
        D1=(B-A1)/2.
        D2=(B-A2)/2.
        SUM1=0.
        SUM2=0.
        DO 13 K =1,12
        E1=C1+D1*Z(K)
        E2=C2+C2*Z(K)
        F1=C1-D1*Z(K)
        F2=C2-D2*Z(K)
        FIRST =XI*(DEXP(UMINUS*E1)/(1.+P1/P0*DEXP(U*E1))
```

```
     .           +DEXP(UMINUS*F1)/(1.+P1/P0*DEXP(U*F1)))
      SECOND=XF*(DEXP(UMINUS*E2)/(1.+P2/P0*DEXP(U*E2))
     .           +DEXP(UMINUS*F2)/(1.+P2/P0*DEXP(U*F2)))
      WTFUN1=WEIGHT(K)*FIRST
      WTFUN2=WEIGHT(K)*SECOND
      SUM1=WTFUN1+SUM1
   13 SUM2=WTFUN2+SUM2
      AREA1=D1*SUM1
      AREA2=D2*SUM2
      CONC(J) = CFINAL+(AREA1-AREA2)*CONCMO
      CONC1(J)=AREA1*CONCMO
      CONC2(J)=AREA2*CONCMO
      YAXIS(J)=(CONC(J)-CINTAL)*SCALE
   14 CONTINUE
      GO TO 3
    2 DO 16 I=1,JJ
   16 WRITE(3,102) I,T(I),CONC(I),CONC1(I),CONC2(I),
     .YAXIS(I)
      N=JJ
      GO TO 500
    3 DO 15 I =1,N
   15 WRITE(3,102) I,T(I),CONC(I),CONC1(I),CONC2(I),
     .YAXIS(I)
  500 WRITE(3,103)' END
  102 FORMAT(1X,I2,4X,F6.0,3(4X,F5.3),4X,F6.2)
  103 FORMAT('0',30X,'END OF SCALE  ',F5.2////////////)
      STOP
      END

$DATA
```

CL = 0.70000000D 00
CM = 0.20000000D 02
C1 = 0.93300000D 00
C2 = 0.60000000D 01
P1 = 0.16212000D-03
P2 = 0.12828000D 01
P0 = 0.60297603D 03
A =-0.83926951D 01
U = 0.48230471D 01
R =-0.45289005D-03
VL = 0.37877025D 01

AS = 0.50000D-02
FVALUE = 0.97500D 00

	TIME(M)	CONC	CONC1	CONC2	Y-AXIS
1	0.	0.830	0.495	5.664	-0.38
2	751.	3.674	0.493	2.819	10.22
3	1503.	4.329	0.491	2.161	12.67
4	2254.	4.656	0.488	1.833	13.89
5	3006.	4.862	0.486	1.624	14.66
6	3757.	5.009	0.483	1.474	15.20
7	4508.	5.120	0.480	1.360	15.62
8	5260.	5.208	0.477	1.268	15.95
9	6011.	5.281	0.474	1.193	16.22
10	6762.	5.342	0.470	1.129	16.44
11	8791.	5.466	0.461	0.995	16.91
12	10820.	5.554	0.451	0.897	17.24
13	12849.	5.621	0.442	0.821	17.49
14	14878.	5.672	0.432	0.759	17.68
15	16906.	5.714	0.422	0.708	17.83
16	18935.	5.748	0.412	0.664	17.96
17	20964.	5.776	0.402	0.627	18.06
18	22993.	5.800	0.393	0.593	18.15
19	25021.	5.820	0.384	0.564	18.23
20	27050.	5.837	0.374	0.537	18.29

END OF SCALE 18.90

APPENDIX II

List of Apparatus Used in Sorption Run

Heating System

Versatherm Model 2156-Proportional Electronic Temperature Controller for cesium source

Fabricated heating coil for cesium source

Custom-made heating jacket for mid-section of sorption rig

Barber Colman Model 122Y - Temperature Controller for heating jacket

Lindberg Model 54032 - Electrical Resistance Furnace

Barber Colman Model 537H - Temperature Controller for Lindberg Furnace

Barber Colman Model CB41 - Proportional Power Controller for Lindberg Furnace

Fabricated Safety Trip Circuit for cutting off furnace power

Thermocouple wires - K-type and J-type

Thermo Electric Digimite Model 31160 - Digital Temperature Indicator

Keithley Model 178 - Digital Multimeter

Counting System

Scintillator NaI (Tl) crystal

Ortec Model 276 - Photomultiplier Base for scintillator

Ortec Model 486 - Pulse Height Analyzer Amplifier

Ortec Model 715 - Dual Counter/Timer

Ortec Model 410 - Linear Amplifier

Ortec Model 419 - Precision Pulse Generator

Ortec Model 456 - High Voltage Power Supply

Ortec Model 401A - Modular System Bin

Ortec Model 402A - Bin Power Supply

Ortec Model 432A - Printout control

Teletype Printer - Teletype Corporation Model

Tracor Northern Model TN-1705 Multi Channel Analyzer

Fabricated Switching unit for automatic counting

APPENDIX III

Liang's Formula for Cesium Vapor Pressure at the Graphite Sample

When a temperature difference exists between the source, T_{SRC} K and the graphite sample T_{SAM} K, a correction can be made by the use of Liang's expression to find the ratio of the cesium vapor pressure over the graphite sample, P_{SAM} to that over the cesium source P_{SRC}. This expression is

$$\frac{P_{SAM}}{P_{SRC}} = \frac{\alpha_{He}(\phi_g \varepsilon)^2 + \beta_{He}(\phi_g \varepsilon) + 1.0}{\alpha_{He}(\phi_g \varepsilon) + \beta_{He}(\phi_g \varepsilon) + \left(\frac{T_{SRC}}{T_{SAM}}\right)^{\frac{1}{2}}} \qquad \text{(AIII-1)}$$

where $\alpha_{He} = 2.13$

$\varepsilon = P_{SRC} d$ (P_{SRC} in units of mm) (AIII-2)

d = tube diameter = 18 mm

$\beta_{He} = 4.83\left[1 - \left(\frac{T_{SRC}}{T_{SAM}}\right)^{\frac{1}{2}}\right]$

r = collision radius of cesium atom = 2.62 Å

$\phi_g = 10^{(\log(2r) - 0.35)10.44} = 6.909$

In the Equation (AIII-2), cesium vapor pressure over the source, P_{SRC} is determined in mm units,

$$P_{SRC} = 10^{AP - BP/T_{SRC}} - CP \times \log(T_{SRC}) \qquad \text{(AIII-3)}$$

where the cesium vapor parameters are given by

AP = 11.38

BP = 4075

CP = 1.45

The vapor pressure at the graphite sample is now found by the product of Equations (AIII-1) and (AIII-3). Sample Calculation: Given temperature of cesium source as 300 K and that of graphite sample as 1272 K, then

Cesium vapor pressure over the source, $P_{SRC} = 1.603 \times 10^{-6}$ mm

$= 2.109 \times 10^{-9}$ atm

$= 2.137 \times 10^{-4}$ Pa,

Cesium vapor pressure over the graphite sample, $P_{SAM} = 3.298 \times 10^{-6}$ mm

$= 4.340 \times 10^{-9}$ atm

$= 4.397 \times 10^{-4}$ Pa

APPENDIX IV

Determination of Activity Coefficients from Thermodynamic Model

In this study, no experiment was performed on pure barium sorption by graphite, therefore it became necessary to use the parameters from a barium sorption work performed in the same graphite (H-451 grade) at General Atomic in 1973. The relationship as reported in General Atomic Report, GA-A14479 is given by

$$\ln P(Pa) = \left[19.37 - \frac{47313}{T(K)}\right] + \left[0.426 + \frac{3728}{T(K)}\right] \ln C(mmol/kg) \qquad \text{(AIV-1)}$$

Using the subscripts 1 for cesium, 2 for barium and the temperature T as 1272 K, the relationship obtained for H-451 graphite is reduced to

$$\ln P_2 = -17.826 + 3.357 \ln C_2 \qquad \text{(AIV-2)}$$

From Equation (AIV-2), the parameters corresponding to equation in the form $\ln P = a + b \ln C$ lead to

$$a_2 = -17.826 \qquad \text{(AIV-3)}$$

and

$$b_2 = 3.357 \qquad \text{(AIV-4)}$$

Comparing Equation (AIV-2) to the Freundlich isotherm relationship

$$P = kC^u \qquad (3.1)$$

the coefficients become

$$k_2 = \exp(a_2) = 1.8129 \times 10^{-8} \qquad \text{(AIV-5)}$$

and $$u_2 = b_2 = 3.357 \qquad \text{(AIV-6)}$$

Similarly the coefficients derived from this experimental study for cesium sorption lead to

$$k_1 = 1.6975 \times 10^{-4} \qquad \text{(AIV-7)}$$

$$u_1 = 5.193 \qquad \text{(AIV-8)}$$

The thermodynamic model for mixed binary Freundlich sorption is given by

$$P_1(\text{ideal}) = \frac{\left[k_1 C_1\ C_1 + (u_2/u_1) C_2\right]^{u_1}}{(C_1 + C_2)} \qquad \text{(3.16)}$$

which is rearranged as

$$P_1(\text{ideal}) = k_1 \frac{C_1}{(C_1+C_2)} (C_1+C_2)^{u_1} \left[\frac{C_1}{C_1 + C_2} + \frac{u_2}{u_1}\left(\frac{C_2}{C_1+C_2}\right)\right]^{u_1} \qquad \text{(AIV-9)}$$

The molefraction of cesium, x_1 is represented by

$$x_1 = \frac{C_1}{C_1 + C_2} \qquad \text{(AIV-10)}$$

therefore the molefraction for barium, x_2 becomes

$$x_2 = 1 - x_1 \qquad \text{(AIV-11)}$$

Substituting the expressions for molefractions in Equation (AIV-9), the cesium pressure relationship obtained is

$$P_1(\text{ideal}) = k_1(C_1+C_2)^{u_1} x_1 \left[\frac{u_2}{u_1} + \left(\frac{u_1 - u_2}{u_1} \right) x_1 \right]^{u_1}$$

or

$$P_1(\text{ideal}) = k_1(C_1 + C_2)^{u_1}(1-x_2) \left[1 - \left(\frac{u_1 - u_2}{u_1} \right) x_2 \right]^{u_1} \qquad \text{(AIV-12)}$$

The activity coefficient for cesium, γ_1 is defined as

$$\gamma_1 = \frac{P_1(\text{true})}{P_1(\text{ideal})} = \frac{P_1(\text{exp})}{P_1(\text{ideal})} \qquad \text{(AIV-13)}$$

where $P_1(\text{exp})$ is the observed experimental value of cesium vapor pressure P_1. It is assumed that the activity coefficient γ_1 is a function of cesium molefraction x_1 (or x_2). Hence,

$$\gamma_1 = f(x_1) \qquad \text{(AIV-14)}$$

gives $\gamma_1 = 1$ when $x_1 = 1$

Similarly if

$$\gamma_1 = f(x_2) \qquad \text{(AIV-15)}$$

then $\gamma_1 = 1$ when $x_2 = 0$.

A possible function that can be assumed is

$$\gamma_1 = \exp\ -f(x_2) \qquad \text{(AIV-16)}$$

or

$$-\ln\gamma_1 = f(x_2) \qquad \text{(AIV-17)}$$

Therefore from Equations (AIV-12), (AIV-13) and (AIV-16), the experimental cesium vapor pressure, $P_1(\text{exp})$ is derived to be

$$P_1(\text{true}) = k_1(C_1 + C_2)^{u_1}(1 - x_2)\left[1 - \frac{(u_1 - u_2)}{u_1}\ x_2\right]^{u_1}\ \gamma_1 \qquad \text{(AIV-18)}$$

The next step is to find the exponential distribution function by plotting $-\ln\gamma_1$ against the barium mole fraction as shown in Figure IV-1 . Various polynomial expressions were applied to the distribution function by using linear least-squares analysis. The best polynomial fit obtained for reduced chi-squared value of 0.06 corresponds to the equation of the form

$$-\ln\gamma_1 = c_1x_2 + c_2x_2^{\ 2} + c_3x_3^{\ 3} \qquad \text{(AIV-19)}$$

where

$c_1 = 3.775$

$c_2 = -10.154$

$c_3 = 11.53$

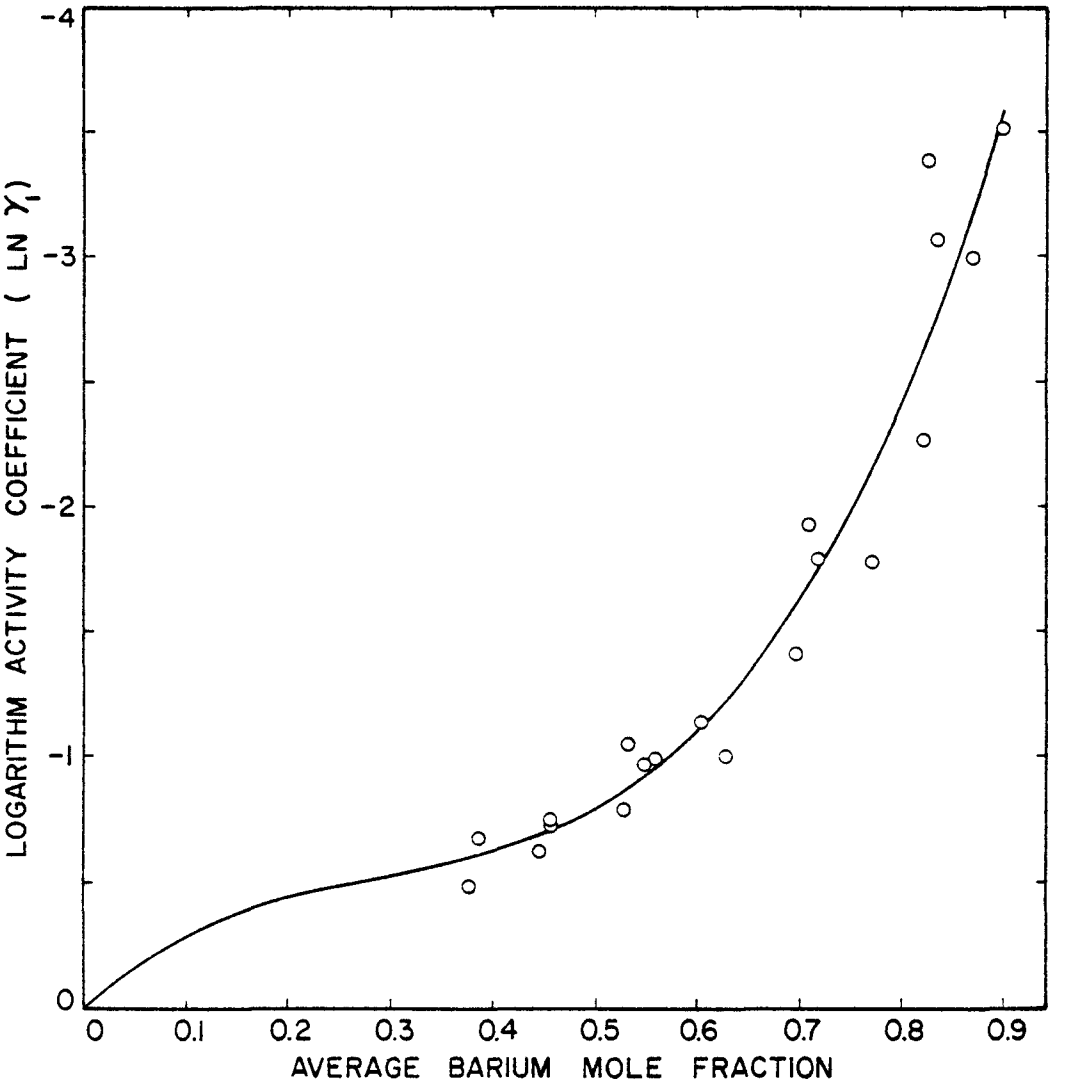

Figure IV-1: Plot of Negative Logarithm Activity Coefficient as a Function of Barium Mole Fraction.

From Equation (AIV-19), the activity coefficient which is a function of barium mole fraction was found to be given by

$$\gamma_1 = \exp\ -(c_1 x_2 + c_2 x_2^{\,2} + c_3 x_2^{\,3}) \qquad \text{(AIV-20)}$$

Equation (AIV-20) was substituted into Equation (AIV-18) and the plot for P(true) which is the same as P(exp) is shown in Figure 5.15 .

APPENDIX V

Experimental Errors

V-1. Background Correction for Cesium and Barium

Tube background correction was imposed on all the concentrations that are plotted on the isotherms. Tube background consists of cesium and barium sorbed on the tantalum liner which serves as a protective sleeve. The graphite sample was maintained at a constant temperature of 1000° C. It rested on the tantalum sleeve which was lined in the Inconel-600 sorption tube. Correction for tube background was made possible by the experiments carried out by Pyecha and Zumwalt (1). They carried out cesium sorption work on tantalum and molybdenum sleeves without the graphite sample. They found that the sleeves adsorbing cesium followed a linear log P-log C relationship until they reached highest sorbed concentration which corresponded to the maximum cesium vapor pressure. The time needed to attain equilibrium was about 200 to 600 minutes. On desorbing the sleeves, they observed no change in the cesium activity in spite of the variation imposed on the temperatures of the main furnace and the cesium source as long as the cesium vapor pressure was lower than the maximum attained earlier. Regarding barium content of the graphite sample, the barium loss during the desorption stage was less than 10%. Hence, the end-of-experiment, barium tube background was assumed and this background correction was applied to the gross desorption results.

V-2. Experimental Errors Arising from Physical Measurements

(i) Graphite Sample Temperature

There was an uncertainty with which the sample temperature was measured. The temperature of the sample was assumed to be the same as

that of the Inconel sorption tube in that region. Measurement of temperature involved the use of a thermocouple and an optical pyrometer. The error in sample temperature is no more than 10^{o} C which was the maximum difference between the pyrometer and thermocouple measurements.

(ii) Isotope Concentration Determination

Another source of error was the determination of cesium and barium content in the graphite sample. The sorbed elements in the sample were tagged by radioisotopes. The isotopic activity of the sample was compared with the activity of the polyvials* containing standard solutions. There was a difference in the geometrical shape between the sample and the polyvials. A correction was made for this difference which corresponded to about 4% in counting efficiency. These polyvials, containing the standard solutions, physically fitted only in the thin-walled tube. Therefore, those experiments that used a slightly thicker walled tube involved a correction that accounted for 7% difference for the combined geometry-attenuation factor.

(iii) Calibration involving counting system

The counting system presented a possibility of a drifting of calibration for the isotope activity since the time span for the experiments was 3 to 6 months. Polyvials containing standard solutions were counted before the start of the experiment and after the conclusion of the experiment. Depending upon the behavior of the electronic counting system, the isotope activity was determined from the average of the two counts and in some cases determined from the end count of the standard solutions. The difference between the two counts was less than 10%. Single channel

---

*The polyvials were snap-lid-closed polyethylene vials of 16mm outer diameter, 55mm length and about 1mm thick.

analyzer (SCA) was continuously used for monitoring the activity to study the kinetics behavior. At the equilibrium stage, gamma-ray spectra indicated that the sleeves were being saturated with cesium. Therefore, it is a simple matter to subtract the end-of-experiment cesium tube background from the gross desorption results. The slope determined from the adsorption isotherm of the tube background experiment was applied to the barium-cesium sorption experiments for tube background correction. The end-of-experiment cesium background found from the same barium-cesium experiments was used as the upper value for the adsorption isotherm for that experiment. The sorption isotherms of cesium background do not have a linear log P-log C relationship but since the cesium tube background constitutes a few percent of the gross cesium content, the error for the net cesium content of the graphite sample is about 2-3%.

The barium-impregnated graphite sample lost a considerable amount of barium during the absorption stage and this barium was subsequently deposited on the tantalum sleeve. Since the barium content was about a couple of mmol/kg as compared to the cesium content on the sleeve which was less than a couple of tenths of mmol/kg, no attempt was made to determine the net barium obtained from the Multi-Channel Analyzer (MCA).

The data were analyzed by a computer code developed by Schonfeld (17). This code took into account gain shift and threshold shift of the counting system. At each equilibrium point, calibration of the counting system was checked with the help of a precision pulse generator and the difference between SCA counts and MCA counts was found to be not more than 5%.